CHARACTERIZATION, LONG-TERM BEHAVIOR EVALUATION AND THERMO-MECHANICAL PROPERTIES OF UNTREATED AND TREATED FLAX FIBER-REINFORCED COMPOSITES

A Dissertation
Submitted to the Graduate Faculty
of the
North Dakota State University
of Agriculture and Applied Science

By

Ali Amiri

In Partial Fulfillment of the Requirements
for the Degree of
DOCTOR OF PHILOSOPHY

Major Department:
Mechanical Engineering

June 2017

Fargo, North Dakota

North Dakota State University

Graduate School

Title

CHARACTERIZATION, LONG-TERM BEHAVIOR EVALUATION AND THERMO-MECHANICAL PROPERTIES OF UNTREATED AND TREATED FLAX FIBER-REINFORCED COMPOSITES

By

Ali Amiri

The Supervisory Committee certifies that this ***disquisition*** complies with North Dakota State University's regulations and meets the accepted standards for the degree of

DOCTOR OF PHILOSOPHY

SUPERVISORY COMMITTEE:

Chad Ulven
Chair

Dilpreet Bajwa

Long Jiang

Sreekala Bajwa

Approved:

6-9-2017
Date

Alan Kallmeyer
Department Chair

ABSTRACT

In recent years there has been a resurgence of interest in the usage of natural fiber reinforced composites in more advanced structural applications. Consequently, the need for improving their mechanical properties as well as service life and long-term behavior modeling and predictions has arisen. In a step towards further development of these materials, in this study, two newly developed biobased resins, derived from soybean oil, methacrylated epoxidized sucrose soyate and double methacrylated epoxidized sucrose soyate are combined with untreated and alkaline treated flax fiber to produce novel biocomposites. Vinyl ester reinforced with flax fiber is used as control in addition to comparing properties of biobased composites against commercial pultruded composites. Effects of alkaline treatment of flax fiber as well as addition of 1% acrylic resin to vinyl ester and the two mentioned biobased resins on mechanical properties are studied. Properties are evaluated in short-term and also, after being exposed to accelerated weathering (i.e. UV and moisture). Moreover, long-term creep of these novel biobased composites and effect of fiber and matrix treatment on viscoelastic behavior is investigated using Time-temperature superposition (TTS) principle. Based on the results of this study, the TTS provides an accelerated method for evaluation of mechanical properties of biobased composites, and satisfactory master curves are achieved by use of this principle. Also, fiber and matrix treatments were effective in increasing mechanical properties of biobased composites in short-term, and treatments delayed the creep response and slowed the process of creep in composites under study in the steady state region. Overall, results of this study reveal the successful production of biocomposites having properties that meet or exceed those of conventional pultruded members while maintaining high biocontent. Composites using treated flax fiber and newly developed resins showed less degradation in properties after accelerated weather exposure. Procedures and methods developed

throughout this study, as well as results presented are essential to further development of these novel materials and utilizing them in more advanced structural applications. Results presented in this dissertation have been published as 5 peer reviewed journal articles, 2 book chapters and have been presented in 6 national and international conferences.

ACKNOWLEDGEMENTS

I would like to express my sincere gratitude to all individuals from whom I received support and encouragement over past four years. Special thanks to my advisor, Dr. Chad Ulven, who has been a great mentor and guide for me throughout this rewarding journey. I would like to thank my committee members whom their valuable advice and comments enhanced the quality of current dissertation. I would also like to thank members of Advanced Materials and Composites Research Laboratory of Dr. Chad Ulven, for last four years, I have benefited from their skills, insight and friendships. I would like to thanks all researchers and scientists who are part of Center for Sustainable Materials Science (CSMS), especially, Dr. Dean Webster and his research team for synthesizing and providing the biobased resins used in this study.

I would like to thank the National Science Foundation (NSF) and ND EPSCoR for providing the funding for this research to be conducted, Composites Innovation Centre of Manitoba conducted the gas pycnometry tests, and AOC Resins generously provided the vinyl ester resin.

Finally, I want to thank my wonderful parents, Nazanin and Gholamreza, and my sister Setare whom always valued education and their selfless love and support taught me the way of life, hard work, perseverance, humility, honesty and integrity. I am forever grateful to you and will always love you.

DEDICATION

To my parents and my sister,

for their endless love, support and encouragement.

TABLE OF CONTENTS

LIST OF TABLES

LIST OF FIGURES

LIST OF APPENDIX TABLES

LIST OF APPENDIX FIGURES

1. INTRODUCTION

Due to their superior advantages, natural fibers such as kenaf, hemp, flax, jute, sisal and nettle have been the center of attention as natural reinforcement in composite materials for the past couple decades. While natural fibers offer competitive strength-to-weight ratio compared to synthetic or mineral fibers, e.g. glass and basalt, other benefits include reduction in CO_2 emission, less dependency on foreign oil resources, reduction in energy consumption and the most important one, recyclability [1]. There have been numerous studies on natural fiber technology [2-4] as well as their use as reinforcement in polymer composites [5-12].

One of the major platforms for natural fiber reinforced composites is in automotive industry in parts such as door panels, headliners, interior parts in addition to underbody shields and covers. Applications of natural fibers in automotive industry dates back to the 1940's when Henry Ford used hemp, wheat straw and soy resin reinforcement in manufacturing some parts for external panels of automobile which had the impact strength 10 times greater than steel [13-16].

However, the growth of natural fiber/thermoplastic composites is somewhat restricted due low degradation temperature of natural fibers. Extended exposure to high temperatures can result in embrittlement of cellulose components and consequently can affect properties such as adhesion bonding of fiber. Therefore temperature profile of composite processing as well as the temperature of fiber surface treatment is matter of great importance [13].

1.1. Flax Fiber

Flax is a type of crop fiber which is grown both for fiber (linen) and for seed oil (linseed). Planting of flax dates back 7000 years ago in Egypt, China and Persia. Canada currently leads the world production of linseed. Flax is also planted in regions with temperate climate such as United States, Russia, India, China and United Kingdom [17]. There are more than 180 species of flax

[18] and depending on the type of flax, the plant is usually sown between March and May and it can reach heights of up to 1m within 100 days. Up to 75% of the plant height will yield to fiber [11].

1.1.1. Structure of Flax Fiber

Flax is a type of multicellular fiber in which its properties are defined by physical, mechanical and chemical properties of the morphological constituents such as cellulose, hemicellulose, lignin and pectin. Cellulose and hemicellulose constitute 70%-95% of the fiber structure and the rest is pectin and lignin which will act as bonding agents [19, 20]. Depending on the variety of flax, other elements can be present in flax structure such as wax, fat, protein, inorganic salts, tannins and dyes [21].

Table 1 summarizes composition of different types of flax fiber reported in literature [22-27]. Also, mechanical properties of flax fiber from literature are presented in Table 2. Pallesen [28] conducted a study in 1996 that showed there are various agricultural factors that can affect composition of flax fiber, such as soil quality, weather conditions, time of harvesting and one of the most important of all, retting process. These factors can even vary for the same farm from year to year [28]. This is the reason variations in cellulose content in different fibers are reported in literature by different authors.

Table 1. Composition of flax fibers reported in literature (%) [22-27]

Reference	Cellulose	Hemi-cellulose	Pectin	Lignin	Wax	Water
[22, 24]	64.1	16.7	1.8	2	1.5	10
[23]	67	11	-	2	-	-
[27]	73.8	13.7	-	2.5	-	1.7
[26]	71	19.6	2	2.2	1.5	-
[25]	60	25	-	8	2	-

Table 2. Literature values for flax fiber [29-35]

Material properties	Flax compiled	Flax [29]	Flax [30]	Flax [31]	Flax [32-35]
Density (kg/m^3)	1400 – 1500	1500	-	1400	-
Tensile modulus (GPa)	12 – 100	100	38.9 – 69.2	50 – 70	12 – 85
Tensile strength (GPa)	0.5 – 2	1.1	0.853–1.825	0.5 – 1.5	0.6 – 2
Max elongation (%)	1 – 4.11	-	2.43 – 4.11	2 – 3	1 – 4
Transverse modulus (GPa)	9.7 – 17.1	-	9.7 – 17.1	-	-
Shear modulus, G_{12} (GPa)	2.4 – 3.4	-	2.4 – 3.4	-	-
Poisson's ratio, υ_{12}	0.183	-	0.131–0.183	-	-

Similar to other natural fibers, flax does not have constant longitudinal dimensions (cross section along its length). Hornsby *et al.* [36], Morvan *et al.* [37] and Stamboulis *et al.* [38] mentioned cross section of flax fiber as polygonal with 5 – 7 sides as it is shown in Figure 1. In general fibers become thinner as one moves from root towards the tip. On average, the width of fiber is 19 µm and the length can be up to 33 mm [30]. However, it is important to note the dispersal of the geometrical dimensions. The transverse and the longitudinal dimensions of the fiber are in the range of 5–76 µm and 4–77 mm, respectively [30, 39].

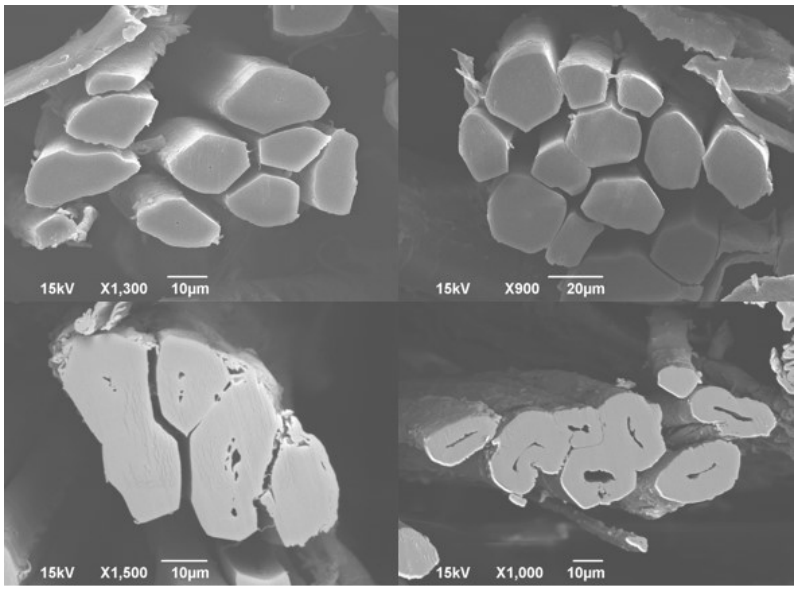

Figure 1. SEM images of cross section of bundles of flax fiber

As shown in Figure 2 there are several layers in a single fiber structure [30, 40-42]. In each single fiber the first layer dispositioning during plant growth is a thin primary wall containing both cellulose and hemicellulose and has a thickness of 0.2 μm [43]. The secondary wall includes three layers consisting of helically wound highly crystalline cellulose chains called micro-fibrils. These micro-fibrils are made up of 30 to 100 cellulose molecule chains which are oriented with 10º angle. Smaller micro-fibrillar angles result in a more rigid fiber [43]. Helically arranged crystalline micro-fibrils of cellulose are held together by amorphous regions consist of hemicellulose and lignin. Hemicellulose molecules are hydrogen bonded to cellulose forming a cellulose-hemicellulose network. The middle layer of the secondary wall is thicker than first and third layer and contributes to the strength of the fiber. According to Bledzki *et al.* [21] the secondary wall contributes to up to 70% of the fiber young's modulus, therefore Higher cellulose content will result in higher tensile modulus [21].

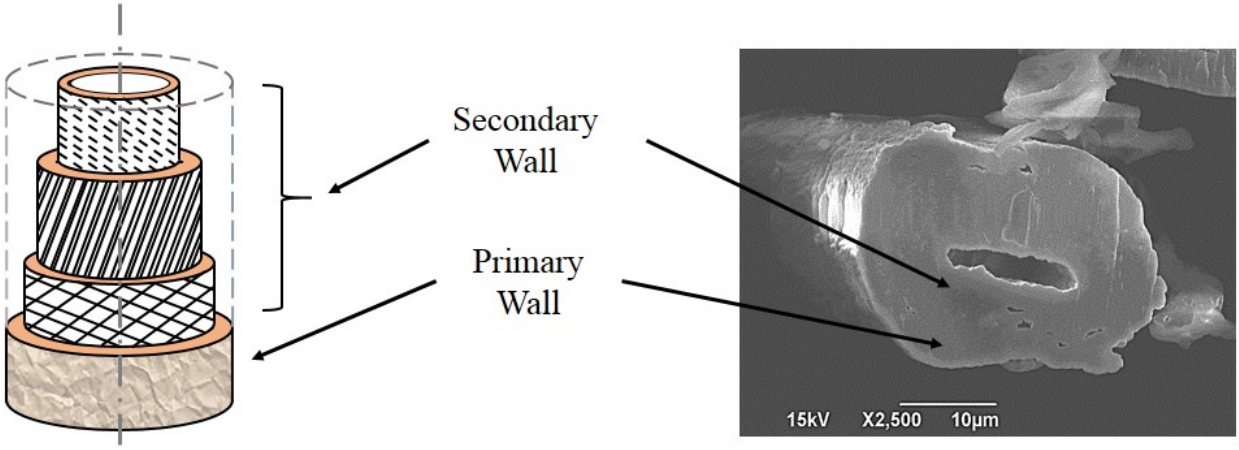

Figure 2. Structural constitution of single flax fiber [30, 40-42]

The lignin network is hydrophobic and will act as a coupling agent increasing the stiffness of cellulose-hemicellulose structure. This will reduce mechanical properties of the fiber as well as interfacial properties of their composites.

As mentioned before, properties of flax depend on cellulose micro-fibrils and their crystallinity. Cellulose is a natural polymer consist of D-anhydro-glucose, $C_6H_{11}O_5$, joining by β-1, 4-glycosidic chains at C1 and C4 locations [44]. A repeating unit of cellulose is shown in Figure 3. Every repeating unit of cellulose has three hydroxyl groups attached to it. The ability of hydroxyl group to form hydrogen bond leads to directing the crystalline packing. Amorphous regions are formed by other molecules with less ordered arrangement. This molecular structure of cellulose dictates its chemical and physical properties. The cellulose content of flax fiber will define the properties of fiber and resultant composites [45]. Also, presence of three hydroxyl groups in each repeating unit, will make cellulose a hydrophilic molecule [21, 46].

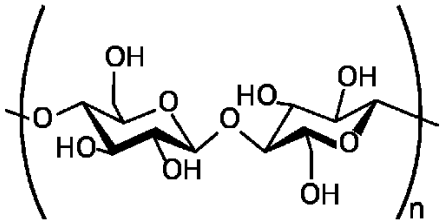

Figure 3. Repeating unit of cellulose

Cellulose can be found in the forms of cellulose I_α and cellulose I_β. Cellulose I_α only exist in some green algae while cellulose I_β can be found in plants or animals [47]. Hemicellulose or polyose is a polymer containing a group of polysaccharides composed of 5-carbon and 6-carbon ring sugars. While cellulose is a linear polymer, hemicellulose has pendant groups attached to its backbone making it an amorphous polymer with shorter chains compared to cellulose [46].

As mentioned in Table 1 lignin will constitute 2-3% of flax fiber structure. Presence of hydroxyl, methoxyl and carbonyl makes structure of lignin complex and hydrophobic [48]. Unlike lignin which will provide stiffness of the plant, pectin which is a type of heteropolysaccaride provides the flexibility to the fiber [46].

1.2. Fiber Treatment and Mechanical Properties

Because of the inherent variations existing in natural fibers [49], the prospect of producing composites using natural fibers poses significant challenges if uniform, quantifiable, reproducible properties are desired [50]. In addition, resin-matrix compatibility issues are a universal hurdle to the use of natural fiber in composites. This incompatibility stems from inherent properties of the materials themselves. In addition, resins are hydrophobic in nature, while natural fibers are hydrophilic. Overcoming this requires treating the fiber in order to modify its surface chemistry, making it behave in a less hydrophilic manner where it interfaces with the matrix. Moreover, due to high concentration of hydroxyl groups on the surface of the cellulose, good wet-out and matrix adhesion are difficult to achieve with natural fibers in their virgin state [51].

In natural fiber reinforced composites, interfacial bonding between fiber and matrix plays a critical role in final composite properties. Hydrophilic nature of flax fiber will lead to absorption of moisture and the result would be presence of voids at the interface of fiber and matrix. Chemical modifications such as alkaline, coupling agents, bleaching, and enzyme, peroxide treatments to remove or reduce non-cellulose content will improve mechanical properties of resulting composites by increasing bonding between the matrix and the fiber and reducing moisture absorption of the fiber.

Belgacem et al. [52] reviewed different methods of natural fiber treatment. In their study, authors concluded that the most effective methods are those that optimize the mechanical properties of the resultant composites by giving continuous rise to covalent bonds between the natural fiber surface and the macromolecular matrix. These methods also will reduce the amount of moisture absorption by natural fibers.

1.2.1. Alkali Treatment

Alkali treatment, also known as mercerization, is removal of hydrogen bonding in the structure of natural fiber. This will result in increase of amorphous cellulose. The alkali treatment is a swelling reaction which can be expressed as the following reaction:

$$\text{Fiber} - \text{OH} + \text{NaOH} \rightarrow \text{Fiber} - \text{O}^{-}\text{Na}^{+} + \text{H}_2\text{O} \quad (1)$$

Cellulose as it occurs in nature has a monoclinic crystalline lattice of cellulose-I. By means of different chemical or thermal treatments this structure can be changed into different polymorphous forms. Cellulose-I, cellulose-II and alkali treated cellulose are shown in Figure 4 [46, 52, 53]. Based on Fengel *et al.* [54] concentration and type of alkali used for treatment affects the degree of lattice transformation in cellulose-II. Also, use of sodium hydroxide will result in higher amount of swelling [54, 55].

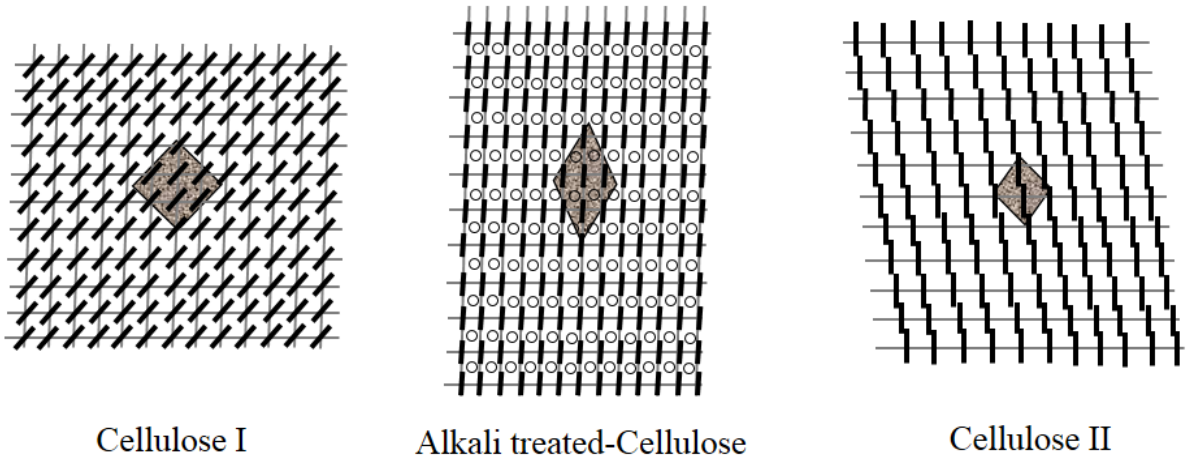

Figure 4. Crystalline lattice of cellulose I, cellulose II and alkali treated cellulose (redrawn from [46, 52, 53])

Alkali treatment can serve two purposes. First, it will increase the surface roughness of the fiber. This will enhance the interfacial adhesion between fiber and matrix or in other words it increases the mechanical interlocking. Second, by increasing the amount of exposed cellulose to

the surface of the fiber, it increases the number of reaction sites and therefore increases better adhesion between fiber and matrix [56, 57]

Van de Weyenberg *et al.* [58] studied the effect of alkali treatment of unidirectional flax fiber on mechanical properties of their ensuing composites. They carried out fiber treatment on aligned normal retted, scutched long flax fibers. The matrix used to make composite panels was epoxy HM 533. For the purpose of alkali treatment, high purity NaOH pellets were dissolved in distilled water to reach desirable concentration. NaOH solution was prepared with 1%, 2% and 3% concentrations and flax fibers were soaked in the solution for 20 minutes at room temperature. Then afterwards fibers were washed with water and acidified water and finally dried in the oven at 80 ºC for 8 hours. Unidirectional flax fiber reinforced composite panels were manufactured manually as well as by use of a drum winder. The resulting composite plates had fiber volume fraction of 40%. Mechanical properties of unidirectional composite panels were measured using flexural and tensile testing. Results of their testing showed significant improvements in tensile and flexural properties of treated fiber composites compared to untreated. The amount of increase for both strength and modulus was about 30% [58]. Similar studies was carried out by Jahn *et al.* [59] and Huo *et al.* [60] and better adhesion between fiber and matrix and increase in mechanical properties of flax reinforced composites was reported.

1.2.2. Coupling Agents – Silane Treatment

A coupling agent contains chemical groups which react both with the fiber surface and the polymer matrix. When coupling agent is used covalent and hydrogen bonds are formed that will enhance the interfacial adhesion [61, 62].

The type of polymer matrix will define what type of coupling agent to be used to treat the fiber. To perform the silane treatment of lingo-cellulosic fibers, first, an alkaline sodium hydroxide

bath is used to activate the OH group of cellulose. Silane is hydrolyzed in water and by reacting with hydroxyl group of the fiber and forms a polysiloxane structure. This reaction is shown in Figure 5 [53, 57, 63].

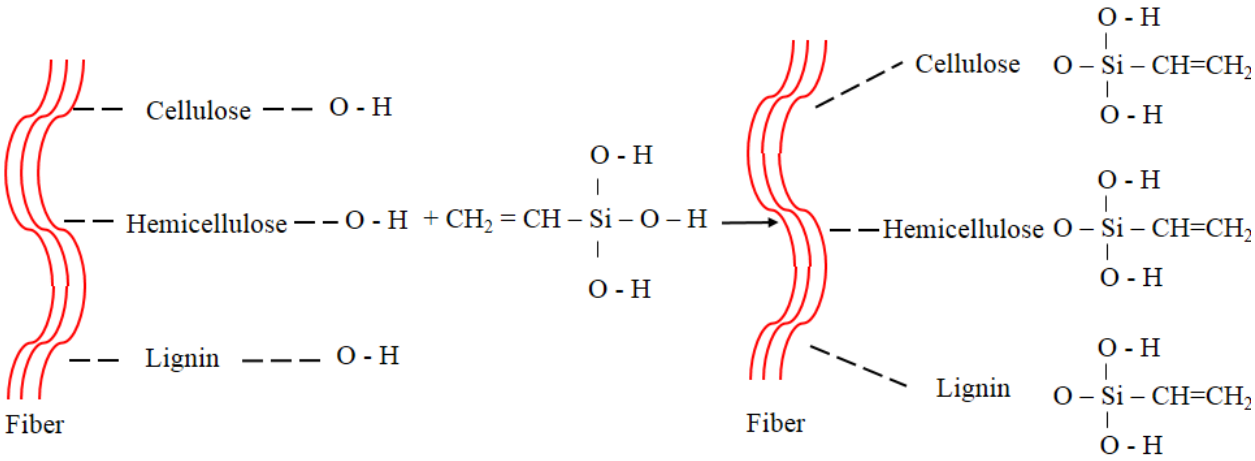

Figure 5. Fiber reaction in silane treatment

Van de Weyenberg et al. [62] studied influence of processing and chemical treatment of flax/epoxy composites. Their results revealed that higher retting degree of flax fiber results in superior mechanical properties of their resultant composites. Authors also investigated effect of silane treatment on mechanical properties of flax/epoxy composites. Table 3 shows the mechanical properties of epoxy resin reinforced with untreated and treated flax fiber. As seen in Table 3, silane treatment was effective on improving mechanical properties of flax/epoxy composites. With 1% silane treatment longitudinal strength and modulus were improved 4.5% and 45% respectively. Transverse properties showed the greatest amount of improvement by 110% for strength and 400% in transverse modulus [62].

In another study Baley *et al.* [64] investigated the effect of chemical treatment of fiber, sodium hydroxide as well as formic acid on adhesion of flax fiber – polyester resin composites. Their results showed that the adhesion between flax fiber and the matrix was improved and

therefore they concluded that composites using treated flax fiber can compete with synthetic glass fiber composites used in advanced industrial applications [64].

Table 3. Mechanical properties of epoxy composites, reinforced with untreated flax fiber vs treated flax fiber [62]

	Tensile strength (MPa)		Flexural strength (MPa)		Tensile modulus (GPa)		Flexural modulus (GPa)	
	untreated	treated	untreated	treated	untreated	treated	untreated	treated
Longitudinal	133	139	218	228	28	41	17.7	26
Transverse	4.5	9.45	8	17	2.7	11	0.36	1.44

1.2.3. Acetylation

Acetylation treatment modifies surface of natural fiber in order to make it more hydrophobic. This treatment includes reaction between OH group of lignin, hemicelluloses and amorphous part of cellulose with acetyl group (CH_3COO^-). This will result in non-polarity of fiber surface and therefore fiber becomes hydrophobic [65]. It will also contribute to dimensional stability of composites [40, 66, 67]. The reaction can be expressed as follow:

$$\text{Fiber-OH} + \text{CH3CO} - \text{O} - \text{OC} - \text{CH3} \rightarrow \text{Fiber} - \text{O} - \text{CO} - \text{CH3} + \text{CH3COOH} \quad (2)$$

Adding acetyl group to the surface of the fiber can be done by using acetate including acetyl chloride, acetic acid and acetic anhydride [68-70], or by use of valerate ($C4H9COO-$). Although Acetylation is one of the most studied reactions of lingo-cellulosic materials [27], but according to Alvarez et al. [71] it is not the most effective treatment. In their study authors compared the effect of two common chemical treatments, alkaline and acetylation on improving mechanical properties of natural fibers. To perform acetylation treatment, fibers were immersed in glacial acetic acid at room temperature for 1, 4 and 24 hours. Then fibers were soaked in acetic anhydride with two drops of sulfuric acid for 5 min. fibers were rinsed with distilled water and finally dried in the oven at 60 ºC. For alkaline treatment fibers were treated with 5% NaOH solution

for 24, 48 and 72 hours at 5, 25 and 40 ºC. Then samples were rinsed with distilled water and dried at 60 ºC. To evaluate mechanical properties of fibers and composites after treatment, mechanical tests such as flexural, adhesion and impact tests were carried out on composite samples.

Based on the results of their study, the interfacial strength does not increase with alkali treatment at room temperature. Authors justified the dispersion seen in the results with the variations in the fiber diameter. Fourier transform infrared spectroscopy (FTIR) tests and SEM images showed that the morphology of the fiber was changed due to the treatments, cellulosic material was removed from surface of the fiber and pores were created. These effects led to a better adhesion between the fiber and the matrix [71].

In other studies Bledzki et al. [8] and Zafeiropoulos et al. [72] found acetylation to be effective in improving the fiber's hydrophobic nature up to 65% for some natural fibers. Also authors enhanced interface of flax fibers and polypropylene matrix. Stress transfer efficiency at interface of fiber/matrix was also improved by acetilation [8, 72].

1.2.4. Enzyme Retting

One of the major processes for preparing bast fibers to be used as reinforcement in composite materials, is retting process [28]. Retting which is the separation of fiber from non-fiber tissues in the stem of the plant. Water-retting is one of the common methods used, however, water retting produces environmentally unacceptable fermentation waste [73]. Fermentation waste and high cost of drying were main reasons for researchers and industrial manufacturer to pursue other methods of fiber retting [74]. An alternative method that has had long-term consideration is enzyme-retting [75]. Research was initiated about a decade ago in the US to evaluate enzyme-retting process for potential to be used in supplying a short staple flax fiber suitable to be blending

with cotton in textile mills. The development of a cost effective, efficient enzyme-retting system still requires additional studies and development [76].

1.2.5. Other Treatments in Literature

Dewaxing is another relatively simple fiber treatment which is accomplished by immersion of fibers in equal parts alcohol and benzene [77]. Mohanty et al. [78] discussed treating natural fibers with maleated forms of polypropylene and polyethylene. Wool and Thielemans [79] reported that deposition of a layer of pine kraft lignin on natural fibers enhances their matrix interactions. They suggested that direct reaction of fibers with the lignin would provide further enhancement. They have also achieved improved fiber/matrix interactions by introducing butyrated kraft lignin to the matrix material prior to composite fabrication [79]. Other methods for chemically modifying natural fibers include benzoylation [80], and acrylation [81] as well as treatment with permanganate [66], peroxides [82] and isocyanates [83]. In addition, cold plasma treatment, corona discharge [84-87], dielectric barrier discharge [88], increase in surface carbonyl group content and porosity of fibers by ultrasound treatment [89] and exposure to ultraviolet radiation have also been shown to improve the polarity of natural fiber [90].

1.3. Vinyl Ester Resin

Vinyl Ester (VE) is a thermosetting resins, typically a di-ester containing recurring ether linkage. The back bone of VE consist of methacrylate oligomer or acrylate and styrene as a reactive diluent [91, 92]. Combination of these materials result in combined mechanical and thermal properties of epoxy resins and unsaturated polyester resins which makes them a great option for high performance fiber reinforced composites [93]. Methacrylate VE resins which contain styrene are typically used in fiberglass reinforces plastics (FRP) and acrylate vinyl ester resins are added during the formulation of UV-cure coatings [91].

Cured VE resins have high resistivity towards solvents, acids and bases. Cured VE has great resistance to degradation in corrosive environments and this makes them suitable for variety of applications such as marine products, i.e. boats, tubs, swimming pools, sewer pipes and solvent storage tanks [94-96]. Other applications of vinyl esters are in high-performance gel coats, pipes and reaction vessels [97].

Properties of VE can be different depending on the type of epoxide molecule in the backbone. Higher molecular weight proxide will provide higher toughness and resiliency but lower solvent and heat resistance. Also, because of lower ester content and vinyl functionality, they have greater resistance to hydrolysis and less shrinkage during cure.

Curing and cross linking process of VE resin initiate with reaction of double bond with a free radical. The initiation step and concentration of free radical will determine the rate of curing. Curing rate plays a fundamental role in VE process. Recently, there have been several studies on cure kinetics of VE using calorimetry and infrared spectroscopy [98, 99].

In [100, 101] authors studied curing process of VE resins. In their studies they investigated effect of factors such as catalyst type and level, laminate thickness and molding temperature on curing behavior of standard vinyl ester and a novolac modified vinyl ester. In series of studies, Han et al. conducted experiments to investigate the influence of prepolymer chemistry and influence of degree of thickening on the chemorheology and cure behavior of VE resins [100, 102, 103].

Palmese et al. [104] studied cure behavior of VE resins when mixed with reinforcement such as glass fiber. The results of their study showed that sizing and surface treatment of fibers can affect cure characteristics of VE because it affects surface interactions between resin and fibers. They used number of commercially sized fiber glass and VE resin systems to study these

effects. The VE resin used contained 50 wt% styrene and 1.75 wt% proxide was used as initiator. The fibers used were four different sized S-2 glass fibers. Neat and fiber reinforced systems were cured and monitored in isothermal environments of 90, 100, 110 and 120 °C and total heat of reaction was measured as a function of time. They Fourier transform infra-red (FTIR) spectroscopy, surface energy measurement methods and differential scanning calorimetry (DSC) were used to characterize fiber surfaces.

In [105] authors observed that sisal reinforced VE resin absorbed 24% less water compared to epoxy resin reinforced with sisal. In addition, VE is one of the effective resins in filling up the flaws of the flax fiber which will lead to better adhesion between fiber and matrix [106].

1.3.1. Treatment of VE Resin

In addition to treatment and modification of fibers, another approach to improve the performance of the composite is to modify the matrix [107]. One method is addition of compatibilizers to the resin in order to decrease the interfacial energy and improve the interfacial adhesion of multiphase polymer [108]. For this method, chemical additives are added to the polymer matrix using chemical or physical interactions to improve the adhesion with the fiber. Addition of compatibilizer with the same repeat unit as the initial matrix will reduce the phase separation of the thermoset resin and result in internal stress and improvement of mechanical performance of the matrix [107, 109]. Huo et al. [106-108] used Acrylic Resin (AR) to manipulate VE system in order to improve mechanical performance of natural fiber reinforced composites. Acrylic resin is a highly viscous liquid, and is used particularly in combination with cellulose nitrate [108].

1.4. Natural Resins from Soybean Oil

The replacement of petroleum-based polymers with biobased counterparts is a recent innovation in the field of "green composites" [64, 110]. Over the last decade, a broad range of chemical routes to utilize natural triglyceride oils to create synthetic-like polymer structure as a basis for coatings, inks, plasticizers, lubricants, and polymers materials has been developed.

Majority of natural resins are derived from botanical and animal oils and these natural oils can be described as triglycerides [111]. The three-member cyclic ether of the epoxy functional group is among the most useful of the potential products of olefinic fatty acids. Consequently, epoxidation is the most common chemical alteration of natural oils [112]. When considering the superlative abundance of soybean oil compared to other vegetable oils, epoxidized soybean oil (ESO) is one of the most significant industrial compounds manufactured from vegetable oils [113, 114]. A depiction of the conversion of soybean oil into ESO can be seen in Figure 6 [115].

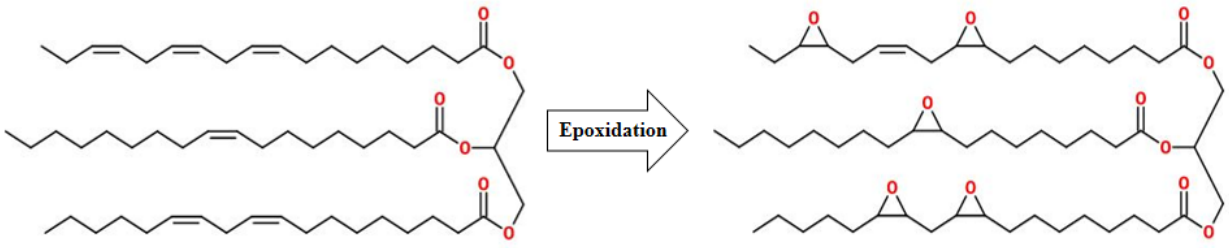

Figure 6. Soybean oil epoxidation adapted from [38]

Much effort has been expended investigating methods of producing biobased resins with respectable performance. Wool et al. pursued various methods of modifying epoxidized forms of soy and other vegetable oils, including acrylation [116], maleinization [117], hydroxylation [118], and phthalation [115]. Adekunle et al. produced methacrylated and acetic anhydride-modified soybean oil [119]. Sithique et al. incorporated bismaleamides [120]. Thulasiraman et. al. reported having created a chlorinated epoxidized soybean oil [121]. These modified ESOs are usually

blended with up to 35 wt% petrochemical based monomers such as styrene [122]. Despite the effort applied in this area, the results generally fail to produce competitive resins without significantly diluting their biobased content. A notable exception, however, is the relatively recent development by Webster et al. of an epoxidized sucrose ester vegetable oil resin, epoxidized sucrose soyate, which exhibits exceptional performance [123, 124].

There were two biobased resins used in this study. First, methacrylated epoxidized sucrose soyate (MESS) resin was made by the reaction of epoxidized sucrose soyate (ESS) and methacrylic acid. ESS was synthesized from fully esterified sucrose soyate as reported previously in [42, 125, 126]. The second resin used was double methacrylated epoxidized sucrose soyate (DMESS). Both of these resins were developed in the Department of Coatings and Polymeric Materials of NDSU by Dr. Dean Webster's research group.

1.5. Long-Term Behavior of Natural Fibers Reinforced Composites

As mentioned before, due to their advantages and also environmental concerns, biobased natural fibers have been replacing synthetic and mineral fibers such as glass or carbon fibers as reinforcement in polymer composites [127-131]. Flax fiber is one of the most popular reinforcement materials in biobased composites. Some advantages of flax fiber is its low density and high specific strength and stiffness, as well as its economically efficient engineering applications [53, 132].

As a result of the viscoelastic nature of both the matrix [133] and the fiber [134], biobased composites exhibit mechanical properties which are time dependent. In recent years there have been numerous studies on viscoelastic behavior of biobased composites [125, 135-138]. Although the service life of bio-composites needs to be adapted to a meet specific application [139], in general, the increase in the interest in use of flax fiber reinforced composites in engineering

applications calls for a minimum of 10 years as their guaranteed service life. Therefore, one important aspect of engineering design development for these materials is long-term creep behavior predictions [140]. In viscoelasticity, there are two common superposition principles that are widely used to predict and model viscoelastic behavior of polymeric materials. The first one is time-temperature superposition developed by Williams, Landel and Ferry (WLF) [141, 142], and the other is the Boltzmann Superposition Principle [142-144]. The time-temperature superposition (TTS) principle can be applied to generate a master curve to describe long-term time dependent deformation based on short-term creep tests at different temperatures. Use of multi-frequency or accelerated temperature measurements is an accepted way to accelerate the time-dependent creep response of biobased composites. In recent years there have been various studies on viscoelastic behavior of biobased composites [125, 135-138] and long term behavior of other polymers [145-148]. Unfortunately, there are not enough studies on applications of mentioned superposition and methods to predict the performance of natural fiber/thermoset resin composites.

1.5.1. Flexural Creep

Creep is a measure of stability of the material and it is of great importance for applications where the material has to sustain load for a long period of time [149, 150]. Three-point bending is one of the methods used to measure creep. Direct measurements of time dependence of strain can be expressed in the form of creep compliance. Creep compliance *J(t)* (1/MPa) in flexure is defined as time-dependent strain per unit stress and is calculated with the following equation [151]:

$$J(t) = \frac{\varepsilon(t)}{\sigma_0} = \frac{4bd^3D(t)}{Pl^3} \quad (3)$$

where *D(t)* is the instantaneous deformation, *P* is the applied load, *b* is the width of the specimen, *d* is the depth of the specimen, and *l* is the support span. Each material has its own creep compliance, as creep compliance is a material property [152]. In three-point bending, the neutral

surface of the sample is assumed to be at the middle of the sample depth and the normal stresses will be shifted from compressive stresses on the top surface of the sample to tensile stresses on the bottom surface across the neutral plane. Also, it is assumed that the entire deformation is due to flexural stress and the deformation due to shear is negligible [153].

1.5.2. Boltzmann Superposition Principle

The Boltzmann Superposition Principle indicates that the effect of mechanical history can linearly be added to determine the total strain response of a single load. The main assumptions for this principle are that (i) the strain of the material depends on the complete loading history of the material, (ii) each loading event should be considered independent, and (iii) the total strain is the addition of strains after each independent event. This principle is expressed with different equations [154, 155]. John Ferry [142] used the following equation to find the total strain $\gamma(t)$ after sequence of finite stress changes σ_i each at any given time u_i :

$$\gamma(t) = \sum_{u_i=-\infty}^{u_i=t} \sigma_i J(t-u_i) \tag{4}$$

where J is creep compliance. When performing creep tests at different temperatures, each temperature step can be considered as a loading event. Therefore, strains from creep measurements at different temperatures can linearly be added together to find the total strain [156].

1.5.3. Time-Temperature Superposition Principle (TTS)

1.5.3.1. Williams – Landel – Ferry Equation for TTS

The basis for time-temperature superposition is the Doolittle equation which relates viscosity of a material, η , to the free volume fraction, f, and has the following form [157]:

$$\eta = A \exp(\frac{B}{f}) \tag{5}$$

in this equation A and B are material constants. It is also known that free volume fraction is dependent on temperature change [157]:

$$f - f_0 = \propto_T (T - T_0) \tag{6}$$

where α is the coefficient of thermal expansion of the material, and f_0 is the free volume fraction at time T_0. The Doolittle equation expresses that the mechanical behavior of a viscoelastic material at different time scales is equivalent to changing their temperatures [158], therefore the temperature shift factor is defined as $a_T = \eta/\eta_0$, where η_0 is the material viscosity at T_0. By taking logarithm of the two sides of this equation and substituting Equation (6) and Equation (5) into the resulting equation we will have the WLF equation as follows [142]:

$$\log a_T = \frac{-C_1(T - T_0)}{C_2 + (T - T_0)} \tag{7}$$

where C_1 and C_2 are empirical constants which depend on material type and reference temperature, T_0.

1.5.3.2. Arrhenius Equation

Arrhenius relation or rate-process theory, describes the relation between rate of reaction and temperature for many reactions. In the case of creep, Arrhenius equation defines the shift factor as ratio of strain rate at an elevated temperature to strain rate at a reference temperature and has the following form [159]:

$$\ln\left(\frac{\dot{\varepsilon_r}}{\dot{\varepsilon}}\right) = \ln(a_T) = \frac{E}{R}\left(\frac{1}{T} - \frac{1}{T_r}\right) \tag{8}$$

where $\dot{\varepsilon_r}$ and $\dot{\varepsilon}$ are strain rate at the reference temperature T_r (K) and arbitrary temperature T (K) at which horizontal shift factor a_T is desired, respectively. In this equation, E is the activation energy (kJ/mol) and R is the universal gas constant (J/mol.K).

Arrhenius equation assumes that creep mechanism remains unchanged at elevated temperature T, in other word, for Equation (8) to be valid, material phase transition should be avoided and in creep process, glass transition temperature, T_g, should not be traversed [156, 160].

1.5.3.3. Time-Temperature Superposition Assumptions

Williams *et al.* [141] and Ferry [142] developed the Time-temperature Superposition (TTS) technique initially for amorphous materials above T_g. They mentioned that equations (7) and (8) is valid in the range T_g+100 º, and below T_g the log(a_T) increases less rapidly with decreasing temperature [141]. In literature, TTS has been applied to predict and model long-term behavior of materials below T_g [161, 162], in the range including T_g [163, 164] and above T_g [165, 166]. TTS is valid when temperature dependence of shift factors a_T, is in the form such as WLF Equation (7) or Arrhenius Equation (8), and a_T has the same value for all viscoelastic functions. Landel and Nielsen [149] and Tajvidi et al. [167] mentioned that TTS could be applied to semicrystalline and crystalline polymers but vertical shift factors are also needed to generate a smooth master curve. The vertical shift factors are the result of change in the structure, degree of crystallinity, and molecular level of the material. Therefore, for TTS of thermoset resins to hold, one should make sure that the resin is fully cured and there is no residual curing and cross-linking of the resin is happening in the test temperature range. The creep test temperature range should be picked in the range lower than degradation of the material being tested [97, 160, 167]. Also, TTS can be applicable to semi-crystalline and crystalline materials if the creep test is conducted under low strain to maintain the material response in the linear viscoelastic range [167, 168].

1.5.4. Creep Modeling

As the interest in natural fiber reinforced composites is growing, so is the necessity for development of models and methods to predict and capture time-dependent properties of biobased

composites [169]. These data and models are essential to the development of biobased composites as they facilitate design engineers in the use of biobased composites in more structural applications [170]. As mentioned previously, thermoset resins reinforced with flax fiber exhibit non-linear behavior when subjected to loading [171, 172]. In addition, the inherent variation present in natural flax fiber [173] as well as polymer matrices make design with of biobased composites a complex task. Therefore empirical models and results are widely used to help designers for their applications [174].

1.5.4.1. Nutting Power Law

Nutting [175] in 1921 proposed an empirical strain-stress-time model which showed good agreement with steady state creep for metals:

$$\varepsilon^c = k\sigma^P t^n \tag{9}$$

where ε^c is the creep strain, σ is the applied stress, *k*, *P* and *n* are temperature-dependent material constants. This model has been used by researchers for viscoelastic materials with satisfactory results for short-term creep [167, 176-178].

1.5.4.2. Modification of Findley Power Law

According to Findley [152] the time-dependent creep compliance, *J(t)*, of a material can be represented by a power function as:

$$J = J_o + J(t) = J_0 + A\, t^n \tag{10}$$

where J_0 is the time-independent or elastic creep compliance, *A* is the time-dependent coefficient, *t* is the time and *n* is stress-independent coefficient. Creep compliance *J(t)* in flexure is defined as the time-dependent strain per unit stress [151]. Therefore Equation (10) can be modified as follows to represent the entire strain creep curve of a material, ε, can be expressed as:

$$\varepsilon = \varepsilon_0 + \varepsilon(t) \tag{11}$$

where ε_0 is the elastic strain, and $\varepsilon(t)$ is the time-dependent strain. From the definition of creep compliance and Equation (10):

$$J(t) = \frac{\varepsilon(t)}{\sigma_0} = At^n \tag{12}$$

Therefore, the modified Findley Power Law for strain creep can be presented as follows:

$$\varepsilon = \varepsilon_0 + A\sigma_0 t^n \tag{13}$$

1.6. Density of Flax Fiber

Density is a fundamental physical property of reinforcement for composites. It appears widely in calculations, which are mostly used for engineering designs. Determining the density of fibers as reinforcement is important issue because beside mechanical performance it is the most important factor that defines the potential application of the fiber as a lightweight construction material [179]. In addition, density measurement in fibers can be used as useful tool of quality control in their production process [180].

The density of homogeneous solid materials is generally straightforward to determine, because it requires only measurements of weight (or mass) and of volume of a specimen. Flax fiber requires a different method of density measurement because it is a porous material. In addition, due to the discussed structure, surface morphology, and also, hydrophilic nature of flax fibers [181], accurately measuring the density of flax fiber is a challenging task to accomplish. Currently there are no standard test methods to suggest how to properly perform the density measurement of flax fiber [182], and the lack of proper and universal method to measure density of flax fiber needs to be addressed by developing a standard method and conditions to measure the density of flax fiber.

In this dissertation, a summary of the research on this issue in collaboration with Composites Innovation Centre, Winnipeg, Manitoba, Canadato develop a standard test method for measuring density of flax fiber under ASTM committee D17.13 will be presented.

In literature as well as previous studies related to flax fiber as reinforcement in composites, different values have been measured and reported for flax fiber density. Tortora and Collier [183] reported the value for density of flax fiber to be 1.54 g/cm^3. some other researchers such as Truong et al. [182] have used this value as a reference for comparison for their work. Arbelaiz et al. [184] used a value of 1.4 g/cm^3 for flax fiber in their study. Flax fiber density values and measurement methods that other researchers from North Dakota State University's Advanced Materials and Composites Research Lab. have used and are reported in publications are as follows; Ehresmann et al. [49] measured the density of flax fiber using Archimedes method and used canola oil as immersion liquid. The reported values for flax fiber density are between 1.28-1.3 g/cm^3. Shanshan Huo [108] used Archimedes method with distilled water as immersion liquid and found the density of linen flax fiber to be 1.42 g/cm^3; Whitacre et al. [181] used the value of 1.44 g/cm^3 for flax fiber used in their studies; and Flynn et al. [185] used the manufacturer value of 1.5 g/cm^3 for their study.

Truong et al. [182] reviewed five different methods of density testing for high-modulus fibers. They mentioned methods to be i) linear density measurement [186], ii) Archimedes or buoyancy method, iii) helium, pycnometry [187], iv) liquid pycnometry [187] and v) gradient column pycnometry. Detailed explanation of each method is provided in [182, 188]. and Truong et al. [182] used this value reported in mentioned study as a reference for their study.

1.7. Objectives

The followings are set as objectives for this study:

1.7.1. Investigating the Effect of Mechanical and Chemical Processes on Performance of Natural Fiber Reinforced Composites

The mechanical and cleaning process of flax fiber prior to use as reinforcement in composite materials as well as increasing and modifying the adhesion between fiber and matrix has been subject of many studies [45, 189-193]. A thorough understanding of different mechanical and cleaning processes of natural fibers is valuable in development of their applications [130], since they can target a specific mechanical property to be improved by use of a certain mechanical process. In this study, short-term and long-term mechanical properties of biobased resins reinforced with flax fiber fibers with different mechanical treatments are compared with composites using Vinyl Ester (VE) as their matrix. Also, two methods of chemical treatments are selected to investigate their effect on improving bonding between fiber and matrix and mechanical properties in short-term and long-term. Results will provide better insight on modification methods of flax fiber and success of mentioned methods on improving short and long-term performance of biobased composites.

1.7.2. Predicting Long-Term Behavior of Natural Fiber/Thermoset Resins

Due to lack of research studies that investigate the modeling and long-term creep behavior of long continuous natural fibers / thermoset resins, in this study, methods and models of predicting long-term behavior of natural fiber/thermoset resins will be studied and investigated. Flax fiber composites are processed with novel natural resins. In the first portion, applicability of existing principles to natural fiber reinforced composites will be investigated. In the second portion, frequency scans of the bio-composite are obtained at different temperatures and storage modulus

and loss modulus are recorded and the application of horizontal and vertical shift factors to these viscoelastic functions are studied.

As mentioned, there are numerous studies which investigate the effect of fiber treatment on mechanical properties of resulting composites. However to the best of authors' knowledge there are not any studies that investigate the effect of these treatments on long-term creep behavior of long continuous natural fibers/thermoset composites. Creep of fiber reinforced composites is a complex phenomenon which depends on many factors such as elastic and fracture behavior of the fibers, creep behavior of matrix, fiber-matrix interfacial properties, efficiency of load transfer from matrix to fiber and even the geometry and arrangement of the fibers in matrix [170]. In the current study, in connection with first objective, effect of two selected methods of treatment on mechanical properties of flax reinforced composites in long-term are studied. Results will provide better insight on which of the mentioned effective factors in long-term behavior is more prone to be affected by these treatments. This information would be essential for engineers and designers for the incorporation of biobased composites in more structural designs.

1.7.3. Developing Composites of Structural Quality from Renewable Resources

One aspect of developing biobased composites for structural applications is their endurance and mechanical performance when exposed to weather conditions is the long-term (UV and moisture). In this part of study, newly developed vegetable oil-based resins reinforced with untreated and alkaline treated flax fiber are manufactured. Properties of these composites are compared against those vinyl ester as their matrices. In addition, accelerated weathering are performed on the manufactured composites to evaluate the mechanical properties after exposing to UV and moisture. The results of this study will be vital to successful production of bio-composites having properties that meet or exceed those of conventional available materials such

as pultruded members while having high biocontent, and therefore their further development to be used in advanced structural applications.

1.7.4. Developing Standard Procedure and Novel Methods of Characterization of Flax Fiber and Biobased Composites

Another difficulty posing challenge in the way of further utilization of natural fibers in fiber reinforced composites is lack of advanced and standard characterization procedures. Therefore, another objective for this study is set to develop a standard test method for measuring density of flax fiber using buoyancy (Archimedes) method and advance method of void fraction calculation for fiber reinforced composites.

First, an alternative standard method of density measurement is developed that can be used in cases gas pycnometry is not available. It is expected that Archimedes method generates less precise results and it can be used when less accurate results are sufficient. In this study, use of Archimedes method as an easy, cheap method is introduced to measure the density of four different types of flax fiber. ASTM E1169-14 is used to perform a ruggedness test on the method provided. Until the date that the process of developing ASTM standard is completed and this test method is available, the results provided in this study are vital to researchers and designers working with flax fiber. In addition, a new advanced method of X-ray 3D imaging using Micro-CT scans employed with a MATLAB image processing code was used to determine void fraction calculation of biobased fiber reinforced composites. Until the date that the process of developing ASTM standard is completed and this test method is available, the results provided in this study are vital to researchers and designers working with flax fiber.

2. RESEARCH METHODOLOGY

It is worth mentioning that throughout the experimental section of this study, all lab safety protocols were complied with. All fibers, and all composite specimens were handles while wearing nitrile powder free gloves. And they were always placed on clean surfaces. All fibers as well as composites specimens were kept in lab controlled environment and dried and conditioned consistently before any processing or testing and all fibers and specimens were stored in press-to-close clear bags.

2.1. Material Used in this Study

2.1.1. Fiber

Based on the information provided in the introduction section and the advantages of flax fiber as a viable form of reinforcement in composite materials, flax fiber was selected as the main material for this study. Six different types of flax fiber were used in this study. Four types of linseed flax, farmed and harvested by the University of Saskatchewan, Saskatoon, SK, Canada. Shive (i.e. woody core of the flax stalk) was removed by passing the fiber through a pilot line eight times at Biolin Research, Inc., Saskatoon, SK, Canada. Three different mechanical processes were carried out (Type 1 through Type 4) in order to clean fibers and align them better for preparation to be used as reinforcement [194]. One type of Chinese linen; retted and separated, with low shive content (<5% by mass) (Type 5). Bidirectional and unidirectional flax fiber mats, Biotex®, obtained from Composites Evolution, Chesterfield, UK (Type 6 and Type 7) were also used. Different types of flax fibers used in this study are described in Table 4.

2.1.2. Enzyme

Enzyme used for the treatment of fiber was provided by Novozymes, Bagsvaerd; Denmark, with the commercial brand of StickAway. The product details are presented in Appendix A.

Table 4. Types of flax fiber used in this study

Fiber Type	Description
Type 1 – Linseed flax	No extra mechanical process was performed on fiber.
Type 2 – Linseed flax	Fiber was combed ten times by "opener" machine in a rough manner.
Type 3 – Linseed flax	A 50/50 blend of optimally retted fiber and over retted fiber.
Type 4 – Linseed flax	Fiber was passed through a pair of small fluted rollers ten times to remove remaining shive.
Type 5 – Chinese Linen flax	Water retted with low shive content
Type 6 – Bidirectional flax fabric	Biotex flax fabric, 2×2 twill, areal density of 400 g/m^2
Type 7 – Unidirectional flax fabric	Biotex flax fabric

2.1.3. Resin

2.1.3.1. Epoxy Araldite 8601

The first resin which was used as control, was Araldite 8601 crosslinked with Aradur 8602 (mixing ratio of 100 to 25 parts by weight). It is a commercially available epoxy/amine combination formulated specifically by Huntsman Corporation (The Woodlands, TX) for VARTM process. Properties of this epoxy resin from literature is provided in Appendix A [195, 196].

2.1.3.2. Vinyl Ester (VE)

The second resin used was a vinyl ester (VE) system Hydropel® R037-YDF-40 provided by AOC resins. The hardener was a 2-butanone peroxide (Luperox® DDM-9) solution, which was obtained from Sigma-Aldrich Co. Mixing ratio of VE and hardener is 100 to 1 weight parts. Acronal® 700L was provided by BASF Aktiengesellschaft, Ludwigshafen, Germany. Acronal® 700L is a type of acrylic resin (AR), which is the copolymer from n-butyl acrylate and vinyl isobutyl ether.

2.1.3.3. Methacrylated Epoxidized Sucrose Soyate (MESS)

The synthesis of the MESS resin was achieved via ring-opening reaction of ESS with methacrylic acid. The reaction was carried out at 90°C, using AMC-2 (source) as the catalyst and hydroquinone as the inhibitor. The molar ratio of methacrylic acid (source) to epoxy was 0.8. The procedure is as follows: ESS (1000.00 g), methacrylic acid (291.831 g, acid to epoxy ratio = 0.8), hydroquinone (source) (6.459 g, 0.5% of total weight) and AMC-2 (12.918 g, 1.0% of total weight) were placed into a three-necked, round-bottomed flask equipped with a mechanical stirrer and a thermocouple. The mixture was heated at 90°C for 24 h. The final resin appeared as a dark green, viscous liquid. No further purification was carried out before incorporation into the composites. The synthesis rout is presented in [123] and in Figure 7.

Procter & Gamble Chemicals (Cincinnati, OH, USA) provided the sucrose soyate (Sefose 1618U), which was the precursor of the starting material. Methacrylic acid and methacrylic anhydride were purchased from Alfa Aesar (Ward Hill, Massachusetts, USA). ATC-3 accelerator was purchased from AMPAC Fine Chemicals (Rancho Cordova, CA, USA), is a 50% solution of trivalent organic chromium complexes in phthalate esters. Hydroquinone was purchased from Sigma Aldrich (St. Louis, MO, USA). All the reagents were used as-received. Epoxidized sucrose soyate (ESS) was synthesized following the procedure in the literature [123]. The epoxy equivalent weight of ESS, which was 246, was determined by epoxy titration according to ASTM D 1652.

2.1.3.4. Double Methacrylated Epoxidized Sucrose Soyate (DMESS)

Synthesis of DMESS is presented in Figure 8. The synthesis of DMESS resin was achieved by the same reaction from ESS with methacrylic acid and subsequent methacrylation with methacrylic anhydride. The reaction was carried out at 100°C, using ATC-3 as the catalyst and hydroquinone as the inhibitor. The molar ratio of methacrylic acid to methacrylic anhydride was

1:9 while the molar ratio of the methacrylating agents (methacrylic acid and methacrylic anhydride) to epoxy was 0.8. The procedure is as follows: ESS (700.00 g), methacrylic acid (19.76 g), hydroquinone (1.04 g, 0.1% of total weight) and ATC-3 (10.38 g, 1.0% of total weight) were placed into a four-necked reaction kettle equipped with a mechanical stirrer and a thermocouple. The mixture was heated to 100°C followed by the dropwise addition (~0.25 mL/min) of methacrylic anhydride (318.45 g). The final resin appeared as a dark green, viscous liquid. No further purification was carried out before incorporation into the composites.

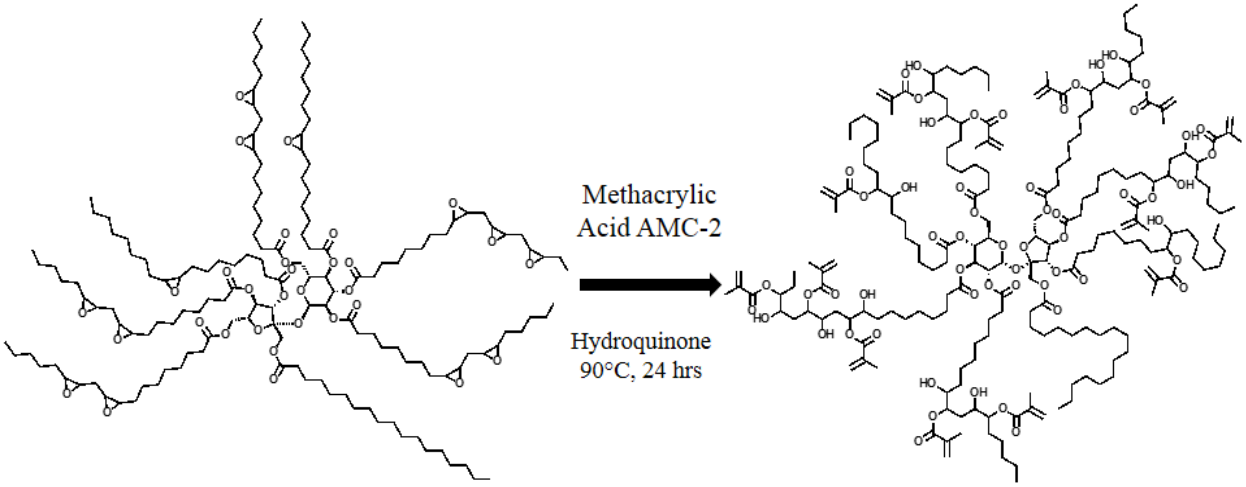

Figure 7. Synthetic route to MESS

The MESS and DMESS resins were too viscous to be used for thermoset formulations. Therefore, styrene was introduced as a reactive diluent to reduce the viscosity, as well as a co-monomer to increase the rigidity of the resulting thermosets. The resulting resins contained 30% styrene. The resin was mixed with tert-butyl peroxybenzoate 98% (Luperox® P) as a high temperature initiator and cumyl hydroperoxide 45% (Trigonox 239A) as a room temperature initiator. The mixing ratio of Luperox® P, Trigonox 239A were 2 and 3 wt%, respectively. The DMESS was also mixed with 2 wt% Luperox 10M75 (Tert-butyl peroxyneodecanoate). Styrene and Luperox® P were purchased from Sigma-Aldrich Co. located in St. Louis, Missouri, USA.

Cumyl Peroxide, commercially available as Trigonox 239A, was generously provided by AkzoNobel Co., Amsterdam, Netherlands. Luperox 10M75 was obtained from Arkema®, Philadelphia, PA.

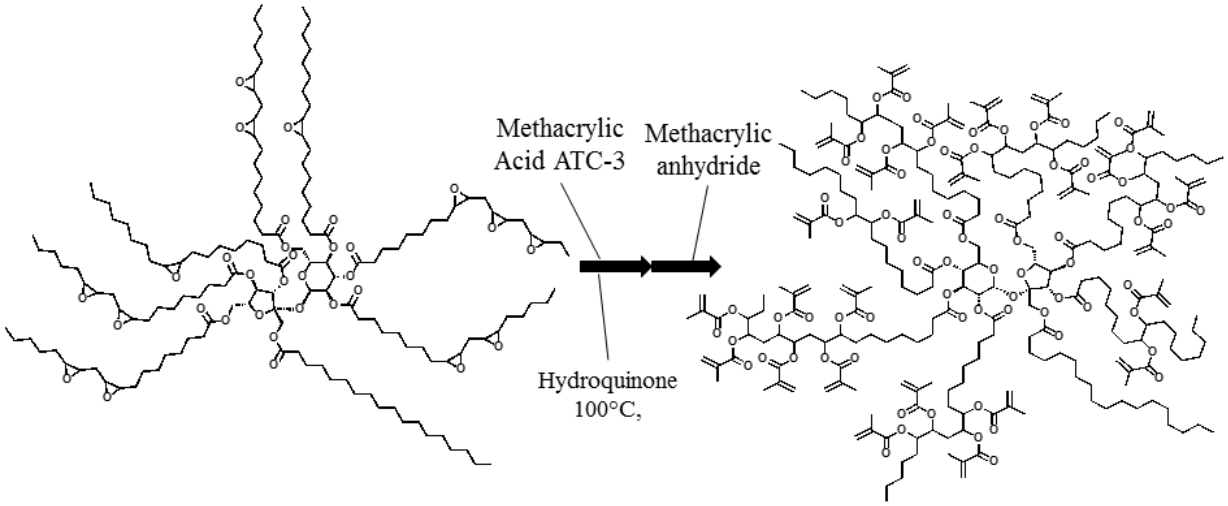

Figure 8. Synthetic route to DMESS

Table 5. Summary of resins used in this study

Resin	Manufacturer	Hardener/initiator	Weight ratio	Cure condition	Post curing
Vinyl Ester	AOC Resins	Luperox DDM9	100 : 1	24 hrs 25 °C	12 hrs 80 °C
Epoxy 8601	Huntsman	Aradur 8601	100 : 4	24 hrs 25 °C	2 hrs 60 °C
MESS	NDSU	Styrene	100 : 30	2 hrs 175 °C	None
		Luperox P	100 : 2		
		Trigonox 239A	100 : 3		
DMESS	NDSU	Styrene	100 : 30	1hr 70 °C	None
		Luperox P	100 : 2	1hr 90 °C	
		Luperox 10M75	100 : 2	1hr 150 °C	

2.1.4. Fluids Used for Density Method Development

Five different types of fluids were used in the density measurement method development study. Two types of canola oil were used, first grocery store grade with the commercial name of Wesson was purchased from Walmart Super Center, and the second one, Canola Oil Certified Organic, from Sigma Aldrich Company, St. Louis, MO, USA, with CAS Number 120962-03-0. Similarly, two types of soybean oil was obtained, grocery store grade with commercial brand of Crisco purchased from Walmart Super Center, and Soybean Oil from Sigma Aldrich Co., with CAS number 8001-22-7. White mineral oil light was purchased from W.S. Dogde Oil Co., Maywood, CA, USA with CAS number 8042-47-5. Summary of fluids used in flax fiber density measurement are presented in Table 6.

Table 6. Properties of fluids used for density measurement of flax fiber

Type of fluid	Manufacturer	CAS Number
Canola Oil - Grocery Store	Wesson	-
Canola Oil – Certified	Sigma Aldrich	120962-03-0
Soybean Oil- Grocery store	Crisco	-
Soybean Oil - Certified	Sigma Aldrich	8001-22-7
White Mineral Oil	W.S. Dodge Oil	8042-47-5

2.2. Treatment Methods

2.2.1. Fiber Lipase Treatment

To find the most significant factor affecting the treatment of the fiber, a central composite design with surface response was used as shown in Table 7. Two factors with three levels were introduced as follows:

Factor 1: X1 = Set time. Levels= 24, 16 and 8 hours

Factor 2: X2 = Solution concentration. Levels = 35.2%, 25.2% and 15.2%

Table 7. Design of experiment for lipase treatment of flax fiber

Sample No.	Set Time (hour)	Solution Concentration (%)	X1	X2	X1X2
1	8	15.2	-1	-1	+1
2	24	15.2	+1	-1	-1
3	8	35.2	-1	+1	-1
4	24	35.2	+1	+1	+1
5	16	25.2	0	0	0
6	16	25.2	0	0	0
7	16	25.2	0	0	0

Enzyme solution was diluted to the concentrations of 25.2% and 15.2%. Type 5 flax fiber samples were cut, weighed and labeled. Each sample was soaked in the solution for 5 minutes. Then samples were set at room temperature in sealed bags for the time periods mentioned in Table 7. Then afterwards, samples were rinsed with tap water and were placed in the oven for 24 hours at 80° C to dry-off. Three smaller samples were picked from each of sample batch 1 through 7 for staining and imaging.

2.2.2. Alkaline Treatment

To study the effect of chemical treatments on mechanical performance of flax fiber reinforced composites, alkaline treatment was selected for treating flax fiber. In order to minimize the effect of shrinkage of the fiber as the result of alkaline treatment [106], NaOH/ethanol solution was used. To treat the fibers, approximately 35 g of NaOH pellets were placed in a 4000 ml beaker and up to 3500 ml of 95% ethanol (100 ml/g NaOH) was added and the beaker was placed on a stirring hotplate and the solution was brought to boil. Maximum of 50 g of Type 1, 6 and 7 fiber per liter of solution were then submerged in the solution, the beaker was cover with aluminum foil and a heavy glass lid for the period of two hours. After two hours of treatment, fibers were rinsed off with cold tap water until there was no treatment solution residue left in the fibers. Fibers were dried in a convection oven (Model 1370FM, VWR) at 60 °C for 12 hours.

For the flax fiber fabric treatment, 9 layers of flax fiber fabric (Type 6, 7) were treated together. In order to keep the alignment of fibers in place after treatment, a sheet of nylon release peel-ply was placed between each layer of flax fiber as well as two slightly larger-cut sheets under and over the stack of fabric. The edges of the oversized sheets of peel-ply were folded back and clamped with small size binder clips. After treatment fibers were washed and rinsed with tap water with the peel-ply sheet in place. The sheets were removed layer by layer right before fabrics were processed to manufacture the composite plates. Figure 9 shows the fibers before, during and after treatment process.

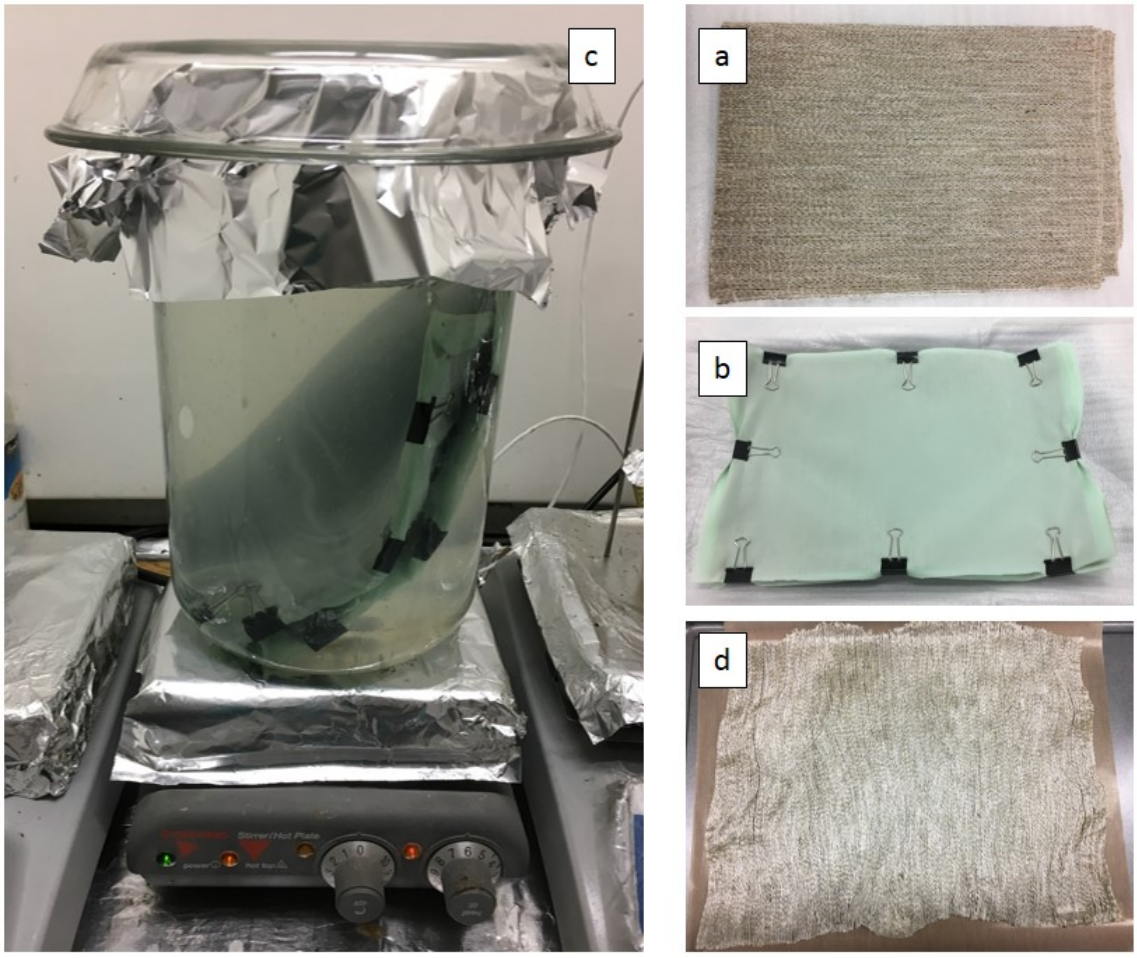

Figure 9. (a) Flax fiber fabric before treatment, (b) flax fiber fabric wrapped in nylon release peel-ply sheets, (c) flax fiber fabric submerged in 4000 ml beaker containing solution of NaOH and 95% ethanol, and (d) flax fiber fabric after treatment (dried)

2.2.3. Vinyl Ester Resin Treatment

1% acrylic resin was also added to the VE resin as a chemical additive to improve the adhesion between the fibers and the resin. Flax/VE with 1wt% acrylic resin composites were also processed by the processes explained in the next section.

2.3. Processing the Composite Panels

2.3.1. Hand Layup Compression Molding

Composite panels were manufactured using a hand-layup compression molding process. To process the composite panels, in case of loose fibers, Type 1-Type 7 fiber roving was processed with a manual drum carder machine model DC-P05-B/A from Strauch Fiber Equipment Co. shown in Figure 10.

Figure 10. Carder machine used in this study and fiber before and after carding process

For each composite panel 50±4 g of fiber was run through carder machine once (500 revolutions). Figure 10 also shows fiber before and after going through carder machine.

Carded fibers were placed on a mold and 350 g of resin was poured onto the mold till fiber was soaked in resin. A nonporous Polytetrafluoroethylene (PTFE) sheet was placed on top of fiber, and a caul plate with dimensions of 200 mm × 150 mm was placed on top of fiber. The entire lay-up was sealed under a layer of vacuum bagging film. The entire set-up was placed in a top bench manual heated press, Carver Model 3856 (Carver Inc., IN, USA). Eight metric tons of force was applied which resulted in 1.6 MPa pressure over the lay-up. VE soaked fibers were in the mold

under mentioned pressure for 24 hours at room temperature and then post cured at 80 ºC for 12 hours. MESS soaked fibers were in the heated press at 175 ºC for two hours. DMESS soaked fibers were under pressure for 1 hour at 70 ºC, 1 hour at 90 ºC and 1 hour at 150 ºC. Cured and processed composite panels were kept under mentioned pressures to cool down to room temperature before they were removed from the press.

Schematic of the composite plate manufacturing layup is shown in Figure 11. The resulting composite plates from this process had average thickness of 2.5 - 3 mm. Figure 12 shows composite panels before, during and after processing.

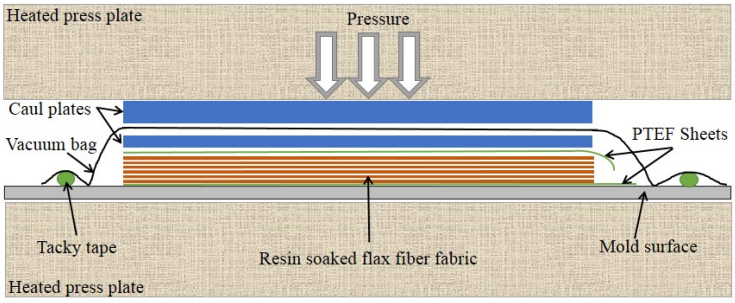

Figure 11. Hand layup composite panel manufacturing layup

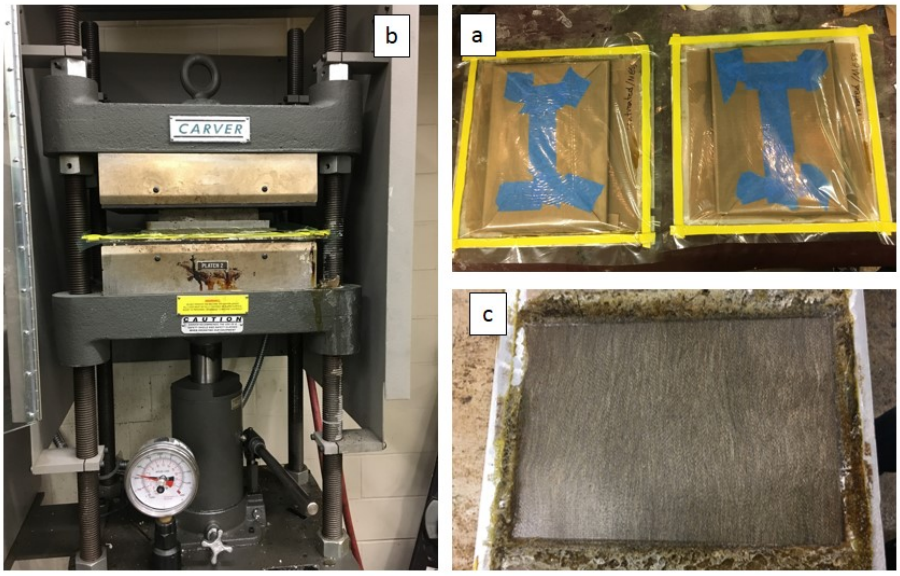

Figure 12. (a) Flax fibers soaked with resin and wrapped in bagging film, (b) panels in the heated press, and (c) a manufactured composite panel

2.3.2. Vacuum Assisted Resin Transfer Molding (VARTM)

Vacuum Assisted Resin Transfer Molding (VARTM) was also used to manufacture composite panels. VARTM method for manufacturing composite has been around for almost 50 years and it's been continuing to develop to achieve better quality. It is an effective method to lower tool costs in manufacturing complex-shaped composite parts, as well as lower void content compared to other manufacturing methods [197-199]. In this process, the reinforcement is assembled in a mold and is sealed inside a vacuum bag. The resin is transferred into the part through a resin inlet under vacuum pressure. Vacuum Assisted Resin Transfer Molding (VARTM) method was used to manufacture composite panels. The mold surface was waxed with mold release agent and six layers of flax fiber mat (or 50 grams of linen flax) were stacked up on each other. One layer of porous polytetrafluoroethylene (PTFE) and one layer of breather cloth was placed on top of all materials. Finally, a layer of vacuum bagging film was applied. Vacuum pressure was applied and resin was infused into the fiber. Once the resin was infused thoroughly and fiber was soaked with resin, the inlet line was shut.

Composite panels using VE were under pressure for 24 hours at room temperature and then post cured at 80 ºC for 12 hours. For Epoxy resin, after 90 min the flow of the resin was stopped and the material was left under vacuum for 24 hours and then post cured at 60°C for two hours as recommended for this matrix. The panels using MESS resins were under pressure for 2 hours at 150 ºC. DMESS soaked fibers were under pressure for 1 hour at 70 ºC, 1 hour at 90 ºC and 1 hour at 150 ºC. To avoid warpage, the panels were cooled down to room temperature under pressure. Figure 13 shows a schematic of the setup for the VARTM process. Figure 14 shows VARTM process, panels being heated and a typical manufactured composite panel. The final composite

plate had a thickness of 3mm. Specimens were cut to size for mechanical testing using an Allied diamond saw.

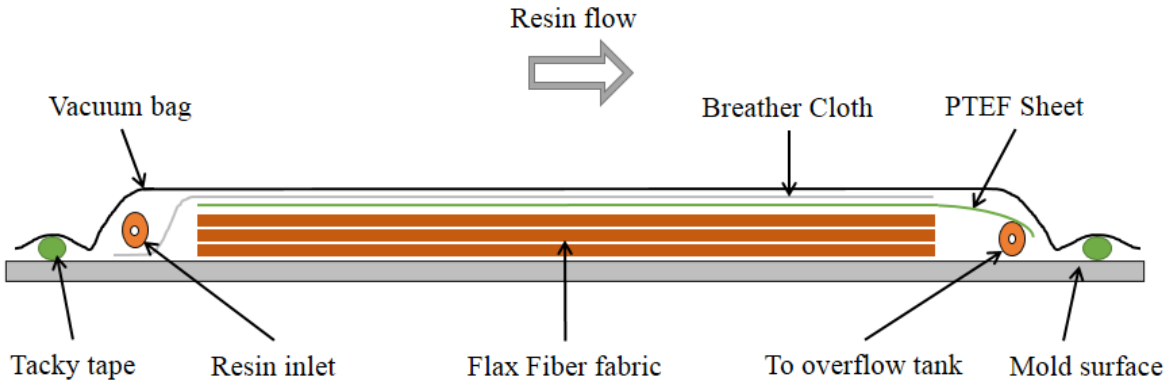

Figure 13. Schematic of the VARTM set-up used to manufacture composite sample

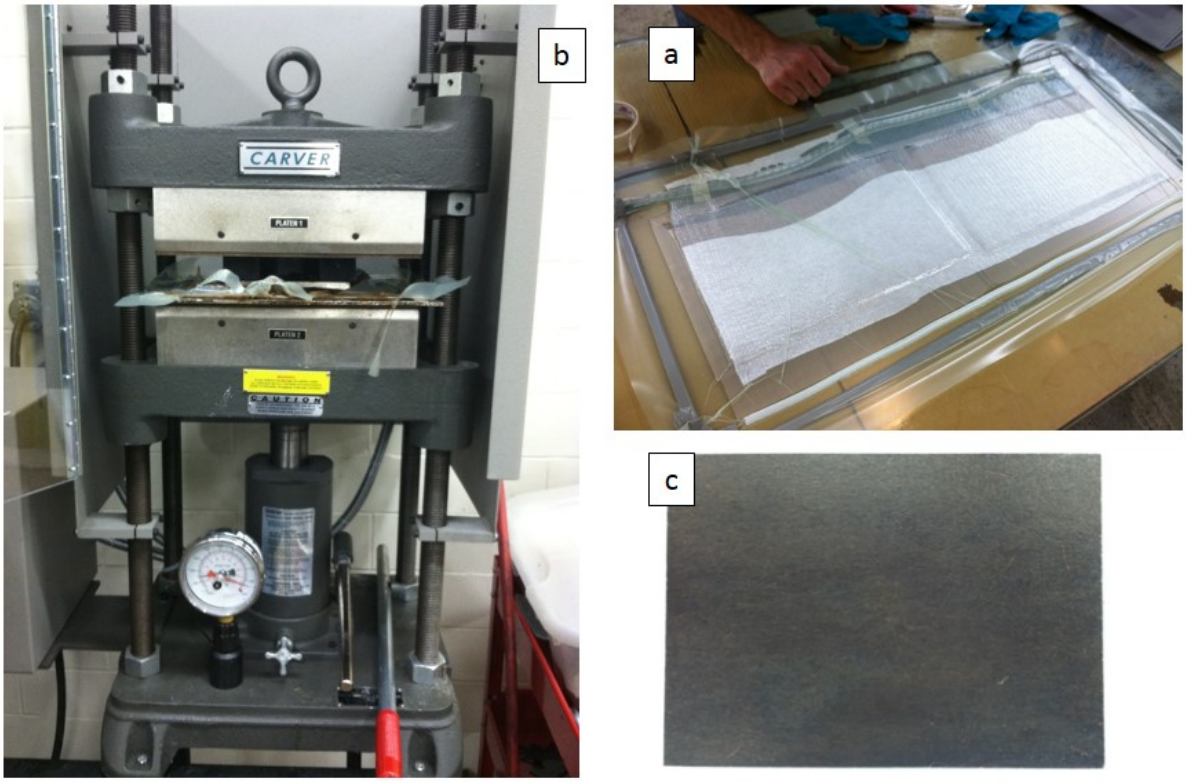

Figure 14. (a) VARTM process, (b) panels in the heated press, and (c) a manufactured composite panel

In general, the VARTM method would yield composites with higher quality and higher fiber volume fraction. However, due to higher viscosity of MESS and DMESS resins and high temperature curing conditions, hand layup compression molding method was found to result in less manufacturing complications when using mentioned resins and consequently resulted in more consistent composite panels.

2.4. Characterization Methods

2.4.1. Characterization of MESS and DMESS

Fourier transform infrared spectroscopy (FTIR) was performed on the resins with a Thermo Scientific Nicolet 8700 with a detector type of DTGS KBr under nitrogen purge. Diluted thin films of the samples were applied on a KBr plate and the absorption spectra were taken with 32 scans at a resolution of 4 cm^{-1}. Molecular weight of the resin was obtained using a gel permeation chromatography (GPC) system (EcoSEC HLC-8320GPC, Tosoh Bioscience, Japan) with a differential refractometer (DRI) detector. Separations were performed using two TSKgel SuperH3000 6.00 mm ID× 15 cm columns with an eluent flow rate of 0.35 ml min^{-1}. The columns and detectors were thermostated at 40°C. The eluent used is tetrahydrofuran (THF). Resin samples were prepared at nominally 1 mg ml^{-1} in an aliquot of the eluent and allowed to dissolve at ambient temperature for several hours and the injection volume was 20µL for each sample. Calibration test of the resin was conducted using polystyrene standards (Agilent EasiVial PS-H 4ml). Proton nuclear magnetic resonance spectroscopy (^{1}H-NMR) was conducted with a Bruker system, Ascend 400 MHz magnet with an Avance III HD console (Bruker BioSpin Corporation, Billerica, Massachusetts, USA), using $CDCl_3$ as the solvent. Acid number titration was carried out according to ASTM D664. The viscosity of the resins was measured at 25°C using an ARES Rheometer (TA Instruments) operating from 0.1 rad/s to 500 rad/s with 0.1% strain.

Results of resin characterization are presented in Appendix B and C for MESS and DMESS, respectively. Detailed analysis of the MESS resin can be found in the published work of Yan and Webster [200]. Detailed analysis of the DMESS resin is currently under review for future publications. Table 5 presents summary of all resins used throughout this study along with the initiator/hardener and curing conditions for the resins.

2.4.2. Tensile Test

At least five tensile test specimens were prepared based on ASTM standard D3039. An Instron 5567 load frame was used for the mechanical processes treatment study. Speed of cross-head was set to 2 mm/min. Ultimate tensile strength and modulus of elasticity was calculated from results of these tensile tests in accordance with ASTM standard D3039 [12]. Strain was measured with MTS extensometer model 632.25B-20 until stress reached 70 MPa, at which the extensometer was removed.

2.4.3. Short Beam Shear Test

Interlaminar properties were evaluated by means of short beam shear test in accordance with ASTM D 2344 using an Instron 5567 load frame. Five samples were tested for each plate in displacement controlled mode with the rate of displacement of cross-head set to 1 mm/min.

2.4.4. Flexural Test

Three-point bending tests were performed on five samples from each plate in accordance with ASTM standard D790 [11]. The support span was set to 50 mm and cross-head displacement rate was 3 mm/min. Maximum flexural stress and flexural modulus calculated according to ASTM standard D790.

2.4.5. Dynamic Mechanical Analyzer (DMA)

2.4.5.1. Creep Testing

Generally, simple equipment is used to measure creep in elastomeric materials. However, in order to precisely record small deformations in rigid composite materials, a more advanced machine is required. In this study Dynamic Mechanical Analyzer Q800 by TA Instruments was used based on ASTM D2990 in flexural bending mode with constant stress of 14 MPa to perform isothermal creep tests. Each sample was subjected to creep for 10 minutes and recovery for 10 min at each temperature step. Starting test temperature was 30 º C and ending temperature was 110 º C with temperature steps of 10 ºC.

Both short-term and long-term creep tests were also performed with the same equipment using a dual cantilever fixture. For short-term creep tests DMA was used in the creep TTS mode at the same temperatures as frequency sweep tests. For frequency sweeps specimens were soaked for 8 minutes at each temperature and then under constant stress of 4.5 MPa for 12 minutes. Long-term creep test was also performed using a dual cantilever fixture and in the DMA creep mode. One creep test was performed at 30 °C with the constant stress of 4.5 MPa for the 24 hours and strain data was collected.

2.4.5.2. Frequency Sweeps

Frequency sweeps were performed using a Dynamic Mechanical Analyzer Q800 by TA Instruments, New Castle, DE, based on ASTM D5418. A dual cantilever fixture was used to perform tests in temperature step/strain mode with the strain amplitude of 0.1%. The frequency range was 0.1-10 Hz in log mode with five measurements in each decade. Storage modulus, loss modulus and tan δ values were recorded at temperatures 30, 40, 50, 60 and 70 °C.

2.4.5.3. Glass transition temperature (T_g)

Glass transition temperature of fiber reinforced composite specimens was measured using a dual cantilever fixture. A 1 Hz scanning frequency with the temperature ramp of 3 °C/min was used to measure the T_g of flax/vinyl ester as well as flax/MESS composite based on ASTM5023. The T_g of cured resin and composite sample was the peak of tanδ curve obtained from the results of the tanδ DMA test.Figure 15 shows a selection of the equipment used for materials characterization in this study.

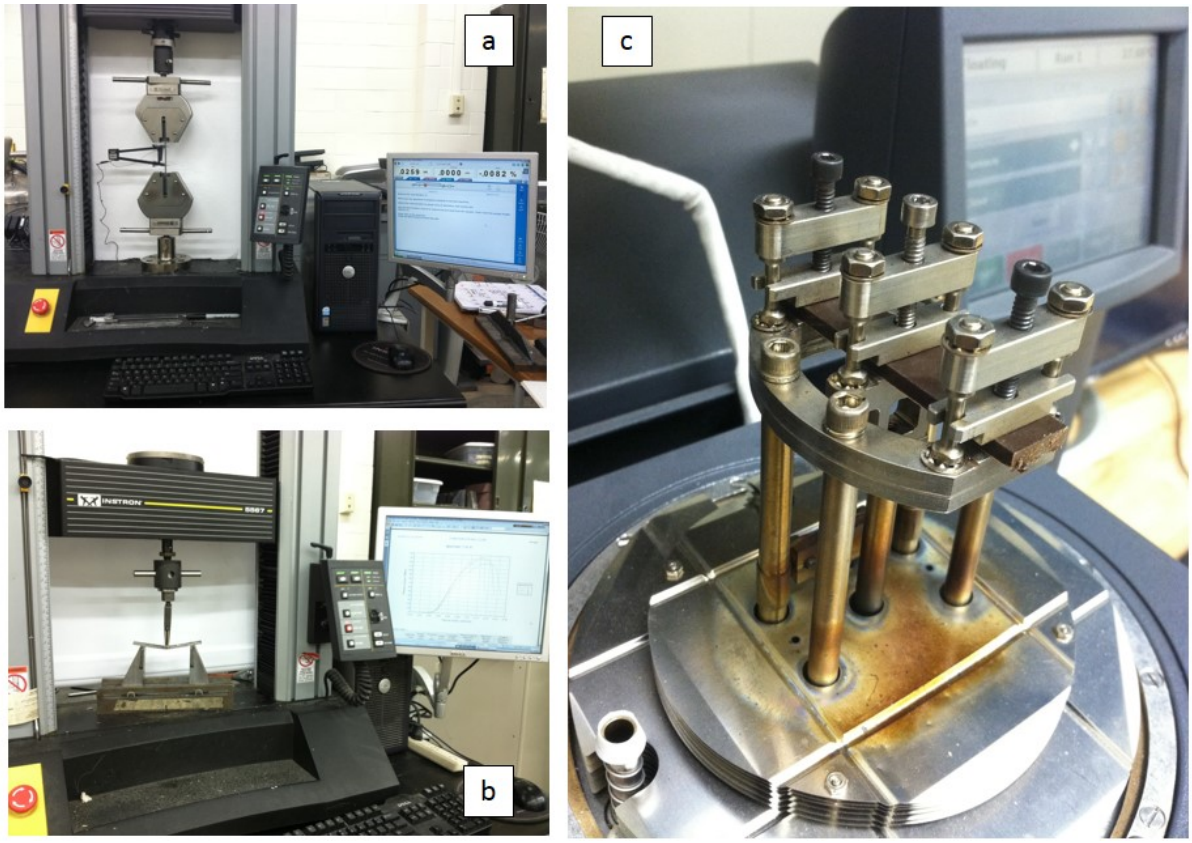

Figure 15. Instron 5567 load frame in (a) tensile test, (b) flexural test, and (c) DMA Q800 with dual cantilever fixture

2.4.6. Thermogravimetric Analysis (TGA)

In order to measure the degradation temperature of flax fiber as well as flax/VE composite, Thermogravimetric Analysis (TGA) was conducted using a TA instrument TGA Q500 with inert

atmosphere based on ASTM E1641. Specimens were heated from room temperature to 450 ºC with temperature ramp of 10 ºC/min.

2.4.7. Differential Scanning Calorimetry (DSC)

Differential Scanning Calorimetry (DSC) was conducted on composite samples to evaluate degree of cure of vinyl ester resin and make sure that no residual cross-linking is present in the material. DSC Q1000 by TA instrument was used to run the analysis based on ASTME2160. Approximately 20 mg samples of material were sealed in aluminum hermetic pans and samples were analyzed under dry nitrogen purge. Samples were heated with the rate of 5 ºC/min from 25 ºC to 200 ºC, and cooled down with the same rate to 25 ºC.

2.4.8. Constituent Analysis

Constituent analysis was conducted at the Animal Science Department of NDSU using an ANKOM 200 Fiber Analyzer (ANKOM Technology, Macedon, NY) following AOAC official method 2001.11. The parameters analyzed included crude protein, neutral detergent fibers, acid detergent fibers, acid detergent lignin, fat, starch, and dry matter content.

2.4.9. Scanning Electron Microscopy (SEM)

Scanning Electron Microscopy (SEM) images of treated and untreated flax fibers, cross sections of flax fibers as well as fractured surface of tensile specimens for each test were captured using a JEOL JSM-6490LV scanning electron microscope at an accelerating voltage of 15 kV.

2.4.10. Cross-Section Imaging of Fibers

Fibers were placed between two pieces of copper tape and cut with a razorblade to expose the edge to be polished. The sample was then mounted to a brass or molybdenum block using 3M XYZ-Axis Electrically Conductive Tape (Ted Pella, Redding CA). Surfaces were exposed using a JEOL IB-09010CP Cross Sectional Polisher (JEOL USA, Peabody MA). Argon milling

conditions were 5kV accelerating voltage for 2 hours or less. The edge of the sample was placed perpendicular to the center of the beam and pivoted +/- 5° during polishing cycle.

2.4.11. Micro Computed Tomography Imaging (Micro-CT)

In order to visually and internally evaluate fiber matrix interaction and quality of manufactured plates, 3D micro-CT scans were acquired using a General Electric 240 kV micro-focus X-ray computed tomography system (v|tome|x micro-CT). This machine is shown in Figure 16.

In order to acquire 3D scans of the composite samples, small specimens were cut out of manufactured samples using a diamond blade saw. The specimens were attached to a glass rod using hot glue and placed into a GE Phoenix v|tome| x s X-ray computed tomography system (MicroCT) (Wunstorf, Germany) equipped with a 180 kV high power nano-focus X-ray tube xs|180nf and a high contrast GE DXR250RT flat panel detector. Nine hundred projections of each sample were acquired at a voltage of 100 kV and a current of 150 mA using a molybdenum target. Detector timing was 1000 ms and the total acquisition time was 1 hour and 6 minutes. Sample magnification varied per sample and approximately 20x producing a voxel size range of around10-12 microns. The acquired images were reconstructed into a volume data set using GE datos|x 3D computer tomography software version 2.2 (Wunstorf, Germany). The reconstructed volume was then viewed and processed using VGStudio Max by Volume Graphics (Charlotte, NC).

2.4.12. Accelerated Weathering

A second set of panels was produced with the intent of weathering them prior to conducting mechanical tests. The samples were placed into a QUV accelerated weathering chamber (Model QUV/S, Q-Lab, Westlake, OH) and one side of them was exposed to alternating cycles of

ultraviolet (UV) radiation and water condensation. 8 hours of UV exposure at 60 ºC and 4 hours of water condensation at 50 ºC were used as suggested by ASTM G154. The chamber produced an irradiance of 1.55 W/m^2.nm using UVA-340 fluorescent lamps. Following 500 hours of treatment, the samples were flipped and the other side was exposed to accelerated weathering in an identical manner. Figure 17 shows accelerated weathering chamber as well as composite panels placed inside the chamber. The same mechanical tests as described previously were performed on five specimens from each composite plate.

Figure 16. GE Phoenix X-ray tomography system located at NDSU Electron Microscopy Center

2.4.12.1. Specular Gloss Testing

A micro-TRI-gloss meter (BYK, Columbia, MD) was used to measure the gloss of the weathered samples at angles of 20°, 60°, and 85° based on ASTM D523 and ASTM D2457. These measurements were made at 0, 250, 500, 750, and 1000 hours.

2.4.12.2. CIELab Color Space Test

In addition, the CIELab color space values of the weathered composites were measured using a Macbeth Color-Eye 7000 (X-Rite Inc., Grand Rapids, MI) operating in reflectance mode

based on ASTM D7856 and ASTM DG155. This data was used to calculate the color changes each panel underwent as a result of weathering.

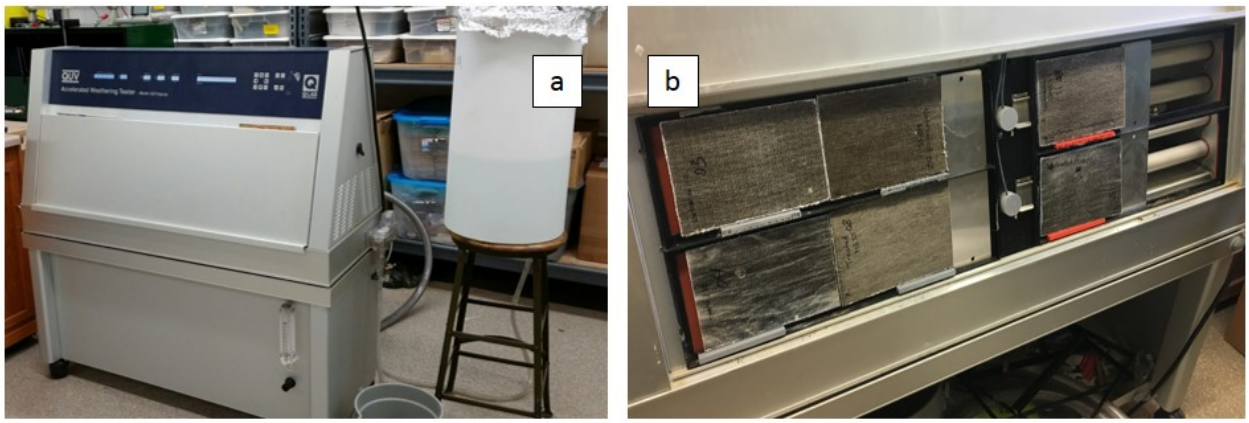

Figure 17. (a) QUV accelerated weathering chamber with water tank supply, and (b) composite panels inside the chamber (UV lights off)

2.4.13. Density Measurement

2.4.13.1. Buoyancy Method

In order to make sure that all specimens used in this study had the same moisture content, prior to all tests, all specimens were dried in a fan-assisted convection oven (from VWR Co., Randorm, PA, USA) at 80 °C for at least 16 hours. The first step was to determine the density of the submersion fluid using a known standard density block. This step was done at the beginning of each new batch of specimens, or when a new batch of immersion fluid was to be used, or there was temperature change greater than ±1ºC. A clean and dry fluid container was filled to 3/4 to 7/8 full with liquid and was allowed to come to temperature equilibrium. The balance was tarred, and the weight of the standard block in air was recorded as $S_{air.}$ Then the standard block was placed on the weighing basket and the submerged weight was recorded as $S_{submerged}$. With the known density of the standard block, ρ_S, the test fluid density, ρ_{fluid} was determined using the following equation:

$$\rho_{fluid} = \frac{S_{air} - S_{submerged}}{S_{air}} \times \rho_S \quad (14)$$

To perform the density measurement using the Archimedes method the flax fiber specimen was wrapped and ends were intertwined. The balance was tarred and the specimen was placed on the weighing pan and weight of the specimen in air was recorded as M_{air}. The specimen was placed onto the weighing basket, the fibers were submerged, and the weight was recorded as $M_{submerged}$. The density of flax fiber is calculated using the following equation:

$$\rho_{flax} = \frac{M_{air}}{M_{air} - M_{submerged}} \times \rho_{fluid} \quad (15)$$

After recording the specimen weight in air, the specimen was submerged in the immersion fluid, the suspension wire was removed and the beaker was placed in the vacuum oven. After the specified amount of time had elapsed, the container was removed from the vacuum oven and placed on the bridge over the weighing pan of the balance. Then suspension wire and weighing basket were put back in place, the balance was tarred again and a utensil was used to transfer the specimen from the bottom of the beaker to the weighing basket without any parts of the specimen being exposed to air. The submerged weight was then recorded. Components of Mettler Toledo density measurement kit are presented in Figure 18.

2.4.13.2. Gas Pycnometry

A Quantachrome auto-pycnometer Ultrapyc 1200e (by Quantachrome Instruments, Boynton Beach, FL, USA) was used to measure the density of flax fibers used in this study to be used as reference based on ASTM D5550, ASTM D70 and ASTM B923. The test was performed using a purge of dry nitrogen for 2.0 minutes. There were 10 runs for each specimen and there were five specimens for each fiber type.

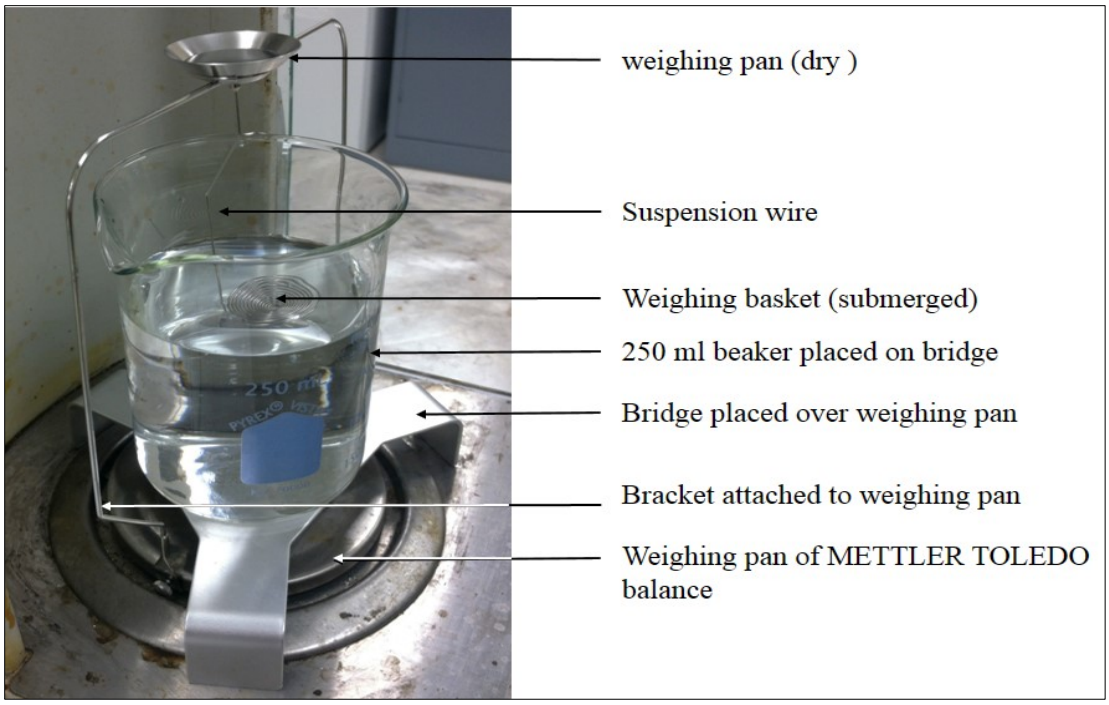

Figure 18. Components of Mettler Toledo density measurement kit

2.4.14. Void Fraction Measurement

2.4.14.1. Conventional Method

For design purposes, also to compare properties of two laminates one should know the fiber volume fraction of the composite. Mechanical properties of composite materials are highly sensitive to fiber volume fraction [60, 106, 181]. Fiber volume fraction is defined as [201]:

$$V_f = Fiber\ volume\ fraction = \frac{volume\ of\ fiber}{volume\ of\ composite} \tag{16}$$

consequently, the void content of composite can be found [201]:

$$V_v = Void\ volume\ fraction = 1 - V_f - V_m = \frac{volume\ of\ voids}{volume\ of\ composite} \tag{17}$$

where V_m is the matrix volume ratio.The void fraction of composite can be found by comparing experimental fiber volume fraction and theoretical fiber volume fraction. The theoretical fiber volume fraction is calculated by [181]:

$$V_f = \frac{\rho_f - \rho_m}{\rho_c - \rho_m} \tag{18}$$

where, ρ_f , ρ_c and ρ_m are the density of fiber, composite and matrix, respectively. The experimental fiber volume fraction is calculated by [181]:

$$V_f = \frac{w_f}{w_c}\frac{\rho_c}{\rho_f} \tag{19}$$

where w_f and w_c are the weights of fiber and composite, respectively.

2.4.14.2. 3D Images Processing

A MATLAB® code was developed to read, analyze, and calculate the void volume in each sample. The developed code is presented in Appendix D. The flowchart of how the MATLAB code operates is presented in Figure 19.

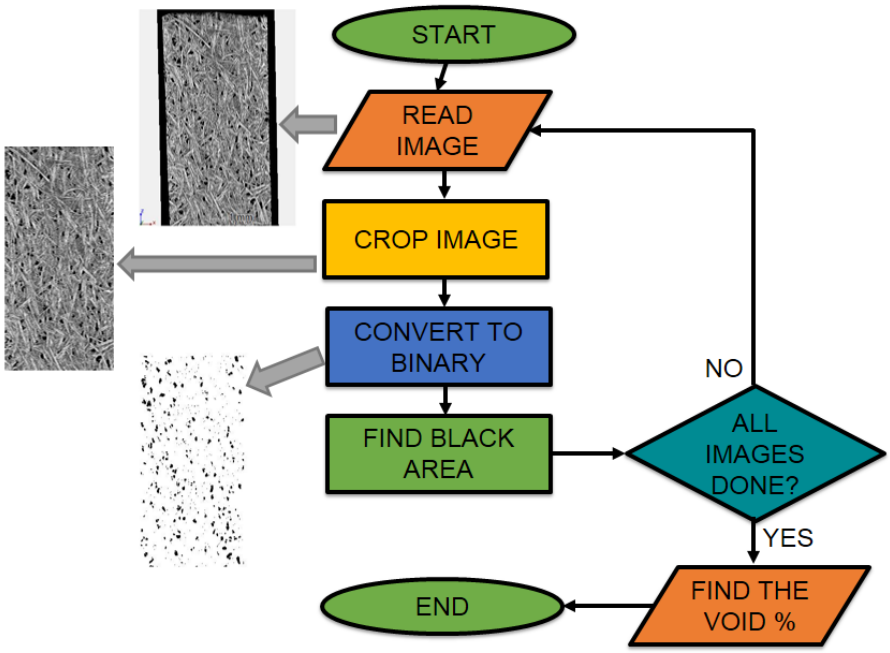

Figure 19. Flowchart of MATLAB code to calculate void fraction using 3D images of composite specimens

A summary of characterization methods, equipment, conditions and standard test methods used in this study are presented in Table 8.

Table 8. Summary of characterization methods, equipment and standards used in this study

Tests	instrument	conditions	Standard
Tensile	Instron 5567	With MTS extensometer 632.25B-20	ASTM D3039
Flexural	Instron 5567	Cross-head speed 3 mm/min	ASTM D790
Interlaminar shear	Instron 5567	Cross-head speed 1 mm/min	ASTM D2344
Creep – TTS	DMA Q800, TA instruments	Flexural bending, constant stress. 30 °C-110 °C with 10 °C steps Creep for 10 minutes, recovery 10 minutes	ASTM D2990
Creep – 24 hours	DMA Q800, TA instruments	Dual cantilever At 30 °C constant temp. Constant stress of 4.5 MPa	ASTM D2990
Frequency sweep	DMA Q800, TA instruments	Dual cantilever Strain amplitude 0.1% 0.1-10 Hz in log mode 30 °C – 70 °C (10°C steps)	ASTM D5418
Glass transition T_g	DMA Q800, TA instruments	Dual cantilever 1 Hz scanning 15 µN preload 25 °C – 200 °C (3°C/min ramp)	ASTM D5023
TGA	TGA Q500, TA Instruments	25 °C to 450 °C (10 °C/min ramp)	ASTM E1641
DSC	DSC Q1000, TA Instruments	20 mg in aluminum hemeric pans Heating: 25 °C -200 °C (5 °C/min) Cooled to 25 °C (5 °C/min)	ASTM E2160
Accelerated weathering	QUV/S, Q-Lab	UVA -340 fluorescent 8 hrs UV at 60 °C 4 hrs condensation at 50 °C	ASTM G154
Density - buoyancy	Mettler Toledo 33360	Submerged in Soybean oil Under 80 kPa vacuum	ASTM E1169
Density – Gas pycnometry	Quantachrome auto-pycnometer Ultrapyc 1200e	Dry nitrogen purge for 2 minutes 10 runs	ASTM B923 ASTM D70 ASTM D5550
SEM	JEOL JSM-6490LV	15 kV Voltage	
Fiber cross section imaging	JEOL IB-09010CP JEOL JSM-6490LV	Argon milling with 5 kV for 2hrs	
Micro - CT	GE Phenix (v|tome|x micro-CT)	180 kV nano-focus X-ray Molybdenum target	
Specular gloss	Micro-TRI gloss meter, BYK	20 °, 60°, 85° angles 0, 250, 500, 750, 1000 hours	ASTM D523 ASTM D2457
CIE Lab color Space	Macbeth Color-eye 700, X-Rite	Reflectance mode	ASTM D7856 ASTM G155
Constituent analysis	ANKOM A200 Fiber analyzer	Min. 5 g of fiber were tested	AOAC 2001.11

2.5. Flax Fiber Density Measurement Method Development Procedure

In order to develop the density measurement method, there were several factors that needed to be determined, such as, type of immersion fluid, use of vacuum chamber, vacuum pressure, duration of exposure to vacuum and minimum specimen size. During this study all of these factors were taken into account and effect of each of them on density measurements of flax fiber was studied. Table 9 presents all different variables and their different values (types) that were investigated in this study.

Table 9. Parameters and their values and types that are investigated in development of density measurement of flax

Variable	Values/types
Specimen size	0.1, 0.25 and 0.5 grams
Immersion fluid	Distilled water, canola oil (grocery store and lab grade), soybean oil (grocery store and lab grade), mineral oil
Vacuum pressure	50 kPa, 90~100 kPa
Vacuum time	3, 6 and 10 minutes

First, distilled water and canola oil were used as immersion fluids without use of vacuum chamber. Then, a vacuum chamber was used with two different pressures and use of canola oil as immersion fluid. ASTM E1169-14 was followed to perform a ruggedness test to determine which factors were significant in influencing the density results. With the parameters determined after ruggedness test method, 5 different immersion fluids were used to perform density measurements of flax fibers with established parameters from ruggedness tests. In each stage results were compared to density of same type of flax fiber measured by gas pychnometery method as a reference. Lab certified soybean oil was chosen as immersion fluid based on the results achieved in the last set of tests and density of four different types of flax fibers were measured.

As mentioned before, a Mettler Toledo 33360 density determination kit was used to perform density measurements. In the experiments where use of vacuum oven was considered, a Lab-Line Squaroid vacuum oven was used to pull vacuum on submerged specimens.

2.5.1. Use of Distilled Water as Submersion Fluid

The first set of data was acquired using five specimens tested in distilled water in ambient pressure and allowed to sit under the water for various amounts of time (1, 3 and 6 minutes). The density determination kit was set up using distilled water and the water's temperature was measured. Each flax specimen was between 0.1 g to 0.3 g. The specimens were rolled between gloved hands in order to compact them enough to stay completely submersed in the test kit but not so much as to trap large air bubbles inside. Specimens were first weighed in air and then submerged in distilled water following the same details as explained in procedure section. Upon submerging the specimens, an initial mass was recorded. The samples were allowed to sit in the basket for 1, 3 and 6 minutes and their masses at these times were recorded. The densities were calculated using these two masses (dry and submerged) and the density of the distilled water at 23 °C.

2.5.2. Use of Canola Oil as Submersion Fluid

The same procedure was set up with canola oil. The only difference from the distilled water was that the oil's temperature was not measured but instead its density was measured using a known standard density block.

Specimens were tested both with and without using a vacuum oven. After weighing the specimens in air, they were submerged in canola oil and placed into a vacuum oven, the pump was started and till the vacuum pressure reached 70 kPa. Specimens were held under vacuum for 6 to 7 minutes at this vacuum pressure. After removing the container from the vacuum oven there were still mini air bubbles in suspension in the oil, which indicates that there was still air trapped in

specimens as well. Therefore, second sets of tests were completed at higher pressure of 100 kPa. After removal of the container from the vacuum oven, almost no bubbles were present in the oil and those that were present could be brought to the surface and removed or burst in order to not interfere with the measurements.

2.5.3. Ruggedness Test for Flax Fiber Density Measurements

ASTM E1169-14 limits the factors to have two levels only. Therefore the type of design used for this study is known to be a Plackett-Burman design [202]. The levels are selected in a way so that the measured effect is reasonably large compared to measurement error.

To perform ruggedness test for density measurement of flax fiber, four factors were selected with two levels for each factor. Table 10 summarizes these selected factors. Recommended design for four factors with two levels from ASTM E1169-14 is shown in Table 11 [202, 203].

The design in Table 11 provides equal numbers of low and high level runs for every factor. In other words, the designs are balanced. Also, for any factor, while it is at its high level, all other factors will be run at equal numbers of high and low levels; similarly, while it is at its low level, all other factors will be run at equal numbers of high and low levels. In the terminology used by statisticians, the design is orthogonal. The tests should be carried out in a random sequence (not the PB orders mentioned) in order to reduce the probability of encountering any potential effects of unknown, time-related factors.

Table 10. Flax fiber density measurement ruggedness test factors, levels and description

Factor Symbol	Variable	Units	Level 1 (-)	Level 2 (+)
A	Vacuum Pressure	kPa	50	90
B	Vacuum Time	minutes	6	10
C	Weight of specimen	grams	0.2±.04	0.5±.04
E	Fluid	-	canola oil	mineral oil

Table 11. Recommended design for four factors with two levels [202, 203]

PB Order	Run #	A	B	C	E	Test Result
1	2	1	1	1	1	
2	4	-1	1	1	-1	
3	6	-1	-1	1	1	
4	8	1	-1	-1	1	
5	5	-1	1	-1	1	
6	3	1	-1	1	-1	
7	1	1	1	-1	-1	
8	7	-1	-1	-1	-1	
Ave +						
Ave -						
Effect						

In this table Ave + is the average of replicate averages corresponding to (1) and Ave – is the average of replicate averages corresponding to (-1). The main effect row is the difference of Ave + and Ave – for each column. Estimate of the standard error of an effect is calculated from [203]:

$$S_{effect} = \sqrt{\frac{4S_{rep}^2}{N \times reps}} \tag{20}$$

with degree of freedom of $(N-1) \times (reps-1)$, and where N is the number of runs in the design, $reps$ is the number of replicates of the design, and S_{rep} is the estimated standard deviation of the test results.

2.5.4. Density Measurements with Different Fluids Using Vacuum Oven

After studying the results of ruggedness tests, five different fluids were selected and minimum of ten specimens were tested for each fluid with the parameters determined by ruggedness test. Parameters for this test are presented in Table 12. To measure the density of flax fiber, same procedure was followed as explained in the procedure section.

Table 12. Parameters used to establish test fluid for density measurement of flax fiber

Parameters	Values/ types
Specimen's mass	0.5 ± 0.1
Immersion oil	Grocery store canola oil, lab grade canola oil, grocery store soybean oil, lab grade soybean oil, mineral oil
Vacuum pressure	90 kPa
Vacuum time	10 min

3. RESULTS AND DISCUSSION

The abbreviations used for addressing the different composites and types of specimens used in this study are presented in Table 13.

Table 13. Abbreviations used to describe the composites and specimens used in this study

Abbreviation	Description
VE	Vinyl ester resin
8601	Epoxy resin
MESS	Methacrylated epoxidized sucrose soyate
DMESS	Double methacrylated epoxidized sucrose soyate
AR	Acrylic resin
VE+AR	Vinyl ester containing 1% acrylic resin
Unt./VE	Vinyl ester resin reinforced with untreated flax fiber
Unt./VE+AR	Vinyl ester resin containing 1% acrylic resin reinforced with untreated flax fiber
Alkaline/VE	Vinyl ester resin reinforced with alkaline treated flax fiber
Alkaline/VE+AR	Vinyl ester resin containing 1% acrylic resin reinforced with alkaline treated flax fiber
UTW-MESS	Untreated, weathered flax fiber / MESS resin
TW-MESS	Alkaline treated, weathered flax fiber / MESS resin
UTUW-DMEE	Untreated, unweathered flax fiber / DMESS resin
TUW-DMESS	Alkaline treated, unweathered flax fiber / DMESS resin
UTW-DMESS	Untreated, weathered flax fiber / DMESS resin
TW-DMESS	Alkaline treated, weathered flax fiber / DMESS resin

3.1. Lipase Treatment of Flax Fiber

Lipase treated fibers were stained and imaged under microscope and the results are shown in Figure 20. Results revealed that fibers treated with lipase with 15.2% concentration and 24 hours set-time had the cleanest surface.

Epoxy resin 8601 was reinforced with treated and untreated flax fiber and two composite panels were manufactured to further assess the effect of treatment on mechanical properties of resulting composites. Results of mechanical tests are presented in Table 14. As seen in Table 14,

lipase treatment has improved flexural strength of the fibers, however, this gain was not statistically significant. Also, it has minimal or no effect on flexural modulus and short beam strength. On the other hand, it has decreased the tensile properties of the fiber significantly. Therefore, although this method was helpful in cleaning up the surface of the fiber, it was decided not to pursue this method further.

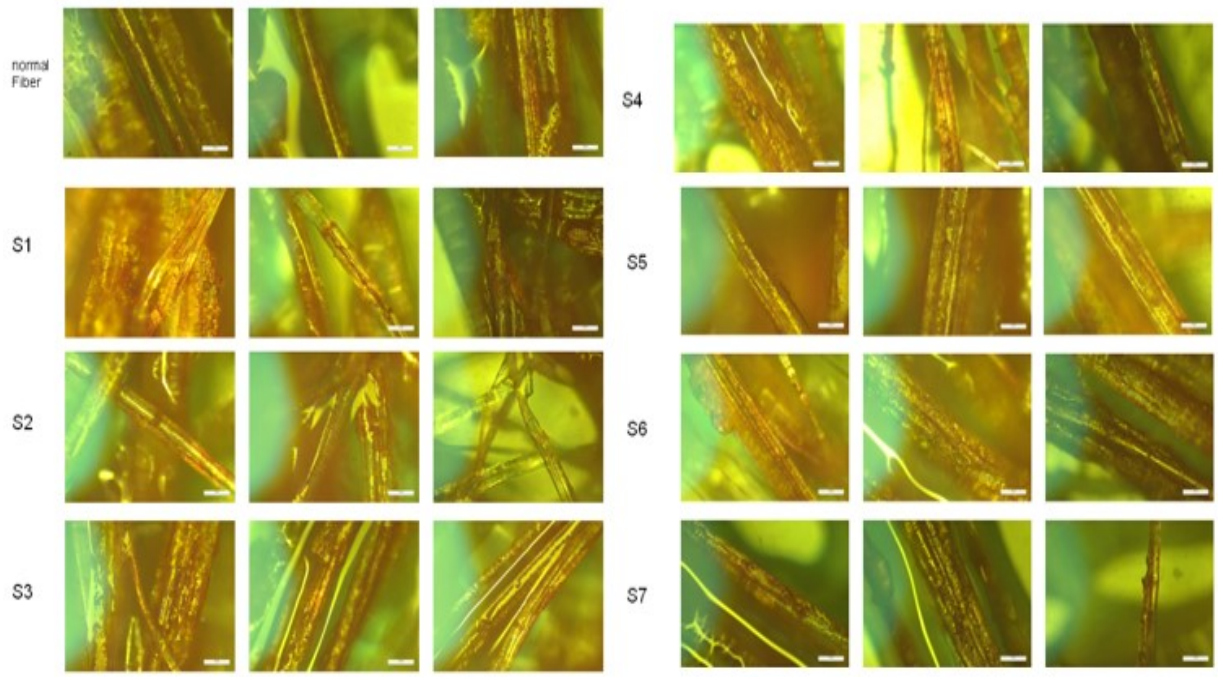

Figure 20. Microscope images of enzyme treated flax fibers

Table 14. Mechanical properties of treated and untreated flax/8601 composites

	Untreated flax/8601		Lipase treated flax/8601	
	Mean value	Std. dev.	Mean value	Std. dev.
Flexural strength (MPa)	123	8.90	130	7.90
Flexural modulus (GPa)	8.2	0.71	7.8	0.28
Interlaminar shear strength (MPa)	16.32	0.80	16	0.50
Tensile strength (MPa)	140.52	15.98	96.26	12.43
Tensile modulus (GPa)	12.67	1.54	11.47	0.41

3.2. Effect of Different Mechanical Treatments

3.2.1. SEM Images

Figure 21 shows SEM images of untreated and mechanically treated fibers. It is observed that mechanical processes were successful to some extent in removal of waxes and pectin from surface of the fibers. As seen, Type 2 and Type 4 fibers show cleaner surfaces compared to Type 1 (untreated). On the other hand, in Type 3, both clean fibers are seen as well as fibers covered in waxes and impurities. One interesting observation seen in SEM images of Type 4 fiber is twisting and entanglement of single fibers and formation of micro-bundles of fibers. The mechanical process used on this type of fiber was use of a pair of fluted rollers. Use of fluted rollers also resulted in less shive content compared to other types of fibers.

3.2.2. Mechanical Properties

To evaluate the effect of different mechanical processes of flax fibers on properties and performance of their ensuing composites, mechanical properties of flax/VE and flax/MESS composites were studied. VE and MESS resins were reinforced with Type 1, 2, 3 and 4 flax fibers.

Mechanical tests, i.e. tensile, flexural and ILSS were carried out using an Instron 5567 load frame. Prior to testing, density tests were completed on three specimens from each sample and fiber volume fraction of samples were calculated. Results are presented in Table 15.

To minimize the effect of variations in fiber volume fraction in different composite plates on mechanical properties, all calculated mechanical properties were normalized to 35% fiber volume fraction. Normalized averages of measured values are presented in Table 16. Radar plots of mechanical properties are presented in Figure 22 and Figure 23 for flax/VE and flax/MESS respectively. Because of the differences in the orders of magnitude of different properties, values have been scaled up or down to show a side by side comparison.

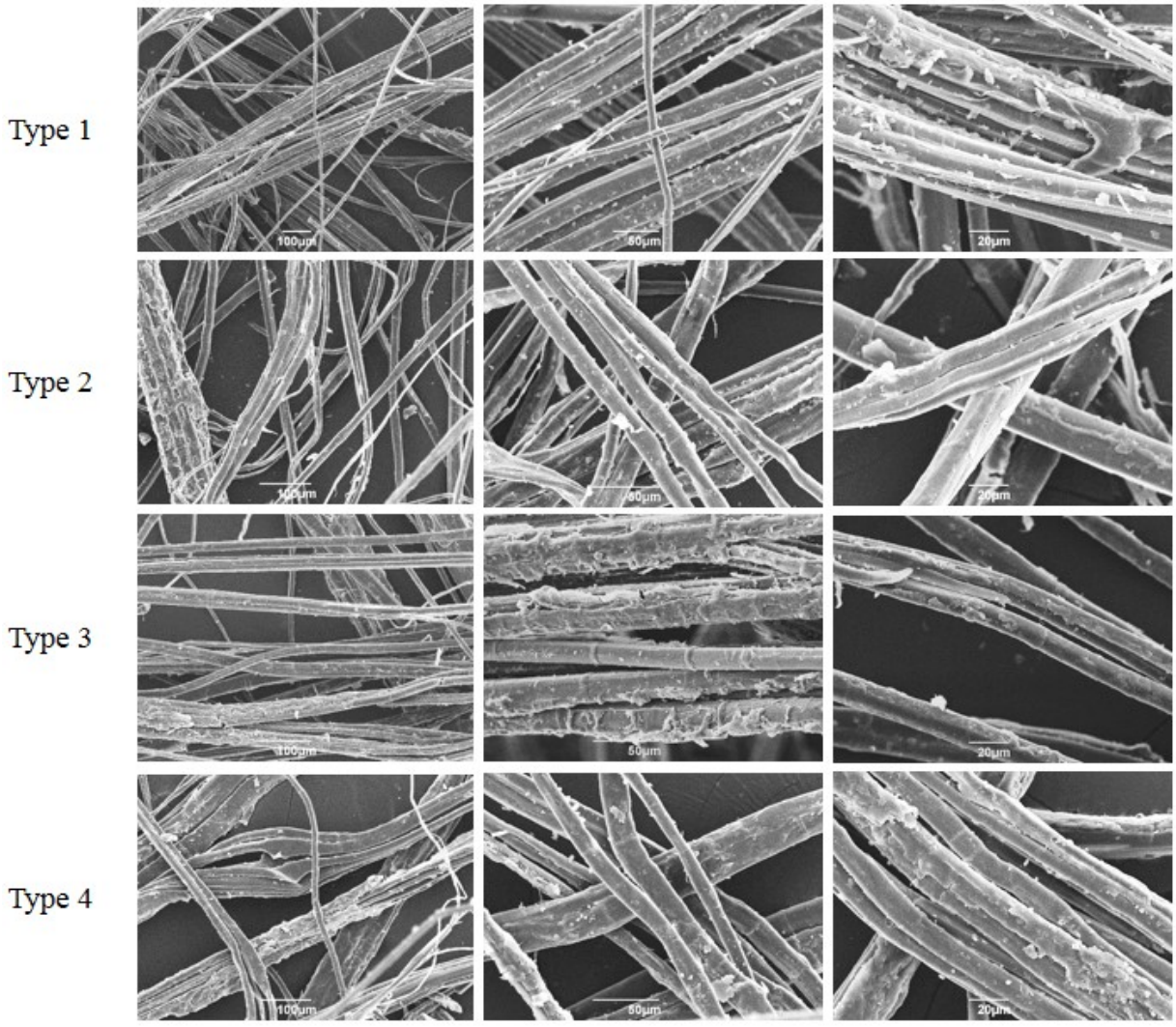

Figure 21. SEM images of flax fiber using four different mechanical processes

Table 15. Density of fibers, resins, composite panels and fiber volume fraction of manufactured panels

Flax Fiber	ρ_{fiber} (g/cm^3)	Resin	ρ_{resin} (g/cm^3)	$\rho_{composite}$ (g/cm^3)	V_f (%)
Type 1	1.52 ± 0.001	VE	1.09 ± 0.003	1.23 ± 0.006	35.50
		MESS	1.15 ± 0.002	1.10 ± 0.024	31.43
Type 2	1.54 ± 0.000	VE	1.09 ± 0.003	1.25 ± 0.032	39.12
		MESS	1.15 ± 0.002	1.11 ± 0.020	33.44
Type 3	1.55 ± 0.000	VE	1.09 ± 0.003	1.22 ± 0.020	37.84
		MESS	1.15 ± 0.002	1.10 ± 0.017	30.10
Type 4	1.54 ± 0.000	VE	1.09 ± 0.003	1.25 ± 0.051	36.60
		MESS	1.15 ± 0.002	1.13 ± 0.024	34.47

Comparing tensile and flexural modulus of Type 1 and 4 composite plates, they showed similar modulus. Type 4 fiber contained less than 5% shive, the cleanest fiber among these four types, and this is reflected in strength of resulting composites in ultimate tensile stress and maximum flexural stress. Observing the properties of Type 2 composites, the mechanical treatment (combing fiber in a rough manner with opener machine has resulted in inferior tensile and flexural strength and modulus compared to standard mechanical treatment (i.e. passing through pilot line). However, the short beam strength of the resulting composite plate has been improved more than 15%.

Table 16. Normalized* mechanical properties of flax/VE and flax/MESS composites

	Tensile Strength (MPa)	Tensile Modulus (GPa)	Flexural Strength (MPa)	Flexural Modulus (GPa)	Interlaminar Shear Strength (MPa)
Type1 – VE	108.08 ± 2.27	15.43 ± 0.45	124.77 ± 3.15	9.30 ± 0.08	12.39 ± 0.70
Type1 - MESS	27.82 ± 1.61	17.06 ± 1.67	41.83 ± 1.46	15.04 ± 0.44	7.97 ± 2.66
Type2 – VE	93.92 ± 3.26	12.87 ± 0.45	114.93 ± 5.54	8.85 ± 0.71	13.06 ± 0.74
Type2 - MESS	42.01 ± 4.69	14.30 ± 0.41	61.92 ± 6.83	14.71 ± 1.70	9.16 ± 1.34
Type3 – VE	81.40 ± 2.67	12.59 ± 0.87	103.61 ± 2.44	6.01 ± 0.34	10.06 ± 0.46
Type3 - MESS	26.30 ± 5.61	12.87 ± 1.26	35.43 ± 5.97	9.59 ± 0.55	4.28 ± 0.67
Type4 – VE	104.95 ± 3.85	14.03 ± 1.00	131.96 ± 3.37	8.51 ± 1.13	10.82 ± 0.69
Type4 - MESS	49.57 ± 5.78	16.41 ± 2.55	64.97 ± 2.63	12.85 ± 1.60	7.03 ± 0.68

* All values are normalized to fiber volume fraction of 35%

Based on the results seen in Table 16, resulting composite panel from fiber Type 3 which contains 50/50 blend of over retted fibers and optimally retted fibers, showed lower mechanical properties compared to other three composite panels. This difference is more noticeable in flexural modulus were the average measured value for flexural modulus is 6.01 GPa for flax/VE composite samples, the lowest of all measurements. The same trend is observed for flax Type 3/ MESS resin

where all the mechanical properties are lower than other three types of fibers. The fiber used to manufacture this composite panel was from straw that was over retted. This resulted in weaker, shorter and finer diameter fiber. Although it is blended 50/50 with optimally retted fiber, still the mechanical properties of resulting composite are inferior to that of others.

For tensile and flexural strength, fiber Type 4 showed comparable properties to untreated/VE composites and better strength compared to untreated/MESS composites and other types of fibers using MESS resin. This can be attributed to two factors, first, lower shive content of fiber, as shive has lower strength compared to flax fiber [204] and second, twisting of fibers and formations of micro-bundles as seen in SEM images. In composites using flax fiber reinforcement with VE resin, untreated fibers showed higher strength than Type 2 fibers while composites using MESS resin Type 2 fiber showed better strength. Moreover, it is observed that Type 2 fibers both with VE and MESS resins showed 5% improvement in shear strength compared to untreated fiber and 20% increase compared to Type 4 treatment.

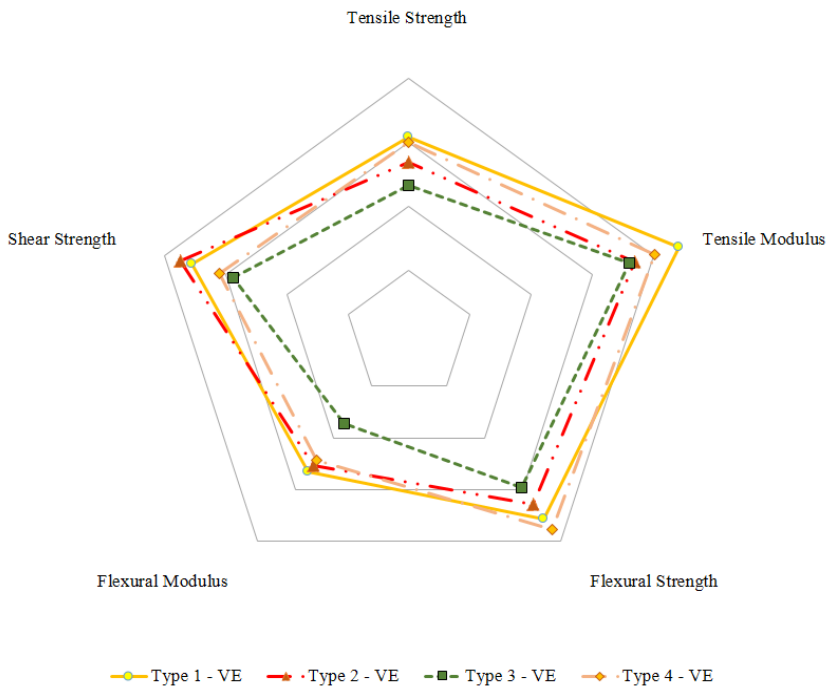

Figure 22. Mechanical Properties of flax/VE composites using four different types of flax fiber

Tensile and flexural moduli of composites were decreased with mechanical processes. In other word, for both VE and MESS resins, untreated fibers exhibited higher flexural and tensile modulus. Comparing the overall results of two types of resins, composites using MESS resin possess higher tensile and flexural modulus. On the other hand, they showed lower tensile, flexural and interlaminar shear strength. This can be the result of higher curing temperature used for MESS resin. As reported by Vold et al. [205], flax shive starts to degrade between 225 ºC and 250 ºC. Composite panels using MESS resin were cured at 200 ºC for two hours, and this can be the reason for lower strength of mentioned composites due to start of degradation of shive content of the fiber.

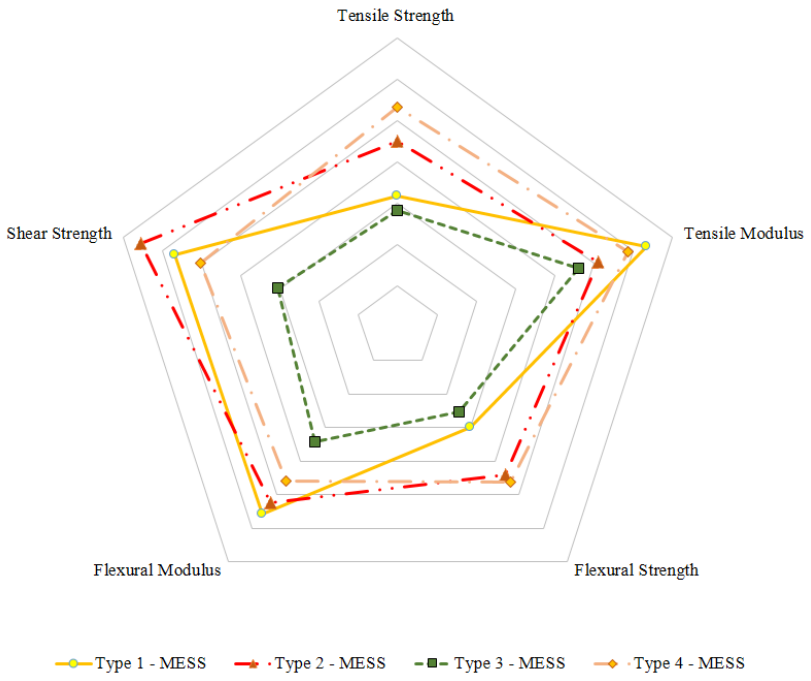

Figure 23. Mechanical Properties of flax/MESS composites using four different types of flax fiber

3.3. Chemical Treatment of Flax Fiber

To compare the effect of chemical treatments on mechanical performance of flax fiber reinforced composites, and based on preliminary studies and previous work of Huo et al. [106] alkali treatment was selected as the method of treatment to be used for this study.

Treated fibers were process as described in the processing the composite section and mechanical tests were carried out to compare the effect of these treatments on mechanical performance of ensuing composites.

The density of flax fiber was measured using immersion density technique and was determined to be 1.42 ± 0.02 g/cm^3. The density of flax/VE composites were observed to be between 1.19 g/cm^3 to 1.32 g/cm^3 and the fiber volume fraction of the flax fiber composites were found to vary between 35% And 39%. To make results of mechanical properties comparable, all results were normalized to 35% fiber volume fraction.

3.3.1.1. Effect of Chemical Treatments on Fiber Morphology

To see the effect of mentioned treatments of the surface of flax fiber and see the changes in the surface morphology, the treated fiber was studied using Scanning Electron Microscopy (SEM). SEM images of treated and untreated fiber are presented in Figure 24 for linseed flax fiber (Type 1) and in Figure 25 for composite specimens after tensile test. By comparing untreated and NaOH treated fiber, it is observed that alkali treatment has been very effective in removing wax, dye, ashes, oils and pectin from external surface of the fiber as expected [106, 206]. Also, addition of NaOH to flax fiber promotes the ionization of the hydroxyl group to the alkoxide, in other words it disrupts the hydrogen bonding in the network structure and increases the surface roughness. This also can be seen in the Figure 24 (b). Alkali treatment can hydrolyze pectin and degrade lignin [58, 184, 206]. Acid treatment also has been very effective regarding removing any external wax and oils. Based on SEM images, alkali treatment has resulted in a much cleaner surface, and from the SEM images with higher magnification, it is observed that surface roughness is also increased. This is consistent with observations of Valadez-Gonzalez et al. [57]. Increasing surface roughness

will result in better interfacial bonding of fiber and matrix and will result in improved mechanical properties.

For the flax fiber fabric (Type 6), the alkaline treatment was successful in removing impurities and excess undesired residue from surface of the fibers. As mentioned before, chemical constituent analysis revealed that alkaline treatment was successful in reducing amount of ash, proteins and other impurities from the surface of the fiber and alkaline treatment resulted in 10% cellulose content of flax fiber.

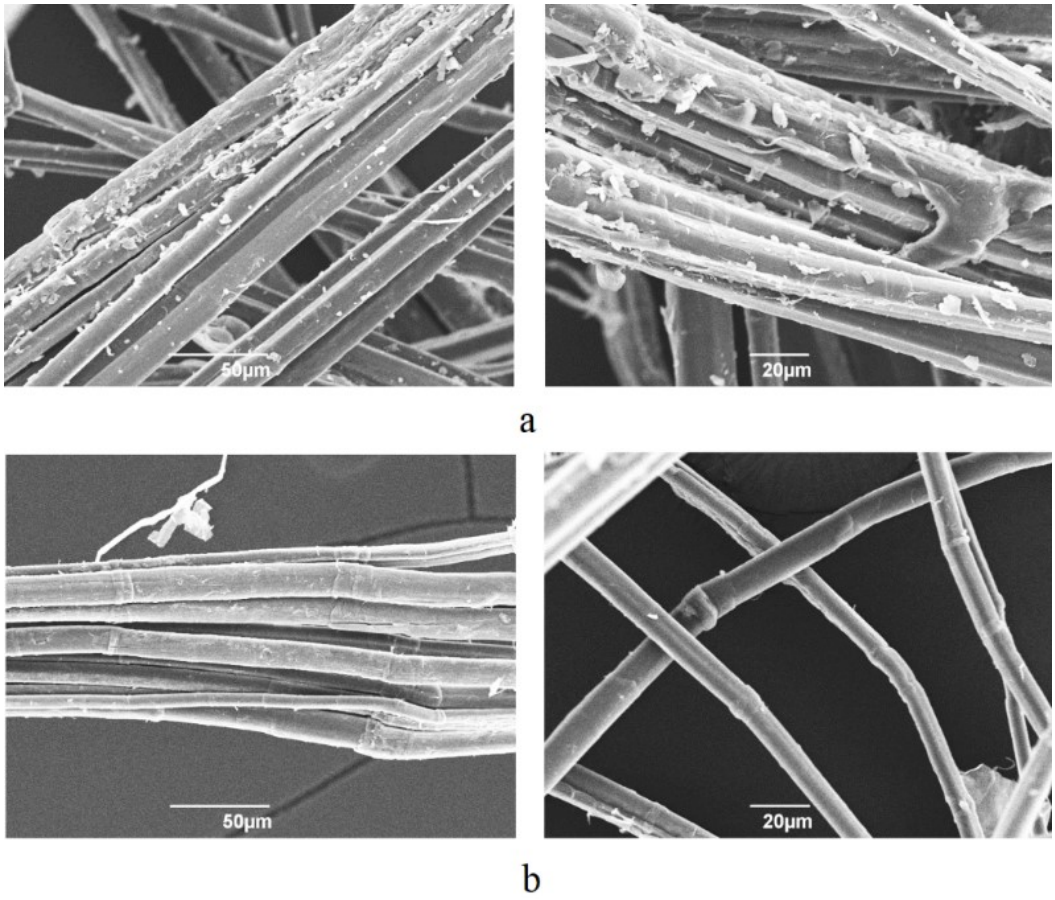

Figure 24. SEM image of linseed flax fiber, Type 1 a) untreated, b) NaOH treatment

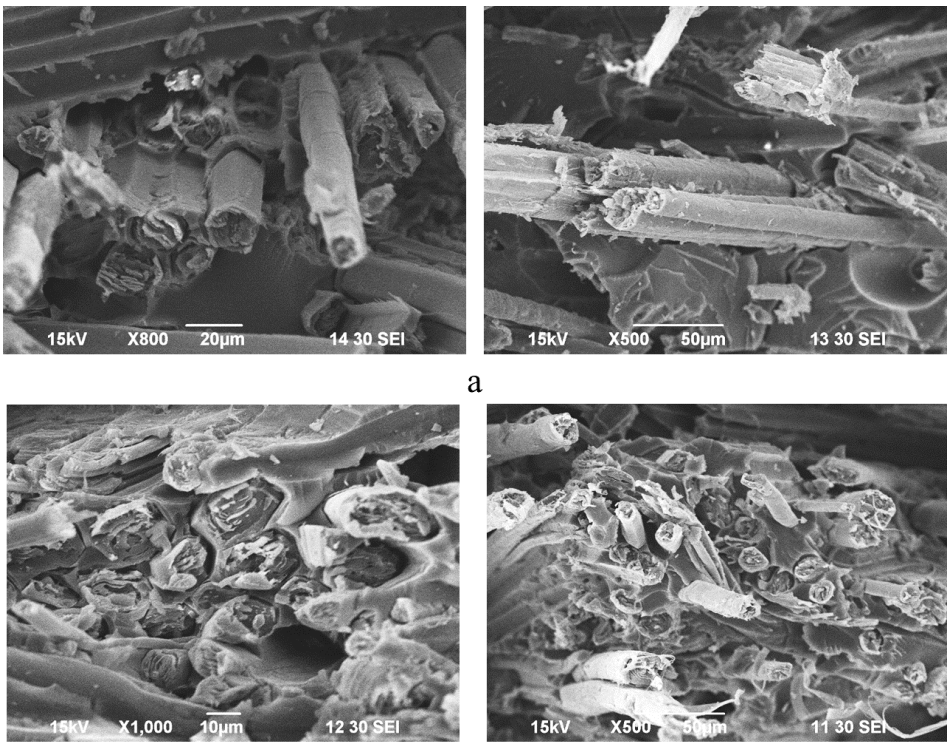

Figure 25. Fractured surface of a) untreated, b) NaOH treated composite after tensile test

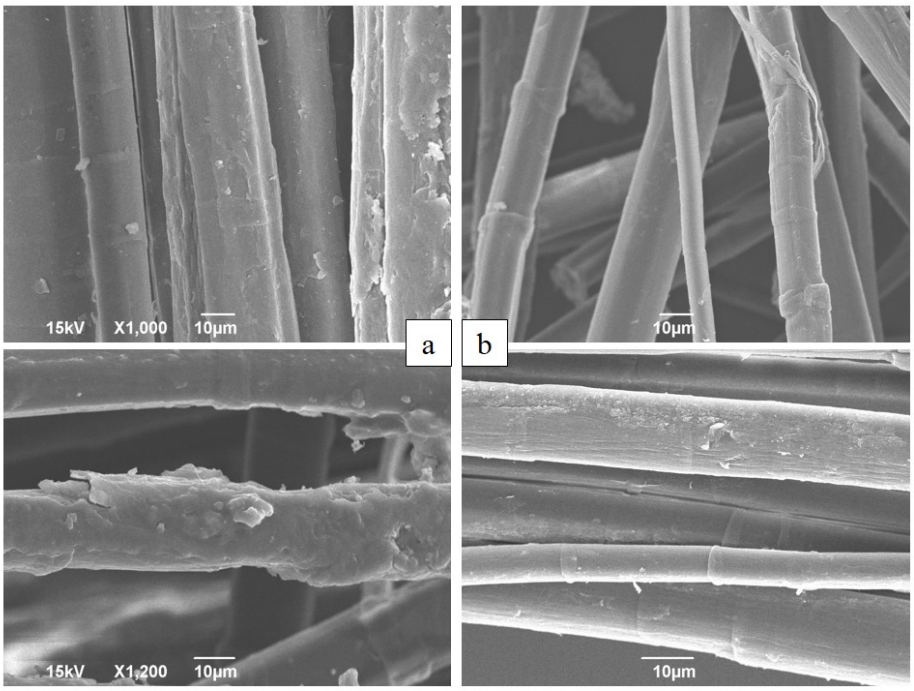

Figure 26. SEM images of (a) untreated, and (b) alkaline treated flax fiber fabric (Type 6)

3.3.2. Effect of Chemical Treatments on Mechanical Properties

3.3.2.1. Linseed Flax Fiber (Type 1) Composites

Constituent analysis results of Type 1 flax fiber before and after alkali treatment are presented in Table 17. Alkaline treatment was successful in reducing amount of ash, proteins and other impurities from the surface of the fiber. In addition, as a result of this treatment the percentage of cellulose has increased by 10%.

Table 17. Constituent analysis of untreated and alkaline treated Type 1 flax fibers

Fiber	Cellulose %	Hemi Cellulose %	Moisture %	Crude Protein %	Crude Fat %	Ash %	Other %
Untreated	79.56	8.76	2.33	2.44	0.40	1.59	0.73
Alkaline Treated	87.81	7.48	1.62	1.22	0.13	0.89	0.42

Table 19 and Figure 30 show the normalized interlaminar shear strength for untreated and treated Type 1 flax fiber composites. These composites used VE and VE+AR as their resins. Statistical analysis of data presented in Table 19 is shown in Appendix G. Both fiber and matrix treatments were effective in increasing interlaminar shear strength. In other words, both treatments were successful in improving bonding between fiber and the matrix as the fiber-to-matrix bonding defines the interfacial and shear properties [207]. Comparing Unt./VE and Alkaline/VE composites, gains of 70% is observed for alkaline treatment.

Table 18. Results of mechanical tests for untreated and treated Type 1 flax fiber with VE and VE+AR resins (raw data)

	Interlaminar shear strength (MPa)	Tensile strength (MPa)	Tensile modulus (GPa)	Flexural strength (MPa)	Flexural modulus (GPa)
Unt./VE	12.22 ± 0.92	100.49 ± 11.02	13.71 ± 2.10	153.25 ± 29.90	12.50 ± 2.90
Unt./VE+AR	15.03 ± 0.95	101.71 ± 3.21	15.03 ± 2.12	145.47 ± 6.79	11.16 ± 0.70
Alkaline/VE	21.48 ± 1.37	108.33 ± 2.90	12.38 ± 1.72	167.69 ± 10.56	11.13 ± 1.19
Alkaline/VE+AR	18.89 ± 1.98	100.20 ± 0.10	11.99 ± 0.14	135.46 ± 17.23	11.67 ± 0.94

Addition of AR resin to VE has increased interlaminar shear strength by 30% for untreated and alkaline treated flax fiber composites. An increase of over 80% in interlaminar shear strength is observed for alkaline treatment with addition of 1% AR to VE. Alkaline treatment will hydrolyze pectin in flax fiber and also remove waxes, dyes and ashes from the fiber surface to result in surface roughness and potentially better adhesion between fiber and matrix [58, 206]. As also seen in Table 17, alkaline treatment of flax fiber has resulted in 55% reduction of ash on the surface of the fiber.

Table 19. Normalized* results of mechanical tests for untreated and treated Type 1 flax fiber with VE and VE+AR resins

	Interlaminar shear strength (MPa)	Tensile strength (MPa)	Tensile modulus (GPa)	Flexural strength (MPa)	Flexural modulus (GPa)
Unt./VE	12.22 ± 0.92	100.49 ± 11.02	13.71 ± 2.10	153.25 ± 29.90	12.50 ± 2.90
Unt./VE+AR	15.94 ± 1.01	107.87 ± 3.40	15.94 ± 2.25	154.29 ± 7.20	11.84 ± 0.75
Alkaline/VE	20.88 ± 0.93	105.32 ± 2.82	12.04 ± 1.67	163.03 ± 10.27	10.82 ± 1.16
Alkaline/VE+AR	22.04 ± 2.31	116.90 ± 0.12	13.99 ± 0.17	158.04 ± 20.10	13.62 ± 1.10

* All values are normalized to fiber volume fraction of 35%

Flexural properties of untreated and treated Type 1 flax fiber with VE and VE+AR resins are presented in Table 19 and Figure 28. Based on statistical analysis presented in Appendix G, the gains of flexural properties are not statistically significant. However, alkaline treatment has improved the flexural strength by 5% compared to composites using untreated flax fiber. Addition of the AR to the VE resin has resulted only in 2% improvement of flexural strength. Fiber treatment or addition of AR to the matrix has resulted in decrease of flexural modulus. However, when both treatments are combined, flexural modulus is increased by 5%. Similar results were observed in the study done by Huo et al. [106, 108]. Alkaline treatment of North American (NA) flax had 5%-10% increasing effect on flexural strength. Flexural modulus, on the other hand was decreased by alkaline treatment. The decrease in flexural strength is attributed to the structural variation in the

structure of flax fiber. This is the result of non-cellulosic content of the flax fiber and microfibrils losing their resistance to deformation and elongation after treatment [208].

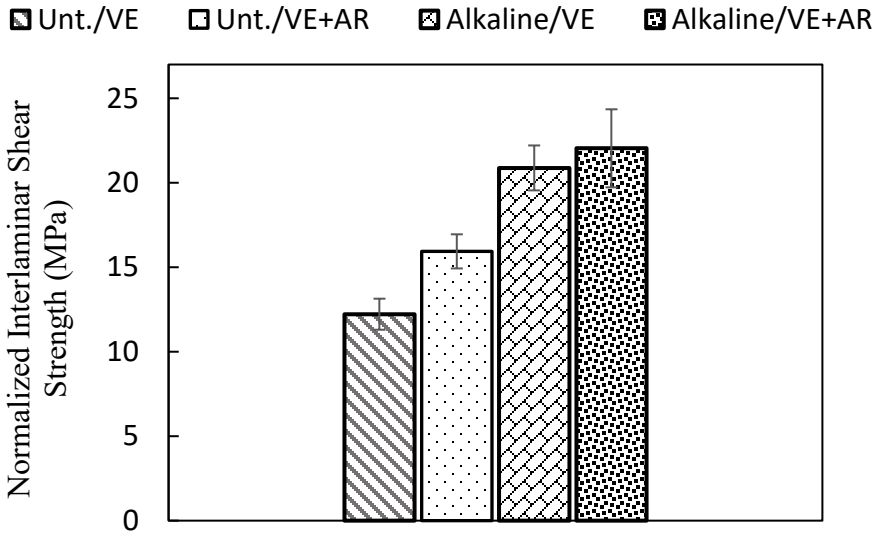

Figure 27. Normalized plots of interlaminar shear strength for different composites

Tensile properties of untreated and treated Type 1 flax fiber with VE and VE+AR are presented in Table 19 and Figure 29. Addition of AR to the VE resin has increased the tensile strength between 8% and 11% for untreated and alkaline treated flax fiber composites, respectively. However, based on results of statistical analysis, the only significant gain in tensile properties is increase in tensile strength when both treatments are combined. This is the indication that as expected, addition of AR has improved the efficiency of load transfer to the matrix [106]. Alkaline treatment has been effective in increasing tensile strength of the composite by 5% and when combined with the addition of AR to the resin, the increase in tensile strength is 17% resulting in the highest tensile strength. This increase in tensile strength can be attributed to the enhanced crystallinity and structure of the cellulose after alkaline treatment as seen in Table 17 [209].

Although the results of tensile modulus are ot statistically significant, reduction in tensile modulus Tensile modulus has been observed in similar studies [106-108, 210]. This decrease is attributed to the breakdown of the flax fiber after alkaline treatment [108], also structural variation in natural fibers will lead to change in the tensile modulus after treatment [211].

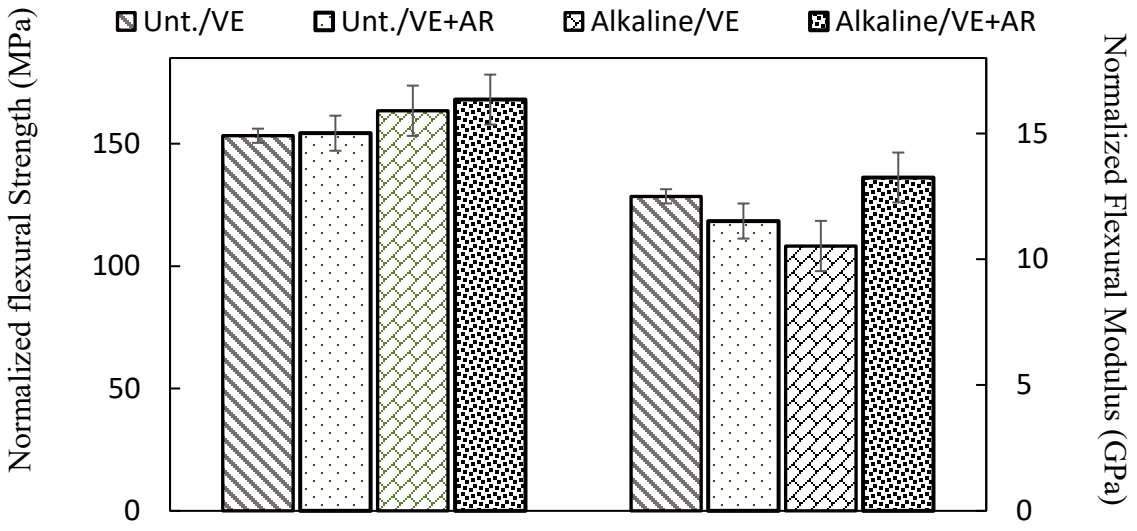

Figure 28. Normalized fleaxural strength and flexural modulus of untreated and treated Type 1 flax/VE composites

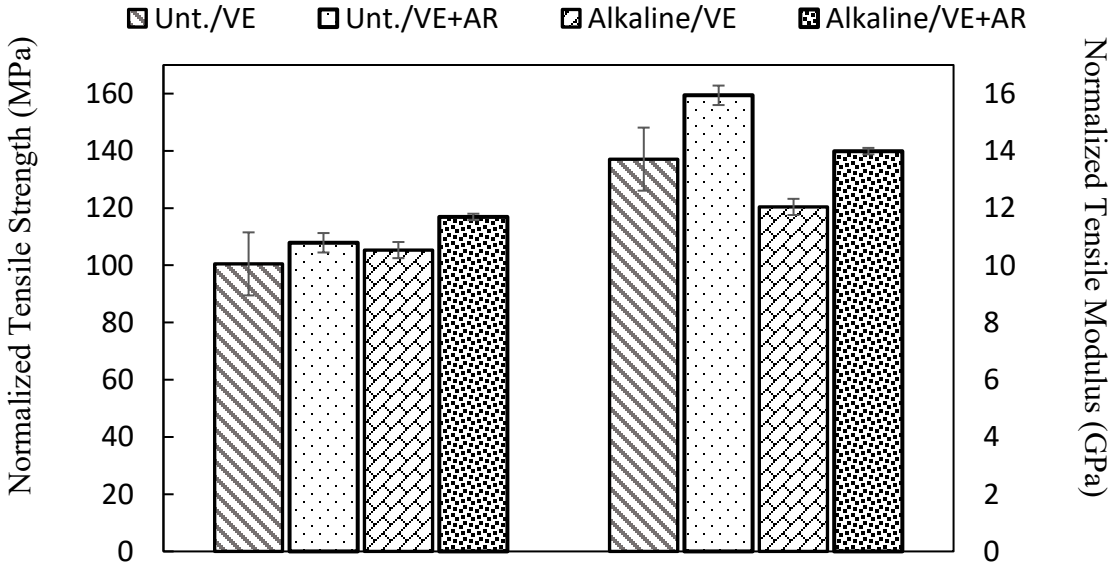

Figure 29. Normalized tensile strength and tensile modulus of untreated and treated Type 1 flax/VE composites

3.3.2.2. Flax Fiber Fabric (Type 6) Composites

An immersion density technique was used to measure the density of the composite plates and cured resins. Density of cured VE, MESS and DMESS was found to be 1.15 g/cm^3, 1.10 g/cm^3, and 1.07 g/cm^3, respectively. The density of flax/VE, flax MESS and flax/DMESS composites were between 1.28 g/cm^3 to 1.33 g/cm^3 and the fiber volume fraction of the flax fiber composites were found to vary between 38% and 56%. In order to make the results of mechanical tests comparable, all presented results are normalized to 50% fiber volume fraction. Normalized results of mechanical tests, before and after treatment, as well as before and after weathering are presented in Table 20. Same as previous studies [212], a target range for desired properties was defined based on data for commercial pultruded fiberglass composites available in literature [68-71]. Statistical analysis of data shown in Table 20 is presented in Appendix G.

Table 20. Normalized results of mechanical tests for untreated and treated, weathered and unweathered flax fiber fabric composites

		Tensile Strength MPa	Tensile Modulus GPa	Flexural Strength MPa	Flexural Modulus GPa	Interlaminar Shear Strength MPa
	Target Properties	200-225	16-18	200-225	11-13	25-30
unweathered	UTUW-VE	182.79±15.00	22.76±1.08	181.53±26.28	18.95±3.72	18.79±1.81
	TUW-VE	209.73±27.46	26.96±3.88	279.03±27.38	25.35±3.24	31.27±1.03
	UTUW-MESS	122.97±2.56	19.23±1.72	136.25±7.09	17.86±4.99	11.68±1.07
	TUW-MESS	207.92±18.13	29.28±13.63	229.07±19.00	26.43±2.73	13.68 ±0.51
	UTUW-DMESS	130.59±11.57	20.28±15.36	133.41±12.02	16.84±1.99	12.72±0.66
	TUW-DMESS	150.39±2.20	24.90±2.14	200.05±40.95	20.35±5.25	18.80±3.73
Weathered	UTW-VE	137.71±7.53	26.49±1.36	161.90±5.47	14.92±1.47	17.94±1.71
	TW-VE	172.23±42.57	31.43±3.43	277.91±14.45	31.16±5.81	27.43±1.32
	UTW-MESS	45.36±3.33	12.92±1.35	105.27±4.86	10.04±1.19	9.40±0.95
	TW-MESS	113.11±18.35	23.78±4.58	129.69±19.00	18.91±2.97	11.63±0.67
	UTW-DMESS	99.65±8.60	12.96±0.93	74.03±11.70	7.62±0.93	7.07±1.17
	TW-DMESS	119.70±12.58	17.10±3.15	120.87±13.64	18.02±4.54	12.76±2.42

* All values are normalized to fiber volume fraction of 50%

Figure 30 show the normalized interlaminar shear strength (ILSS) for untreated and treated flax fiber composites. In all three composites, fiber treatment was effective in increasing interlaminar shear strength, however, based on statistical analysis, gains for shear properties of composites using MESS resin was not significant. Based on the results, the treatment was effective in improving bonding between fiber and the matrix as the fiber-to-matrix bonding defines the interfacial and shear properties [207]. The biggest gain of ILSS was observed for flax-VE composites with the value of 66%. This corresponds to a 70% improvement in ILSS after alkaline treatment for flax-VE composites as observed in a linseed flax treatment. As expected, alkaline treatment, by hydrolyzing pectin in flax fiber and also removing waxes, dyes and ashes from the fiber surface has resulted in better adhesion between fiber and matrix due to increased surface roughness [58, 206]. In addition, by employing alkaline treatment, the ILSS of flax-VE has exceeded the maximum target properties and ILSS of flax/DMESS got very close to the range of target properties.

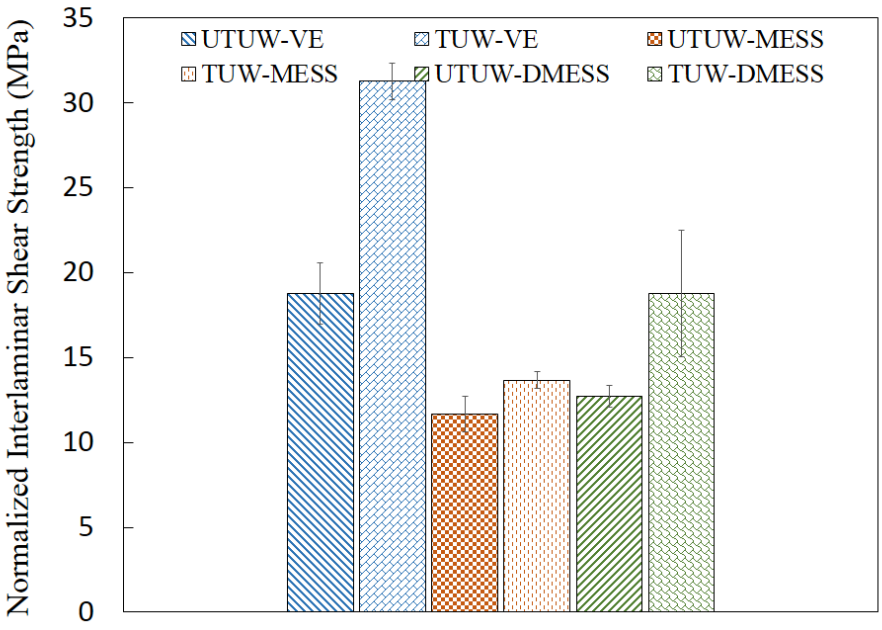

Figure 30. Normalized plots of Interlaminar shear strength for different flax fiber composites

Flexural properties of untreated and treated flax fiber composites are presented in Figure 31. Alkaline treatment has improved the flexural properties. However, the gain in flexural modulus of composites using flax/DMESS is not statistically significant. The biggest gain was for flexural strength of flax-MESS resin, 68%, followed by 55% for flax-VE and 50% for flax-DMESS. With this increase, flexural strength of all composites has met the target range set, and for flax-VE and flax-MESS this value has exceeded the maximum benchmark. In similar studies [51, 60, 108] a reduction in flexural modulus was observed after alkaline treatment. This is due to structural variation present in structure of flax fiber such as presence of non-cellulosic content [208]. Observing the Figure 8, there is no reduction is flexural modulus in this case. Flexural moduli of all composites were increased after alkaline treatment. Before and after fiber treatment, flexural moduli are well above the maximum target value set, and after treatment almost in all composites, the moduli are 200% of the maximum benchmark.

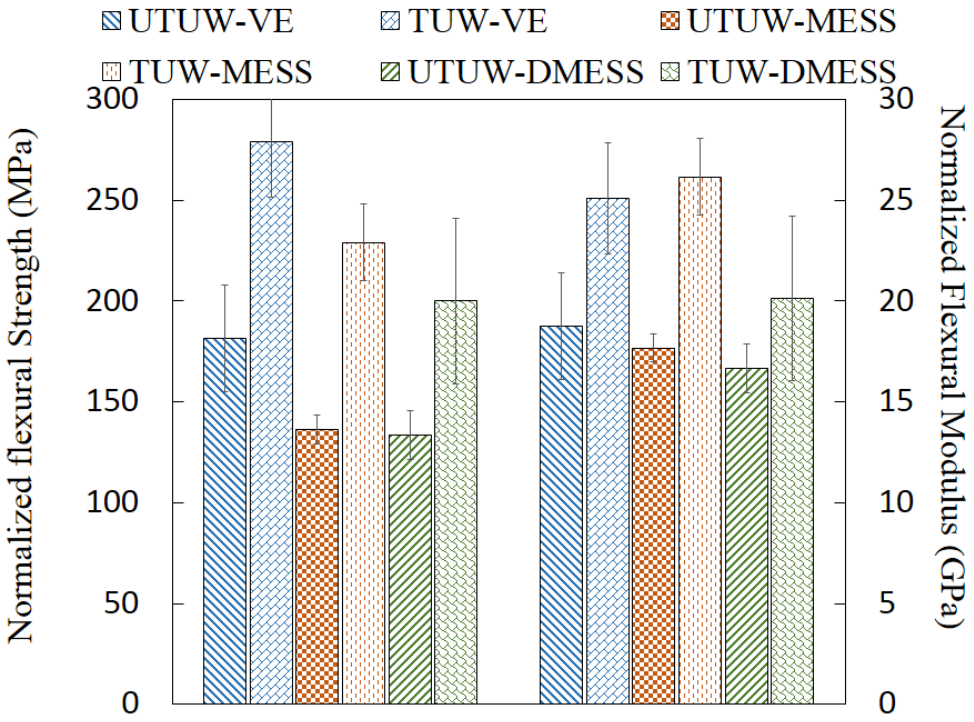

Figure 31. Normalized fleaxural strength and flexural modulus of different flax fiber composites

Tensile properties of untreated and treated flax fiber composites are presented in Figure 32. Alkaline treatment has increased the tensile strength between 15% and 68% compared to tensile strength of composites using untreated flax fiber. This increase is between 25% and 73% for tensile modulus. Same as before, the gains of tensile properties of composites using DMESS resin is not statistically significant; this is due to bigger variance in measured values for flax/DMESS resin. The increase in tensile strength can be attributed to the enhanced crystallinity and structure of the cellulose, which is expected to happen after alkaline treatment [209]. In some cases in similar studies [51, 106-108, 210], a decrease of tensile modulus was observed after alkaline treatment of flax fiber. This decrease is due to the breakdown of the flax fiber after alkaline treatment [108] which varies depending on structural variation in natural fibers [211]. However, same as flexural modulus, no decrease in tensile modulus was observed after alkaline treatment. All tensile moduli, before and after treatment are higher than the set target range as seen in Table 20.

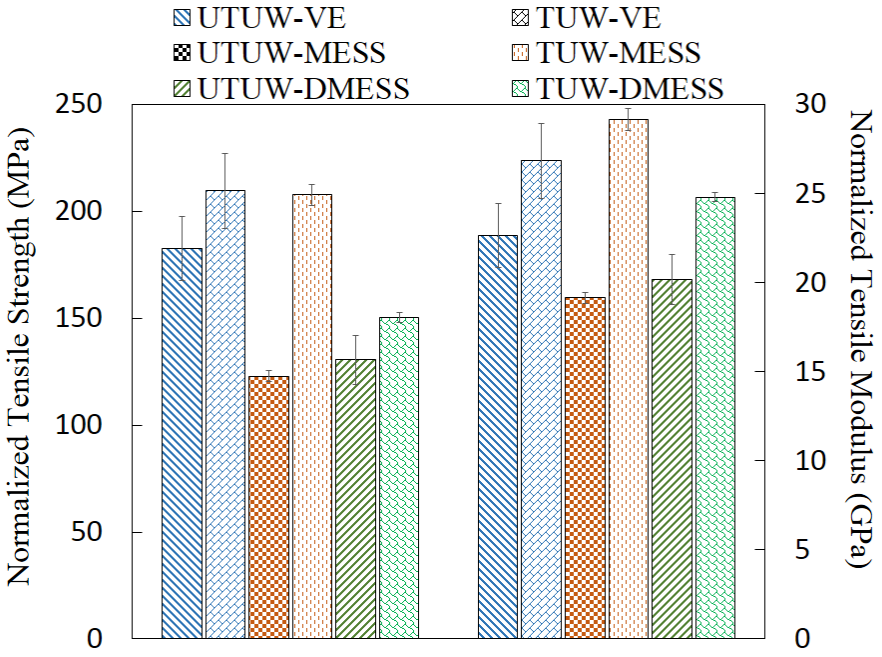

Figure 32. Normalized tensile strength and tensile modulus of different flax fiber composites

3.4. Long-Term Behavior of Flax Fiber - Creep

3.4.1. Thermal Analysis

Figure 33 shows tan δ curves of cured VE resin and flax/VE composite. The peak position and transition breath of tan δ curves were determined using cross-link density. T_g of VE was determined to be 127.83 ºC and T_g of flax/VE to be 126.85 ºC. Huo et al. [106] reported T_g of the same VE resin (Hydropel® R037-YDF-40 with 30% styrene content from AOC resins) to be 128 ºC and Herzog et al. measured T_g of vinyl ester resin [213] to be 132.8 ºC and cured VE + AR (Hydropel® R037-YDF-40 with 30% styrene content with 1% Acronal® 700L) is reported by Huo et al. to be 126.85 ºC [106].

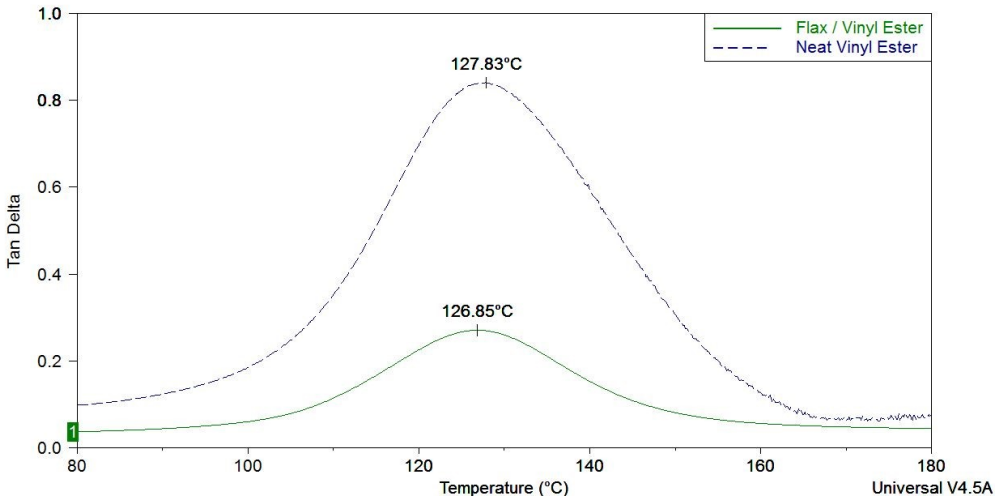

Figure 33. DMA plots of flax/VE and neat vinyl ester resin

Figure 34 shows the typical thermal behavior of flax fiber/VE and flax/VE+AR composite as temperature is increased. Thermogravimetric curve in its original and differentiated state (DTG) is presented. The peaks of DTG curve are marked at 298.87 ºC, 368.37 ºC and 415.96 ºC and correspond to the maximum changes in the slope of TGA curve. Up to 298.87 ºC which is the onset of the major weight loss the degradation in weight is 7.2%. The significance of TGA analysis for this study is to make sure that the material under creep test is not degrading in the temperature

range the tests is conducted. In the range between 30 ºC – 110 ºC that creep tests were carried out, there is only 0.49% decrease in weight of specimen, which could be attributed to moisture and unreacted monomers present in the material. Addition of AR to VE has not changed the degradation temperature of flax/VE composites and it starts to degrade around 320 ºC.

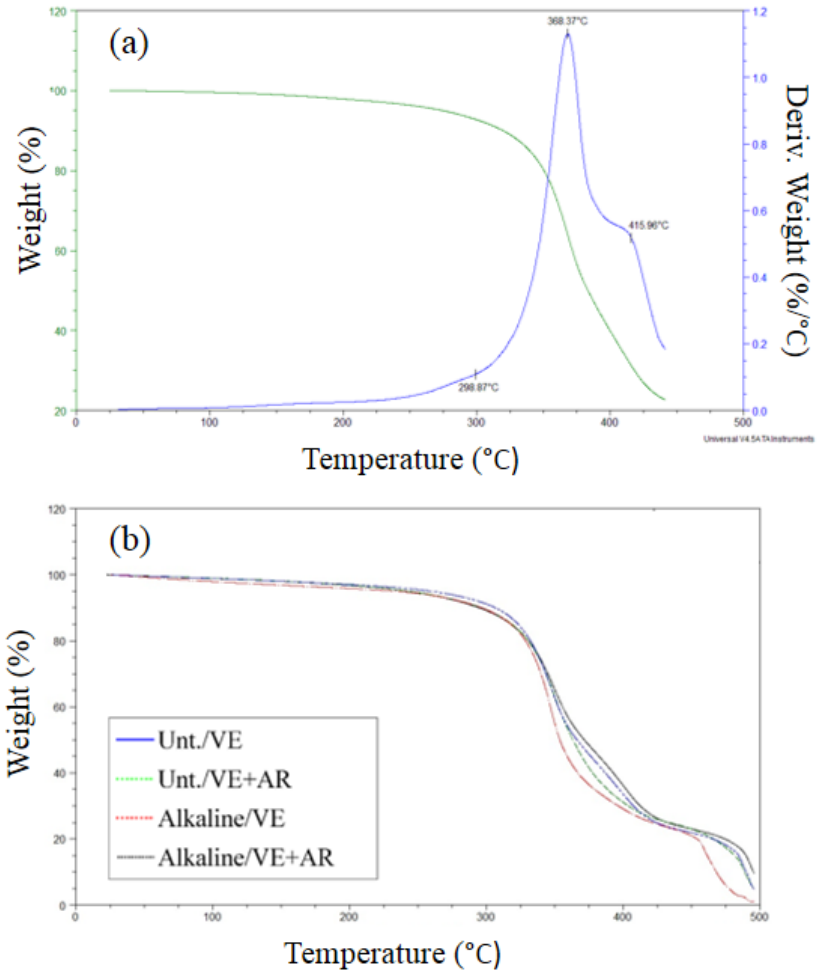

Figure 34. TGA curves (a) in its original and differentiated state for flax/VE and (b) typical TGA curves of flax/VE and flax/VE+AR

DSC tests were run in order to make sure there is no crosslinking or curing happening at the temperature range that creep tests are performed. A typical DSC trace for heating of flax/VE and flax/VE+AR are presented in Figure 35. As mentioned before, the creep measurements are

valid if there is no residual curing happening during creep tests and there is no structure change in the material under study, and the specimen is not degrading in the temperature range.

The degree of cure of resin was calculated using the following equation [214]:

$$Degree\ of\ cure = \frac{\Delta H_{reaction} - \Delta H_{res}}{\Delta H_{reaction}} \quad (21)$$

where $\Delta H_{reaction}$ is the total heat of reaction and ΔH_{res} is the residual heat after curing. In Figure 35, there was some residual curing approximately around 136 ºC and 138 ºC and the degree of cure for VE and VE+AR was calculated to be 99.40% and 99.61% respectively. Based on the results from DSC and TGA, it is concluded that the material does not undergo any degradation or crosslinking at the temperature range selected for the creep tests, i.e. 30 ºC-110 ºC.

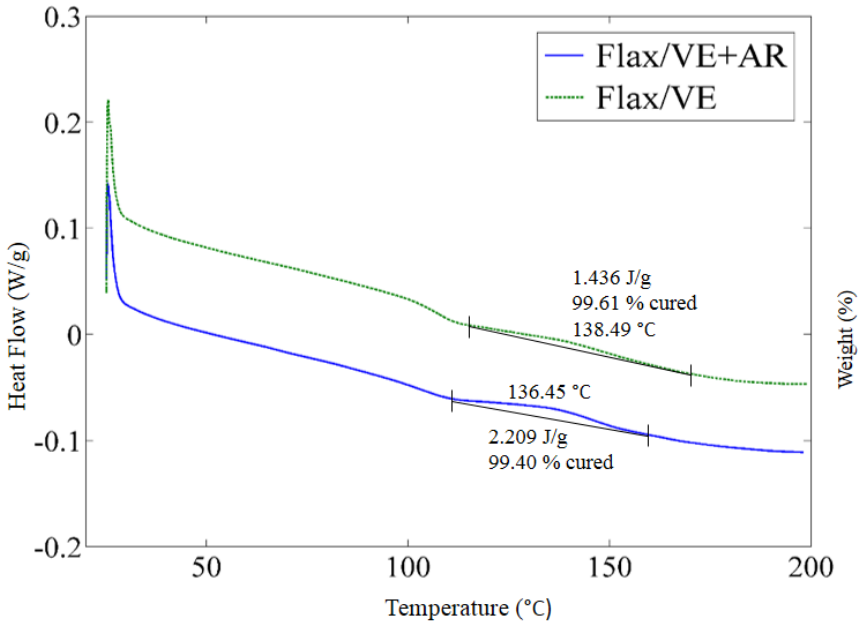

Figure 35. DSC trace for heating of flax/VE and flax/VE+AR from 25 ºC to 200 ºC

3.4.2. Generating Master Creep Compliance Curves

Static three point bending tests at room temperature as well as creep tests at different temperatures were carried out on flax/vinyl ester composite samples. Three point bending tests were performed on five samples using an Instron 5567 load frame in accordance with ASTM D790

[215] to measure the flexural strength. The average flexural strength of the flax/vinyl ester composite studied was found to be 153±29 MPa.

Creep compliance curves measured at different temperatures can be horizontally shifted in reference to a specific temperature to generate a master compliance curve. A master compliance curve provides information for the long-term behavior of a material at a reference temperature.

Creep behavior of flax/vinyl ester composite at different temperatures is shown in Figure 36. With constant stress, increasing temperature accelerates the rate that the samples are strained. The strain curves for 30 ºC and 40 ºC are very similar and nearly coincide with each other. It is from 40 ºC and above that the difference between creep behaviors at different temperatures can be distinguished from each other. As mentioned previously creep compliance *J(t)* is defined as ratio of time-dependent strain to the constant stress applied. The creep compliance curves are shown in Figure 37. As expected, by increasing temperature, the creep compliance is increased as well which is a non-linear creep behavior from material results of change in time scale. The material creeps faster at higher temperatures. This is consistent with the findings of creep behavior of flax fiber reinforced composites as seen in other studies [162, 165] .

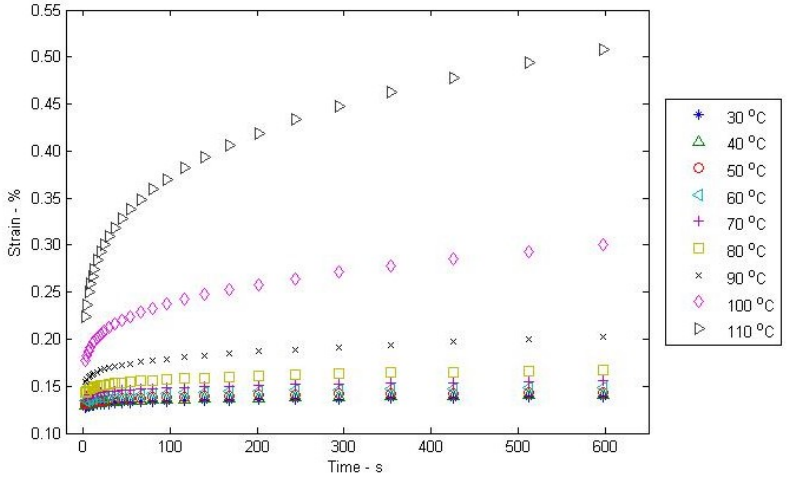

Figure 36. Creep strains vs time at different temperatures for flax/VE composite

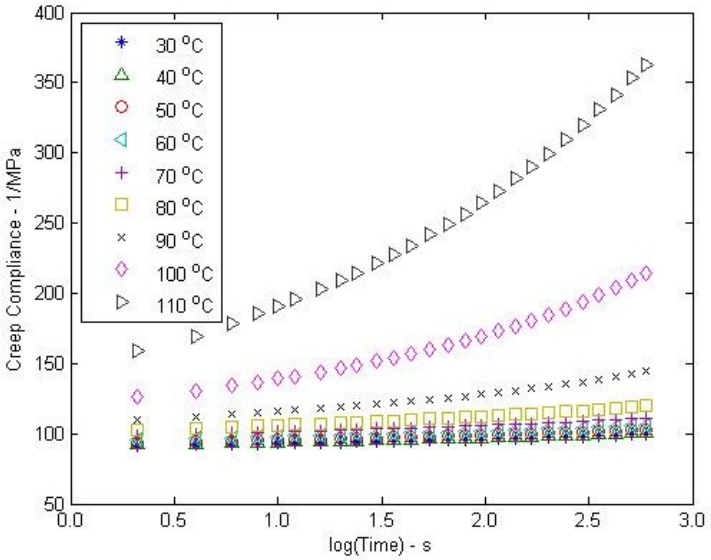

Figure 37. Creep compliance curve at different temperatures for flax/VE composites

By observing creep compliance and creep strain curves, the 30 ºC curve was selected as the reference compliance curve and all other curves have been shifted to the right on time axis to build the master curve for this experiment. A MATLAB® code was used to calculate shift factors in order to minimize the difference between the shifted curve and the reference compliance curve. The result of the shifted curves is shown in Figure 38.

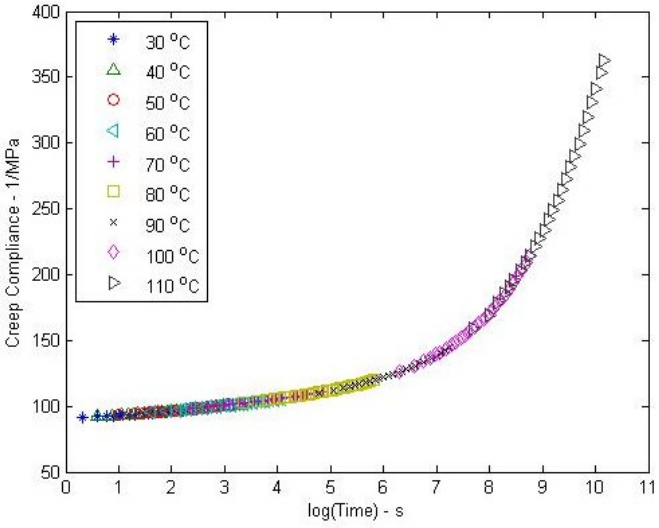

Figure 38. The master curve for creep compliance at 30 ºC for flax/VE composites

Temperature shift factors are plotted in Figure 39. Using least square method to fit Arrhenius to the data in Figure 39, activation energy of flax/VE composites is calculated to be in 124.66 kJ/mol.

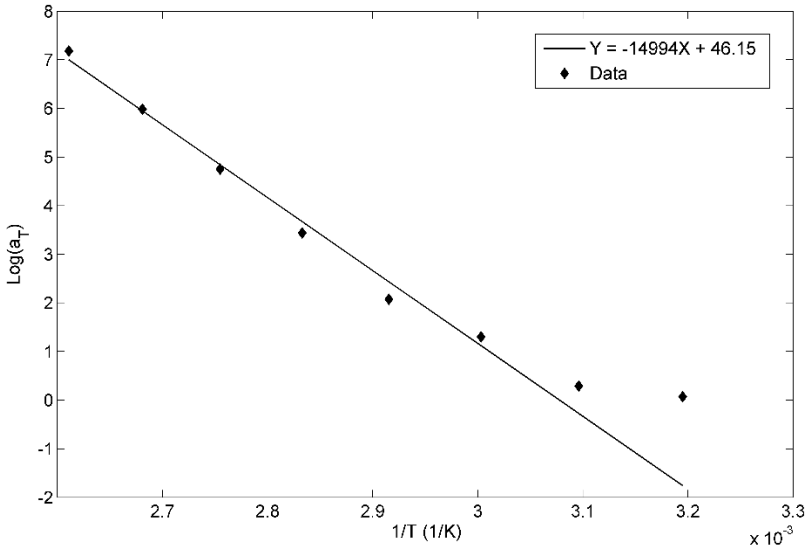

Figure 39. Temperature shifts factors vs temperature difference

For the compliance master curve in Figure 38, the Findley Power Law equation (22) was adapted. Calculated coefficients and the resulting equation is as:

$$J = 100.8 + 0001325 \times t^{5.248} \tag{22}$$

The fitted curve versus experimental data is shown in Figure 40. Despite the slight deviation from experimental data in the early stages of creep, the simulated curve agrees with the experimental results over time. Thus, there is an agreement between the Findley Power Law and the experimental results.

Creep tests with constant stress were carried out at different temperature intervals on flax/vinyl ester composite. A creep compliance master curve was generated by shifting creep

compliance data along time scale in reference to a compliance curve at 30 ºC. Activation energy of the flax/VE composite was found to be 124.66 kJ/mol.

The coefficients in Findley Power Law were computed and a strong agreement between experimental and simulated results was observed.

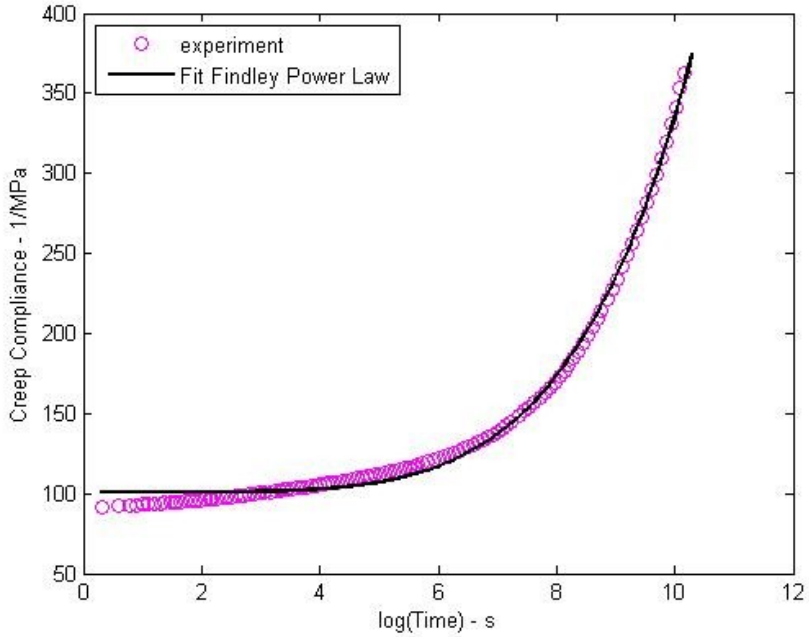

Figure 40. The master curve of creep compliance for flax/VE composites at 30 ºC and Findely Power Law fit

The resulting master curve and power law equation provides accelerated creep characterization up to 10^{10} seconds (20 years if we use temperature up to 100 ºC). As a result, to predict creep behavior of a flax/vinyl ester composite material in 20 years at 30 ºC, one needs to run creep tests at 100 ºC for 10 minutes.

3.4.3. Calculation of Activation Energy for Flax/VE Composite

Horowitz and Metzger in 1963 [216] proposed a new method of calculating activation energy from thermogravimetric curves. They mentioned that the activation energy can be calculated from following equation [216]:

$$\ln\left(\ln\left(\frac{W_o - W_f}{W - W_f}\right)\right) = \frac{E(T_s - T)}{RT_s^2} \quad (23)$$

where W_o is the weight at the beginning of the range, W_f is the weight at the end of the range, W is the weight at absolute temperature T, and T_s is the reference temperature in such way that at T_s, $\frac{W}{W_o} = 1/e^1$. Figure 41 shows plot of $\ln(\ln(\frac{W_o - W_f}{W - W_f}))$ vs. $(T_s - T)$. For the TGA curve shown in Figure 34, T_s was found to be 385 ºC. A straight line was fitted through data points using the method of least squares. The slope of the straight line was found to be 0.036. Therefore, activation energy based on Equation (23) was 129.587 kJ/mol. The value found in this study is in good agreement with that found by other researchers for this material. Velde and Kiekens [217] used the same method and they measured activation energy of six different types of flax fiber in the air and in the nitrogen. Their average value of activation energy for flax fibers in nitrogen was 135.33 kJ/mol.

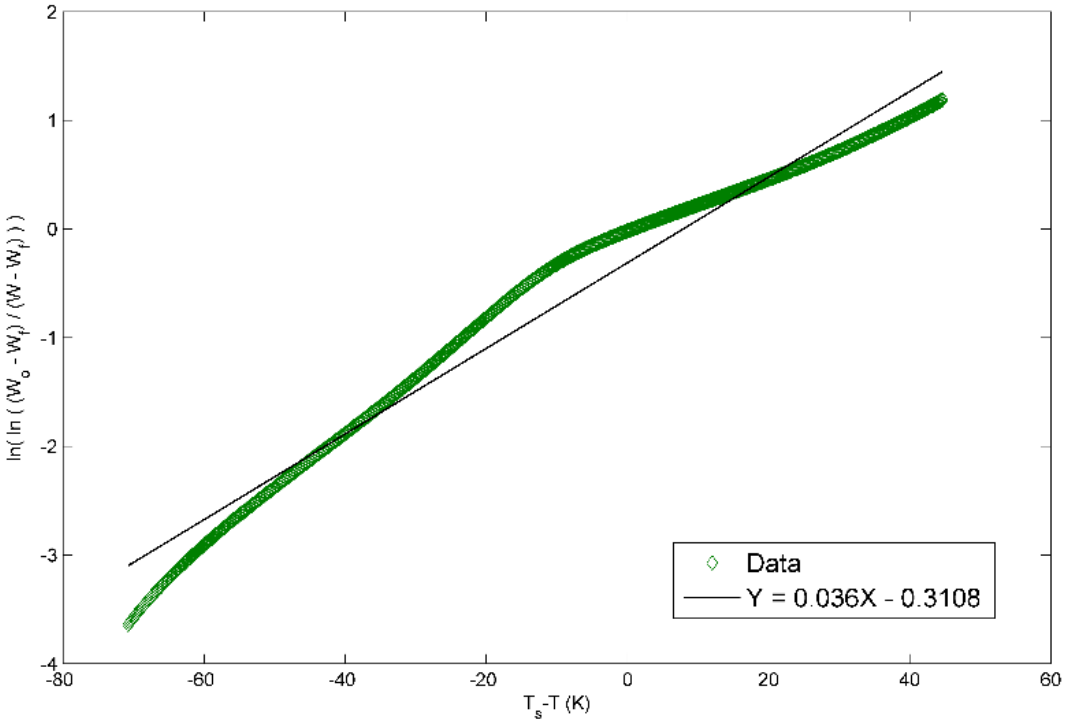

Figure 41. Calculation of activation energy for flax/VE composite

3.4.4. Effect of Chemical Treatment on Creep Behavior of Biobased Composites

Creep behavior of untreated and alkaline treated flax with VE and VE+AR composites are presented in Figure 42. Similar to the work presented in [214] creep compliance master curves are generated by shifting the individual creep compliance curves at different temperatures along logarithmic time axis. The creep compliance curve at 30 ºC was selected as the reference curve and all other curves were shifted to the right. Resulting creep compliance master curves are presented in Figure 43. The curves presented are normalized to 35% fiber volume fraction to be comparable.

In Figure 43, up to $10^{4.5}$ and 10^{6} seconds, can be considered as steady state creep for Alkaline/VE and Unt./VE, respectively. For the composites with VE+AR resin up to $10^{6.5}$ can be considered as steady state region. The slope of the steady state region is the creep rate. Based on the slopes calculated from the steady state of the curves, the highest to the lowest creep rates are Alkaline/VE+AR, Unt./VE+AR, Unt./VE and Alkaline/VE, respectively. In general, composites with neat VE have lower strain rates in the steady state region, but composites with VE+AR have longer steady state region and the onset of tertiary state has been retarded.

As seen in Figure 43, the composite with alkaline treatment and addition of AR has the lowest amount of creep after 10^{8} seconds. This is consistent with results of chemical treatment presented in previous sections. As discussed previously, alkaline treatment and addition of AR to VE resulted in the highest amount of flexural modulus. However, after 10^{8} the rate that the composite with untreated fiber and VE resin starts to creep faster and the order of creep curves is changed.

It is known that increasing the degree of crosslinking of a polymer pushes for the secondary bonding between polymer chains and consequently the polymer becomes more resistant to creep

[150]. Addition of AR to VE resin will result in decreasing cross-linking density of the matrix [106], therefore it is expected for the composites using VE+AR to exhibit less resistance to creep. Interestingly this is not the case here. As mentioned before, creep of fiber reinforced composites is a complex phenomenon which depends on many factors such as creep behavior of matrix, fiber-matrix interfacial properties and load transfer from matrix to fiber [170]. As observed in the results of interlaminar shear strength, addition of AR to VE resin has resulted in an increase in the interfacial bonding between fiber and matrix. In addition, as observed in the results of tensile strength, addition of AR to VE increased the efficiency of load transfer to the matrix.

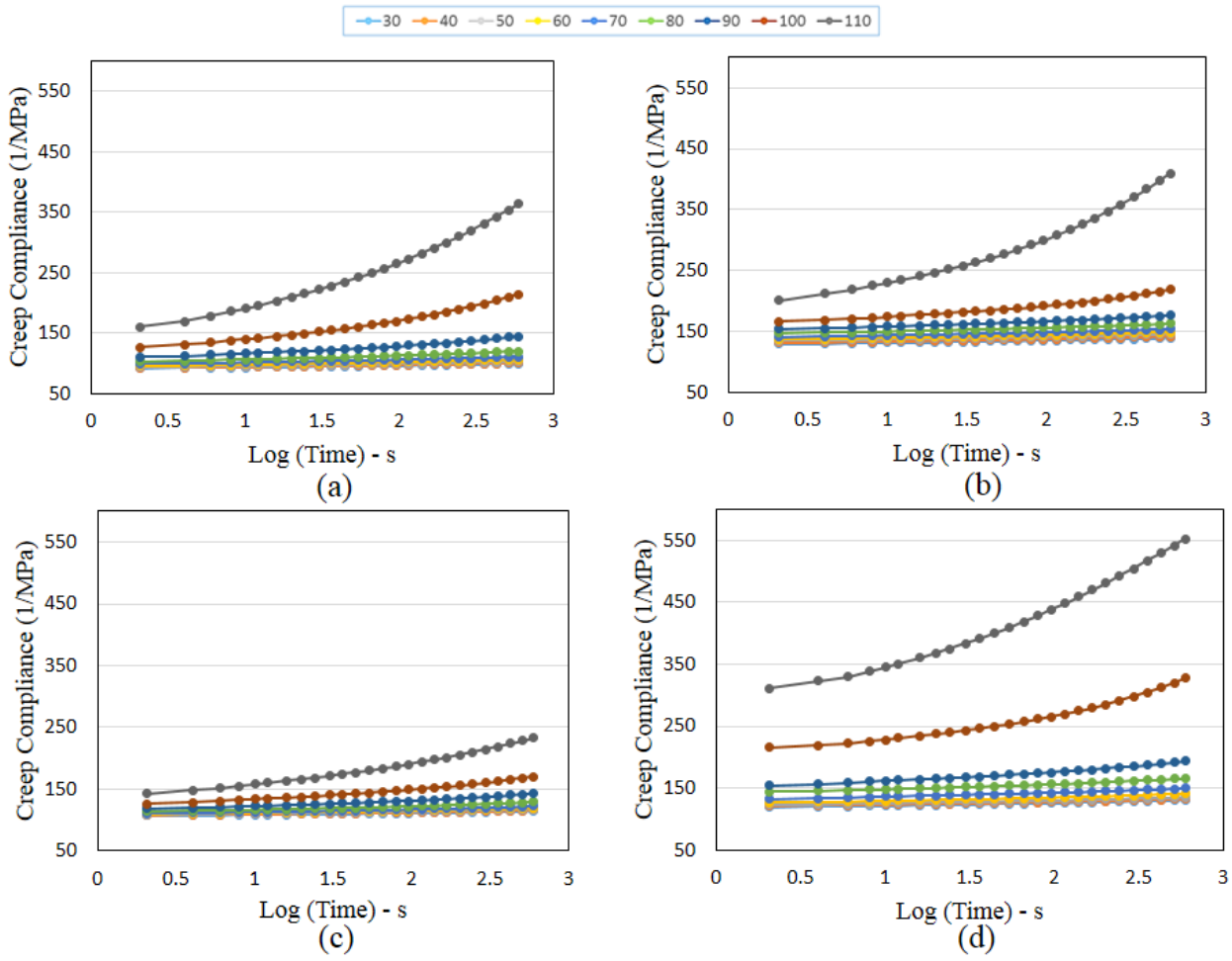

Figure 42. Creep compliance of (a) Unt./VE; (b) Unt./VE+AR; (c) Alkaline/VE; (d) Alkaline/VE+AR at different temperatures

From the results presented in Figure 43, it is perceived that the resultant of the effects of three factors (creep behavior of matrix, fiber-matrix interfacial properties and load transfer from matrix to fiber) has been higher resistance of composite to creep after addition of AR to VE resin. The results are consistent with findings of similar studies. Hue and Ulven [218] studied the effect of addition of AR to VE on interlocking of flax fiber and resin. Based on their results, the AR additive increased the coefficient of thermal contraction of VE during cooling. Also, the compressive stresses on the interface of flax/VE in increased which leads to stronger mechanical interlocking between fiber and matrix.

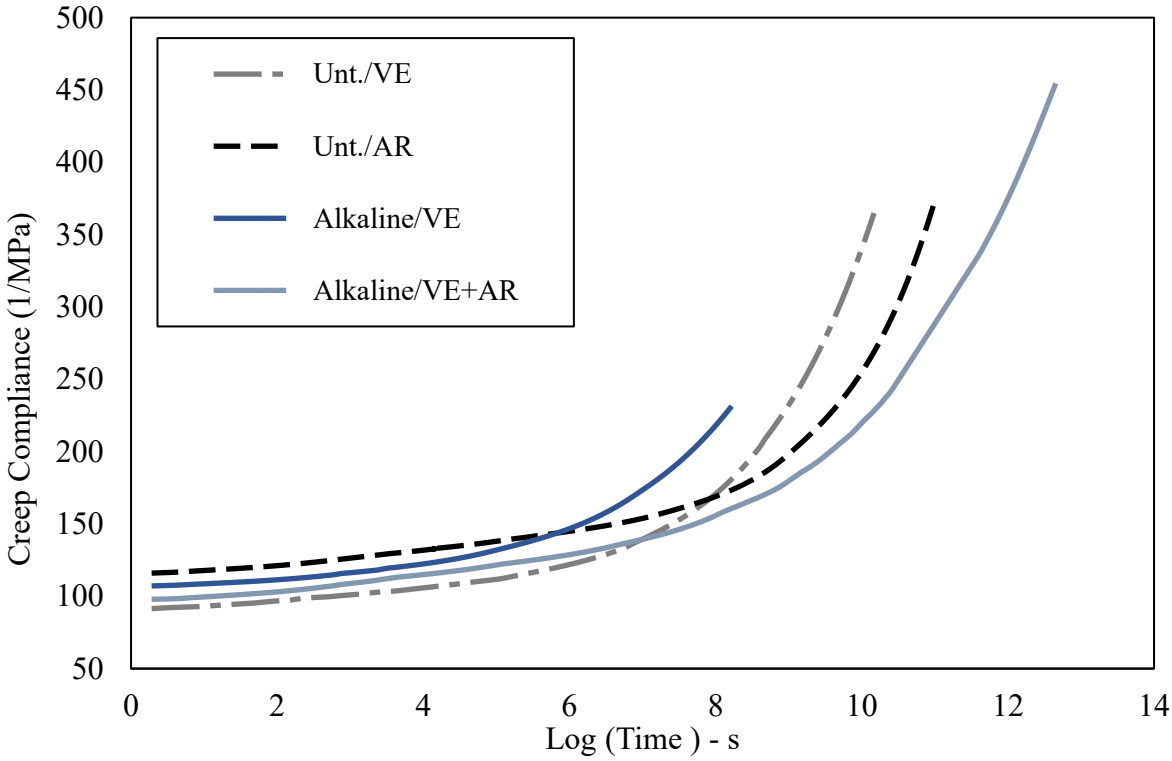

Figure 43. Creep compliance master curves for untreated and treated flax fiber with VE and VE+AR resins

According to William Findley [152], the time-dependent creep compliance of a material can be represented by the Equation (10). For each generated master curve, Findley Power Law was adapted and calculated coefficients and R-square of the fits are presented in Table 21.

As mentioned, A is temperature-independent variable, so in the curve fitting process, A was kept at a constant value of 0.00135 which was calculated for Unt./VE composites at 30 ºC. As seen in Figure 43, master curves for composites with VE resin are parallel to each other with the values of stress-independent coefficient of $n = 5.24$ for untreated and $n = 5.418$ for alkaline treated flax fiber. Likewise, curves for VER+AR reinforced with flax are parallel to each other with the values of $n = 5.007$ for untreated and $n = 4.903$ for alkaline treated flax fibers. Therefore, addition of AR to VE has resulted in the reduction of the stress-independent coefficient.

Table 21. Parameters in Findley Power Law equation for different composites under study

Composite	J_0 (1/MPa)	A	n	R-Square
Unt./VE	100.8 ± 1.4	0.00135 ± 0.003	5.24 ± 0.154	0.9960
Unt./VE + AR	126.2 ± 1.7	0.00135 ± 0.003	5.007 ± 0.012	0.9961
Alkaline/VE	117.5 ± 1.2	0.00135 ± 0.003	5.418 ± 0.073	0.9966
Alkaline/VE + AR	112.8 ± 2.1	0.00135 ± 0.003	4.903 ± 0.082	0.9957

3.4.5. Frequency Sweep of Flax/VE

According to TTS assumptions, same shifting factors should be valid for all viscoelastic parameters [157, 219]. To further validate this assumption of TTS principle foe flax/VE composites, frequency sweeps of flax/VE specimens were conducted and storage and loss moduli as well as tan δ were measured. Results of frequency sweeps are presented in Figure 44. A horizontal shifting of the storage modulus values was performed using TA Instruments Data Analysis software. To perform the shifting process, storage modulus curve at 30 °C was selected as the reference curve, and all other curves shifted to the left. In this process, loss modulus curves and tan δ curves were also shifted with the same values for shift factors. The resulting plots are presented in Figure 45.

Based on Figure 45, although a smooth master curve is obtained for storage modulus, the curves for loss modulus and tan δ are not satisfactory. This is indication of the fact that only one set of horizontal shift factors is not enough for all three sets of curves.

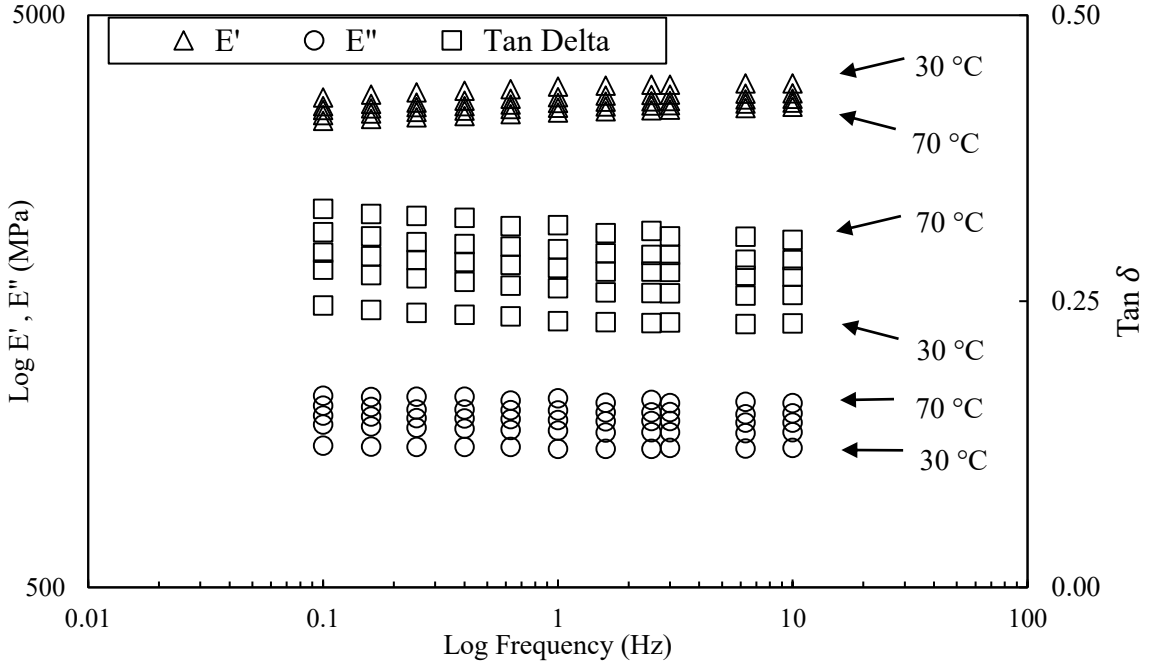

Figure 44. Frequency sweep of flax/VE composite at different temperatures

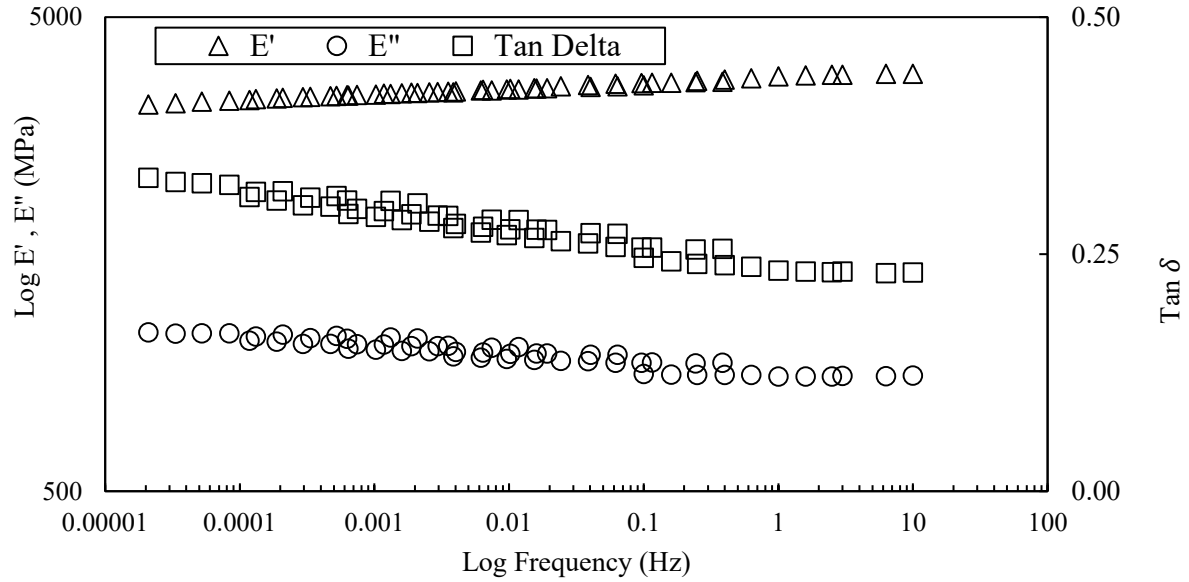

Figure 45. Flax/VE master curves generated by horizontal shifting of storage modulus curve

TA Instruments Data Analysis was employed to move curves simultaneously and shift them both horizontally and vertically. Resulting master curves are presented in Figure 46. Much smoother master curves are obtained with this approach. Based on these results it is valid to conclude that vinyl ester resin reinforced with flax is thermoheologically complex material and to generate a smooth master curve both horizontal and vertical shift factors are necessary [220].

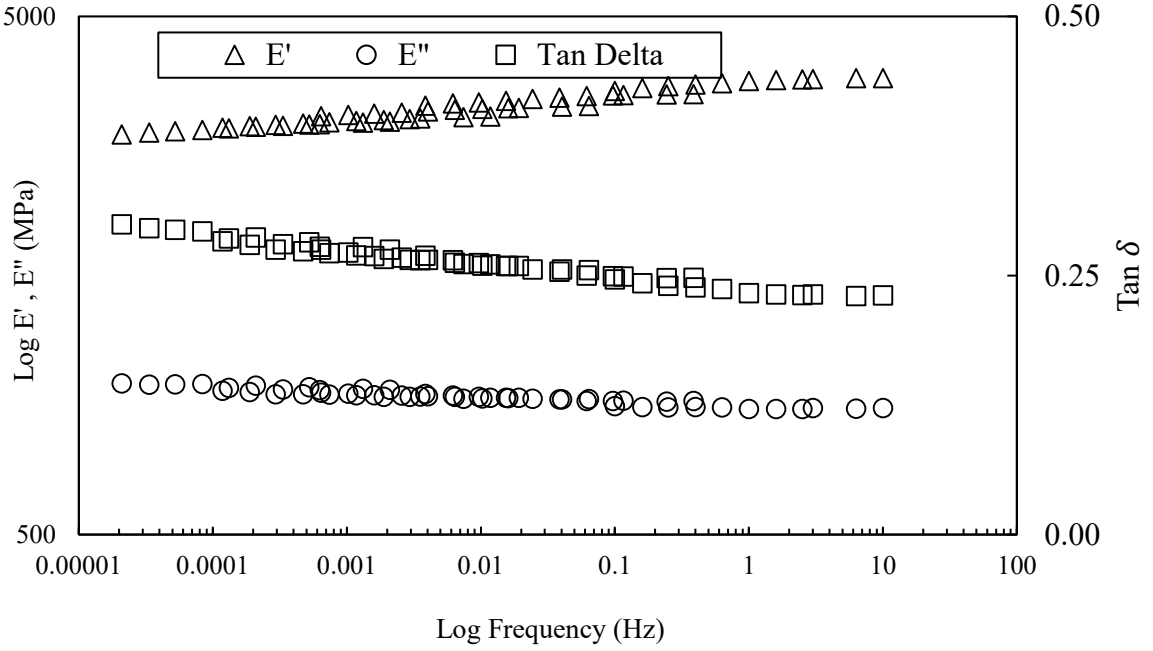

Figure 46. Flax/VE master curves obtained by horizontal and vertical shifting of the frequency sweeps

Figure 47 shows creep data collected at different temperatures. Similar to the work of other researchers for natural fiber/thermoplastics [221] and natural fiber/thermosets [214] whom only have applied horizontal shift factors and neglect the application of shift factors to other viscoelastic properties, strain curves are horizontally shifted in reference to the strain curve at 30 °C to generate creep master curve presented in Figure 48. As observed, an acceptable smooth master curve is obtained by this method.

Now the horizontal shift factors obtained from shifting the storage modulus curve (Figure 45) will be applied. The results are presented in Figure 49. As seen, the creep curves do not superimpose and no master curve is generated. Once more this is the indication that horizontal shift factors are not solely sufficient to generate a master curve. In the next step, both horizontal and vertical shift factors obtained from shifting storage, loss modulus and tan δ curves (Figure 46) are used to shift creep data and the result master curve shown in Figure 50. A smooth master curve is obtained by this method. In addition, by comparing the master curve obtained by horizontal shifting of creep data, with the curve obtained with horizontal and vertical shifts, it is perceived that the latter covers wider range on the time axis.

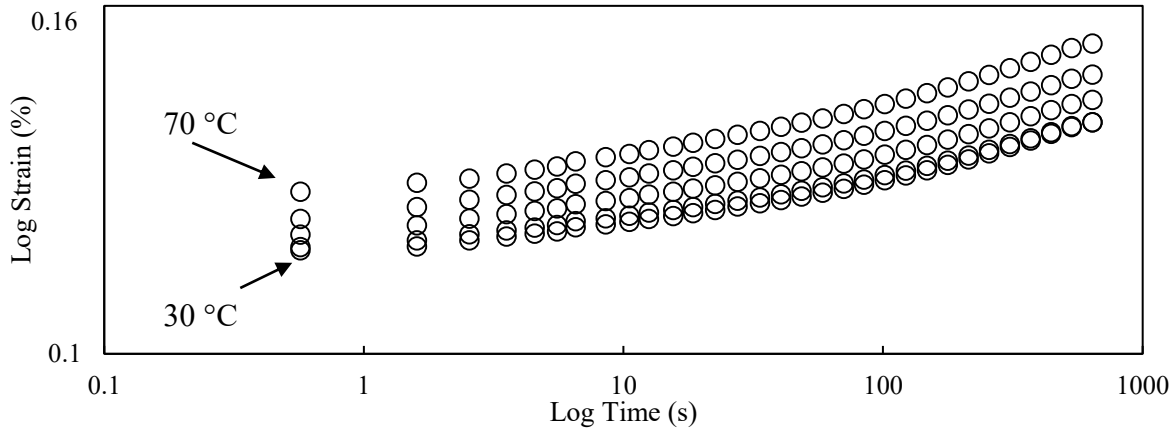

Figure 47. Creep strain vs time at different temperatures for flax/VE composites

As mentioned before, a creep test was performed at 30 °C for 24 hours to check the validity of the obtained master curves. Creep data at 30 °C was used to find the parameters in Findley and Nutting Power Laws. The parameters then were used to extrapolate the creep data to 24 hours. Extrapolated curves and actual creep data for 24 hrs are presented in Figure 51. At longer times there is deviation between both models and actual creep data. However, Findley Power Law stays closer to the actual creep data. In addition Findley Power Law over estimates the strain creep values therefore provides more conservative values of creep strain.

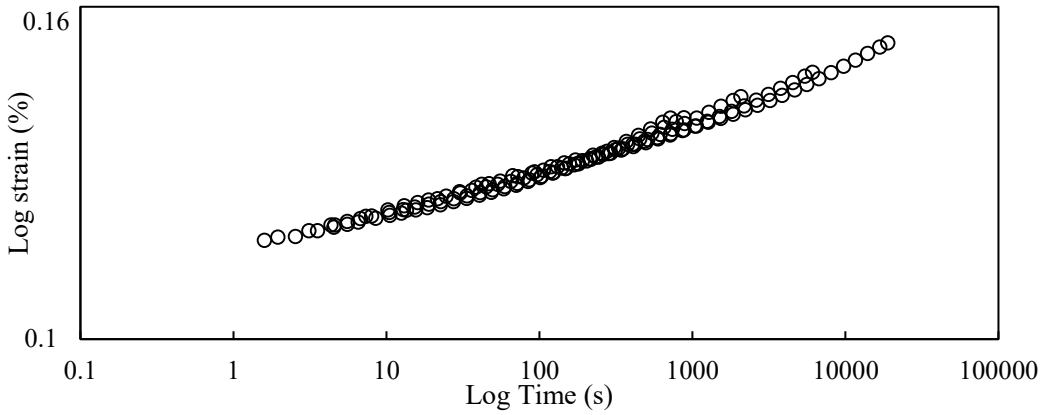

Figure 48. Creep strain master curve at 30 °C obtained by horizontal shifting of creep data at different temperatures for flax/VE composites

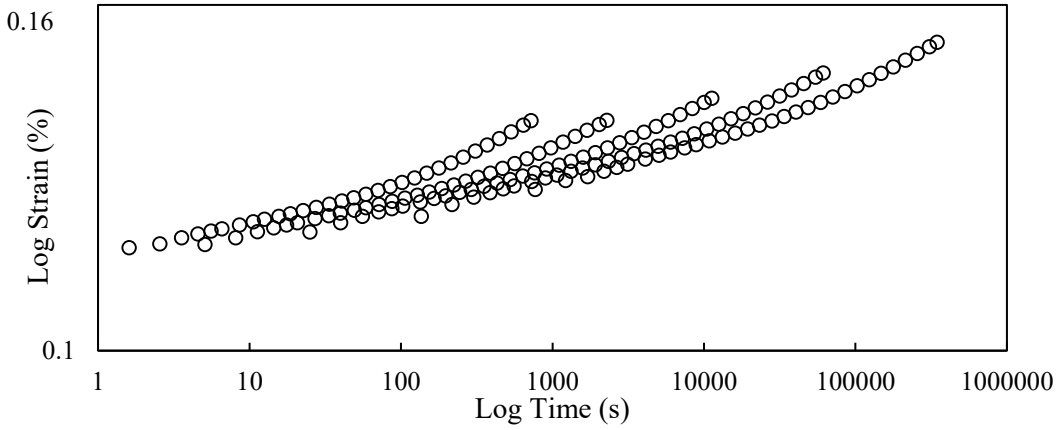

Figure 49. Creep strain curves at different temperatures shifted by the horizontal shift factors obtained from storage modulus master curve for flax/VE composites

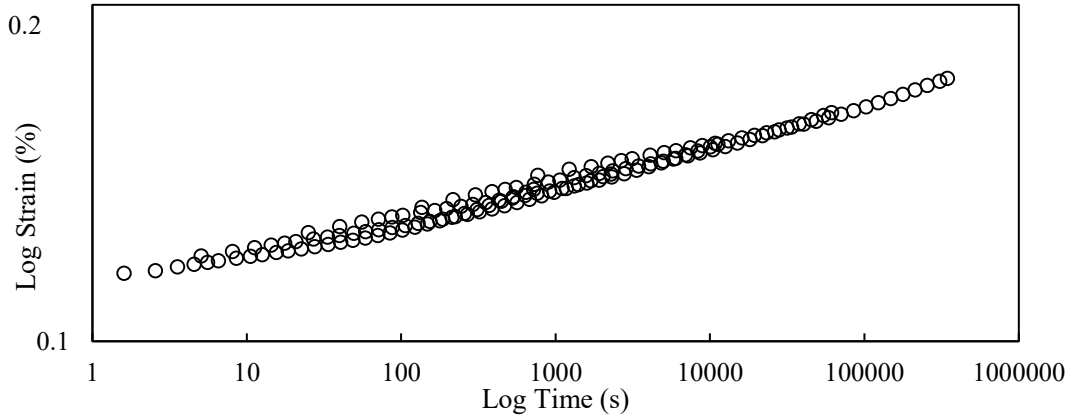

Figure 50. Flax/ VE creep strain master curve generated by horizontal and vertical shift factors

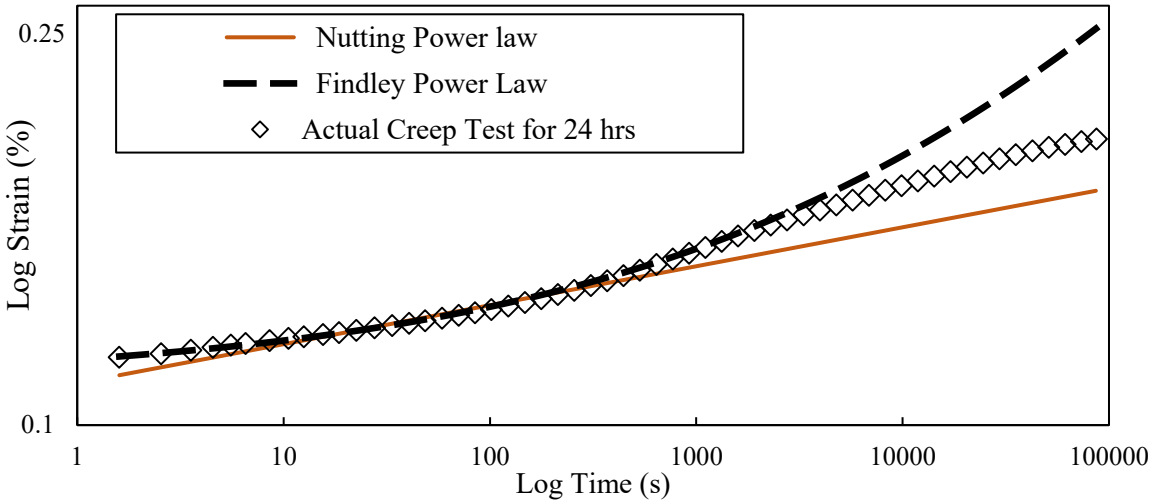

Figure 51. Comparison of extrapolated creep data with Nutting and Findley Power Laws with actual creep data for 24 hours for flax/VE composites

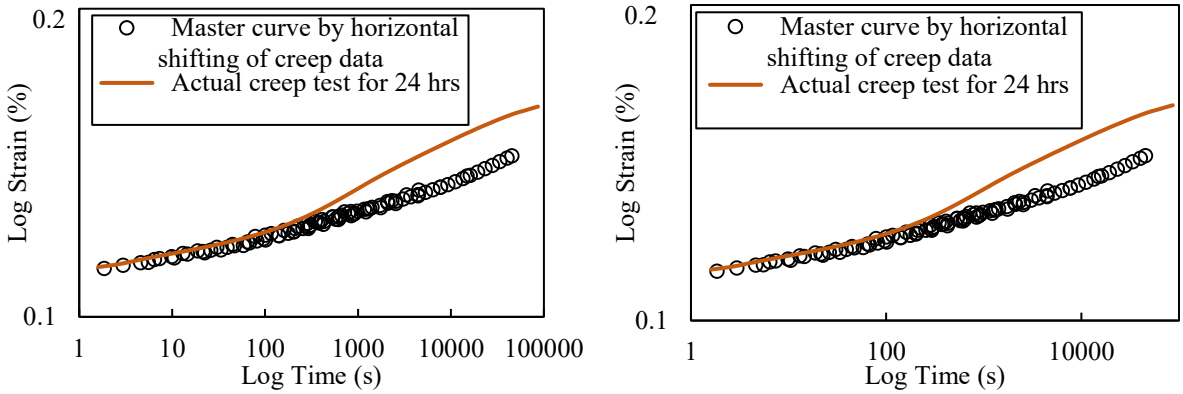

Figure 52. Comparison of actual creep data for 24 hours with (a) master curve generated by horizontal shifting of creep data, (b) master curve generated by horizontal and vertical shift of creep data for flax/VE composites

Figure 52 shows the comparison of the actual creep data with two master curves generated with horizontal shift factors, and horizontal and vertical shift factors. There is not noticeable difference between two master curves and in both curves, there is deviation from actual creep data at longer times and both master curves tend to underestimate creep strain. Future studies are required to investigate the reason behind this behavior which will be addressed later in this dissertation.

3.4.6. Frequency Sweep of Flax/MESS

Results of frequency sweeps are presented in Figure 53. A horizontal shifting of the storage modulus values was performed using TA Instruments Data Analysis software. To perform the shifting process, storage modulus curve at 30 °C was selected as the reference curve, and all other curves were shifted to the left. In this process, loss modulus curves and tan δ curves were also shifted with the same values of shift factors. The resulting plots are presented in Figure 54.

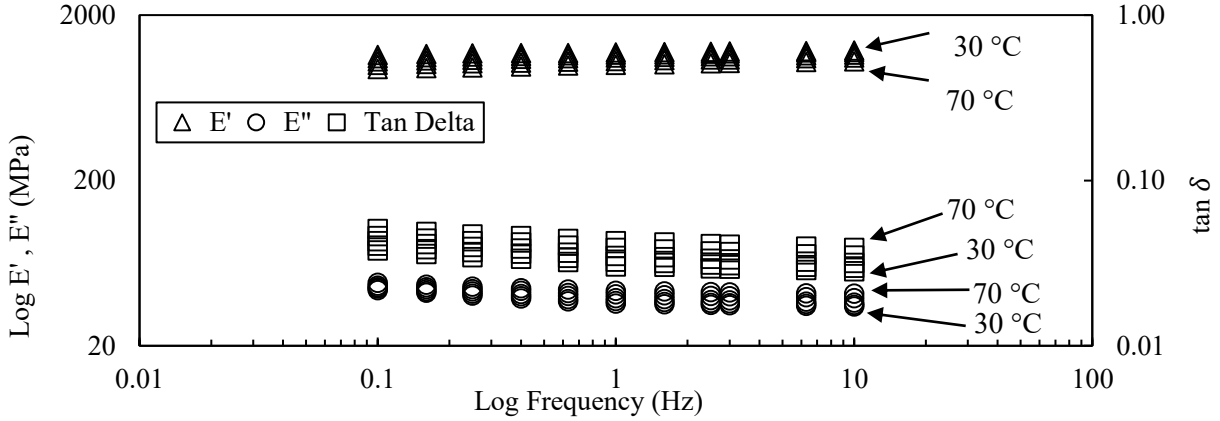

Figure 53. Frequency sweep of flax/MESS composite at different temperatures

Based on Figure 54, although a smooth master curve is obtained for the storage modulus, the curves for loss modulus and tan δ are not satisfactory. This is indication of the fact that again only one set of horizontal shift factors is not enough for all three sets of curves.

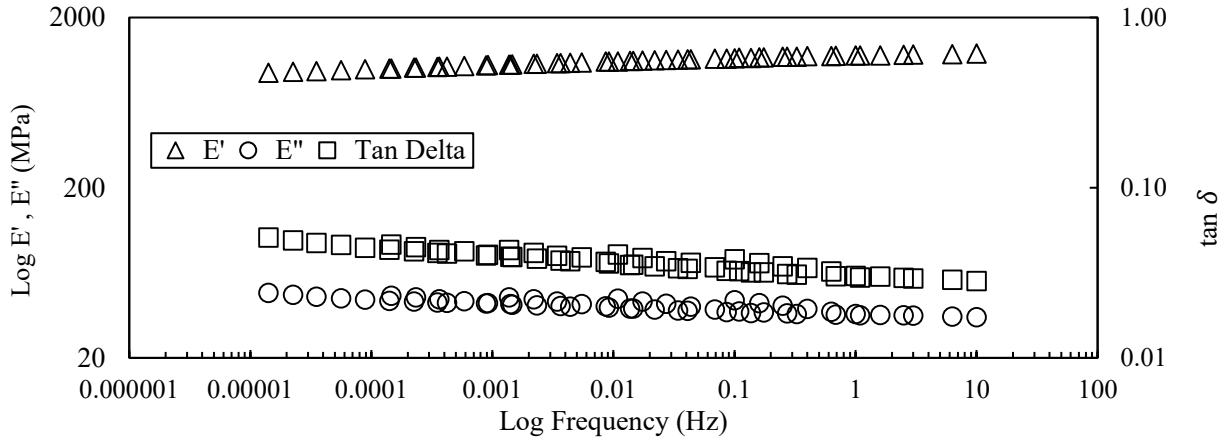

Figure 54. Flax/MESS master curves generated by horizontal shifting of storage modulus curve

TA Instruments Data Analysis was again employed to move curves simultaneously and shift them both horizontally and vertically. The resulting master curves are presented in Figure 55. Much smoother master curves are obtained with this approach. Based on these results it is valid to conclude that MESS resin reinforced with flax fiber is thermorheologically complex material and to generate a smooth master curve both horizontal and vertical shift factors are necessary [220].

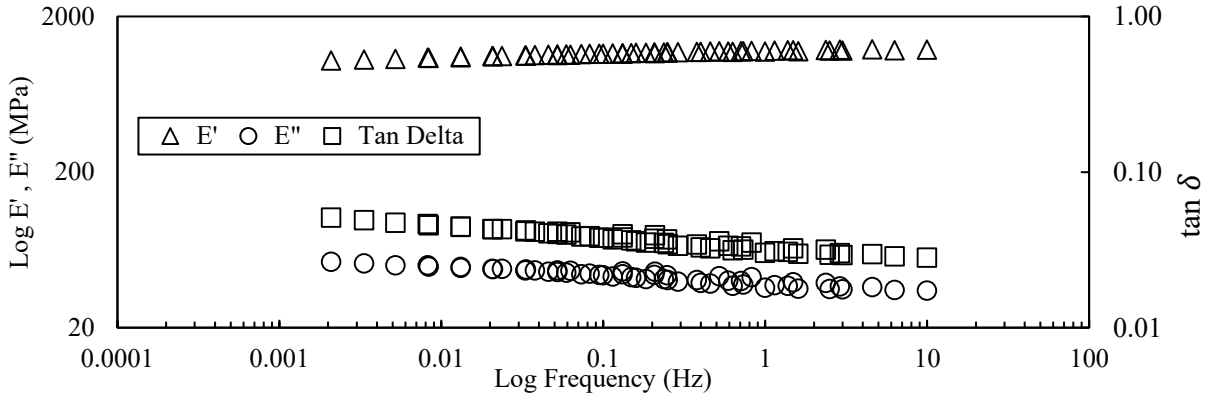

Figure 55. Flax/MESS master curves obtained by horizontal and vertical shifting of the frequency sweeps

Horizontal shift factors used in Figure 54 are plotted in Figure 56a. Horizontal and vertical shift factors used in Figure 55 are plotted in Figure 56b. The dependency on temperatures of shift factors, both for horizontals and vertical shift factors, complies with the Arrhenius equation, which has the following form [214]:

$$\ln(a_T) = \frac{Q}{R}\left(\frac{1}{T} - \frac{1}{T_r}\right) \tag{24}$$

where a_T is the shift factor, T_r (K) is the reference temperature and T (K) is an arbitrary temperature at which horizontal shift factor a_T is desired. In this equation, Q is the activation energy (kJ/mol) and R is the universal gas constant (J/mol·K).

Based on Figure 56, the corresponding values for Q could be calculated using Equation (24). The calculated value for activation energy is 47.52 (kJ/mol) considering only horizontal shift

factors of Figure 56a. If both horizontal and vertical shift factors of Figure 56b are considered, the values of Q are calculated to be 55.48 (kJ/mol) and 42.95 (kJ/mol) based on horizontal shift factors and vertical shift factors, respectively.

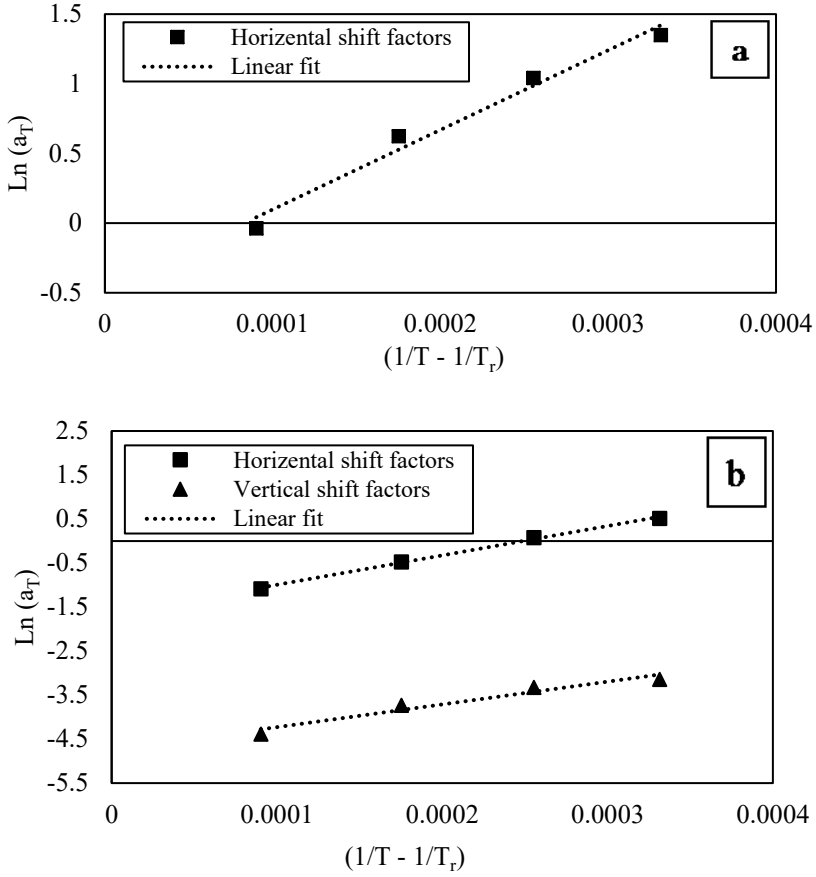

Figure 56. (a) Horizontal shift factors when only horizontal shift factors are used; (b) horizontal and vertical shift factors when both are used for flax/MESS composites

Figure 57 shows creep data collected at different temperatures. Similar to work of other researchers for natural fiber/thermoplastics [221] and natural fiber/thermosets [214] whom only have applied horizontal shift factors and neglected the application of shift factors to other viscoelastic properties, strain curves are horizontally shifted in reference to the strain curve at 30 °C to generate creep master curves presented in Figure 58. As observed, an acceptably smooth master curve is obtained by this method.

Horizontal shift factors obtained from shifting the storage modulus curve in Figure 54 were applied. The results are presented in Figure 59. As seen, the creep curves do not superimpose and no satisfactory master curve is generated. Once more this is an indication that horizontal shift factors are not solely sufficient to generate a master curve. In the next step, both horizontal and vertical shift factors obtained from shifting storage, loss modulus and tan δ curves in Figure 55 is used to shift creep data. The result is a master curve shown in Figure 60. A smooth master curve is obtained by this method. In addition, by comparing the master curve obtained by horizontal shifting of creep data, with the curve obtained with horizontal and vertical shifts, it is perceived that the latter covers a wider range on the time axis.

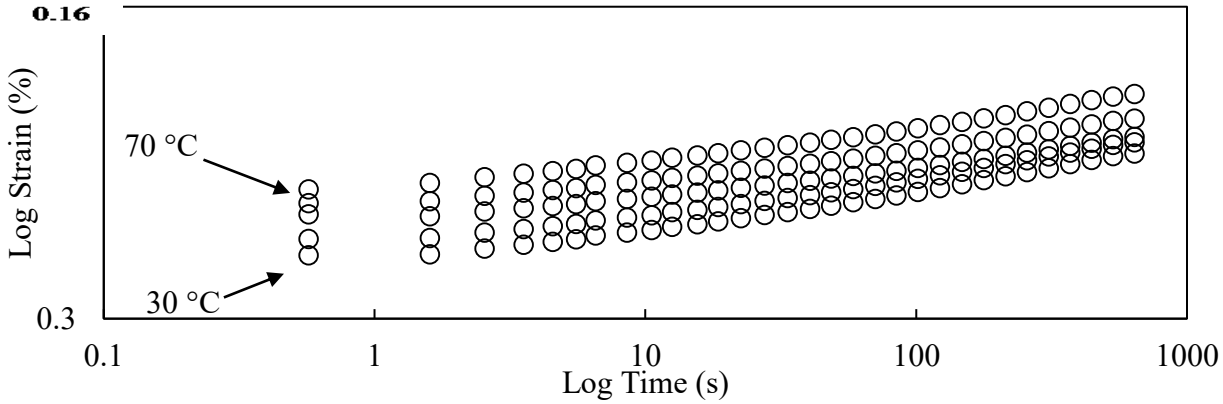

Figure 57. Creep strain vs time at different temperatures for flax/MESS composites

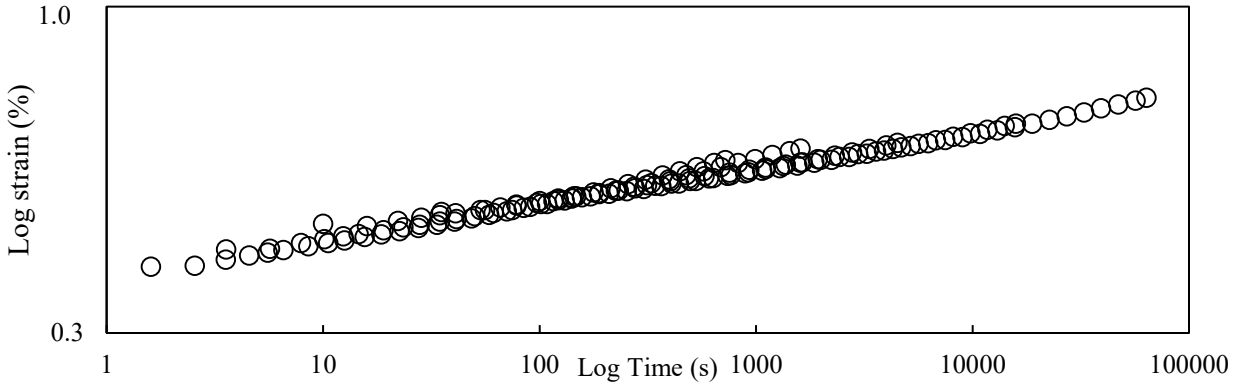

Figure 58. Creep strain master curve at 30 °C obtained by horizontal shifting of creep data at different temperatures for flax/MESS composites

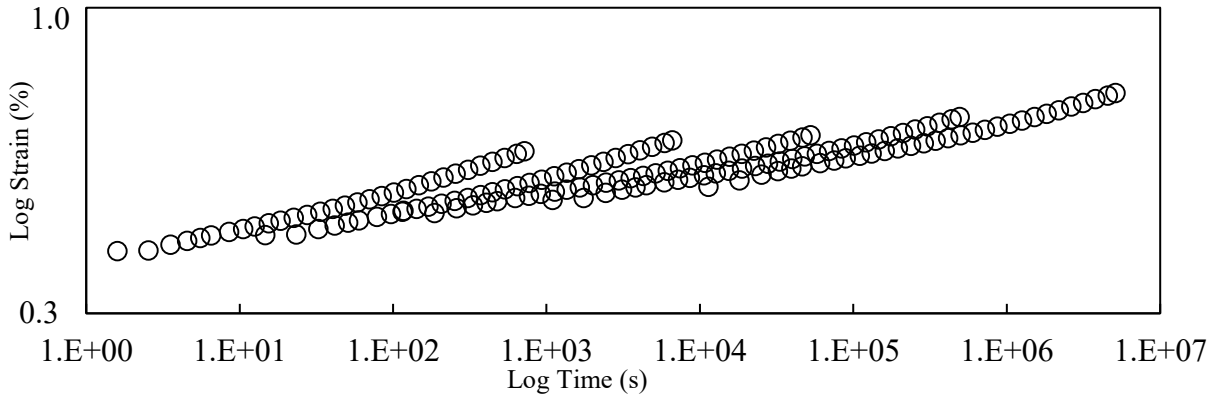

Figure 59. Creep strain curves at different temperatures shifted by the horizontal shift factors obtained from storage modulus master curve for flax/MESS composites

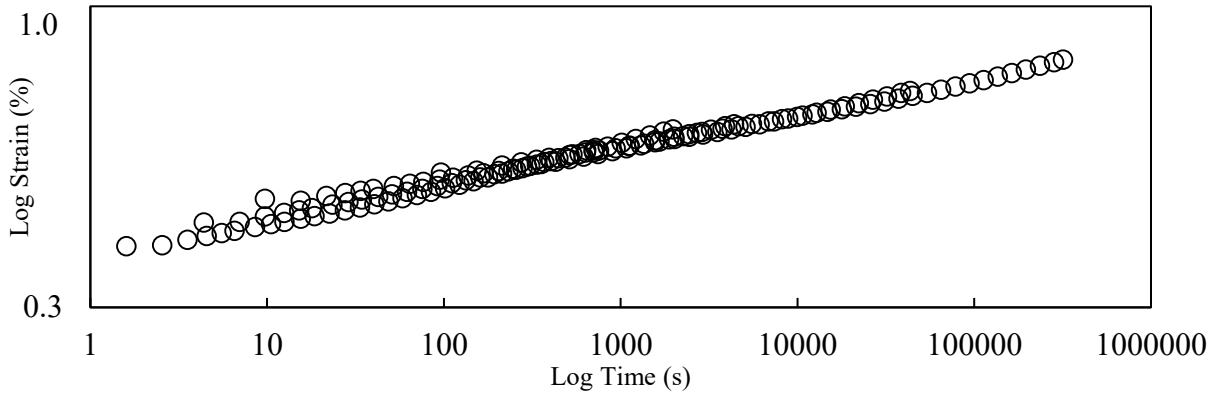

Figure 60. Creep strain master curve generated by horizontal and vertical shift factors for flax/MESS composites

As mentioned before, a long-term creep test was performed at 30 °C for 24 hours to check the validity of the obtained master curves. Creep data at 30 °C was used to find the parameters in Findley Power Law and Nutting Power Law. The parameters then were used to extrapolate the creep data to 24 hours. Extrapolated curves based on Findley Power Law and actual creep data for 24 hours are presented in Figure 61. At longer times there is deviation between Findley model and actual creep data. However this model over estimates the strain creep values therefore provides more conservative values of creep strain. On the other hand, Nutting Power Law has a much better estimate of the creep data and stays closer to actual data.

Figure 62 shows the comparison of the actual creep data with two master curves generated with horizontal shift factors, and horizontal and vertical shift factors. In both curves, there is a deviation from the actual creep data at longer times and both master curves tend to underestimate the creep strain.

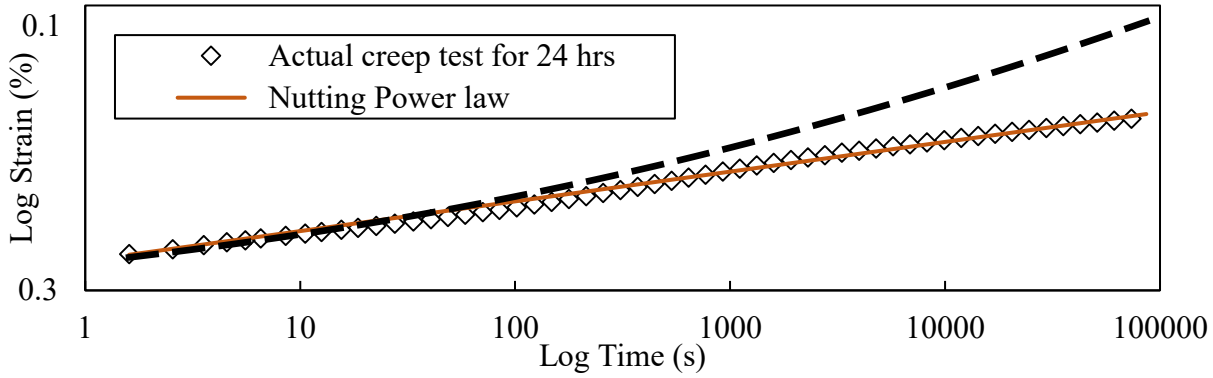

Figure 61. Comparison of extrapolated creep data with Nutting and Findley Power Laws with actual creep data for 24 hours for flax/MESS composites

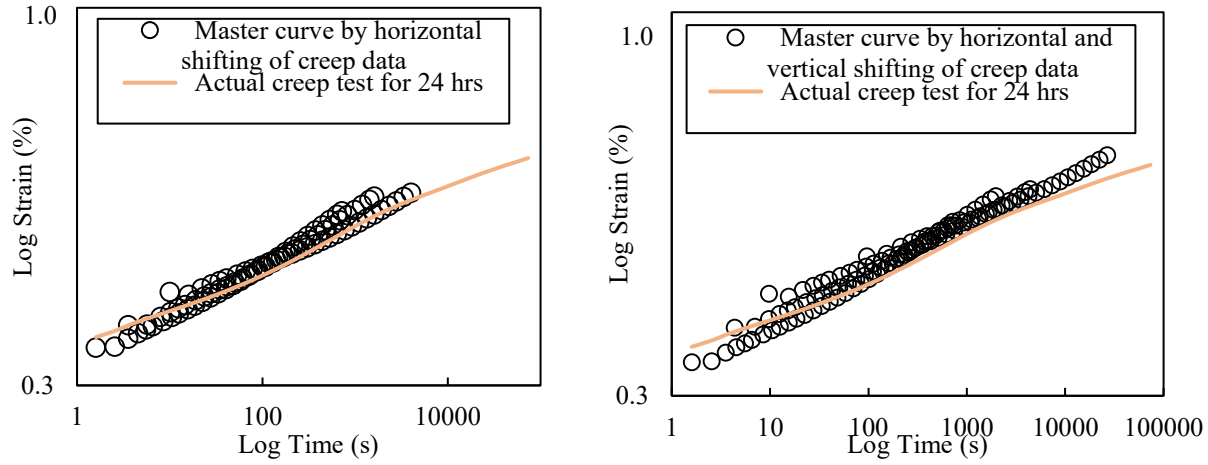

Figure 62. Comparison of actual creep data for 24 hours with (a) master curve generated by horizontal shifting of creep data, (b) master curve generated by horizontal and vertical shift of creep data for flax/MESS composites

Figure 62 shows the comparison of the actual creep data with two master curves generated with horizontal shift factors, and horizontal and vertical shift factors. In both curves, there is a

deviation from the actual creep data at longer times and both master curves tend to underestimate the creep strain.

Based on results presented in Figure 51 and Figure 61, it is observed that flax/VE experimental results agree better with Findley power law, while Nutting power law is a better representation of experimental creep data for flax/MESS composites. The reason behind this behavior lies within the differences between the structures of these two resins. MESS resin has more functional group compares to VE, and therefore has a higher cross linking density after curing. Higher crosslinking density will result in a more brittle resin; therefore, the flax/MESS composite will have a higher resistance to creep deformation. Nutting power law is generally a more conservative model compared to Findeley, and consequently would agree better with results of creep deformation for flax/MESS composite.

3.5. Long-Term Behavior - Accelerated Weathering

3.5.1. SEM Images

SEM images were taken of the tensile tested unweathered treated and untreated fiber composites. Figure 63 shows adhesion of resin to fiber before and after treatment. The untreated fibers of matrix materials VE, MESS, and DMESS show relatively little residual resin on the pulled out fibers. While the fibers appear clean, small pieces of resin did adhere in areas of uneven fiber surface. The treated fibers are noticeably less clean with multiple and larges areas of matrix adhered material. Figure 64 provides more detail regarding the pull out area of the fibers. As anticipated, the untreated fibers pulled out of the matrix material, and ultimate composite facture was due to fiber strength only. This is obvious by comparing Figure 64a and Figure 64b where there are lots of sites where fibers were pulled out, while in Figure 64 d and Figure 64e this trend is not as apparent.

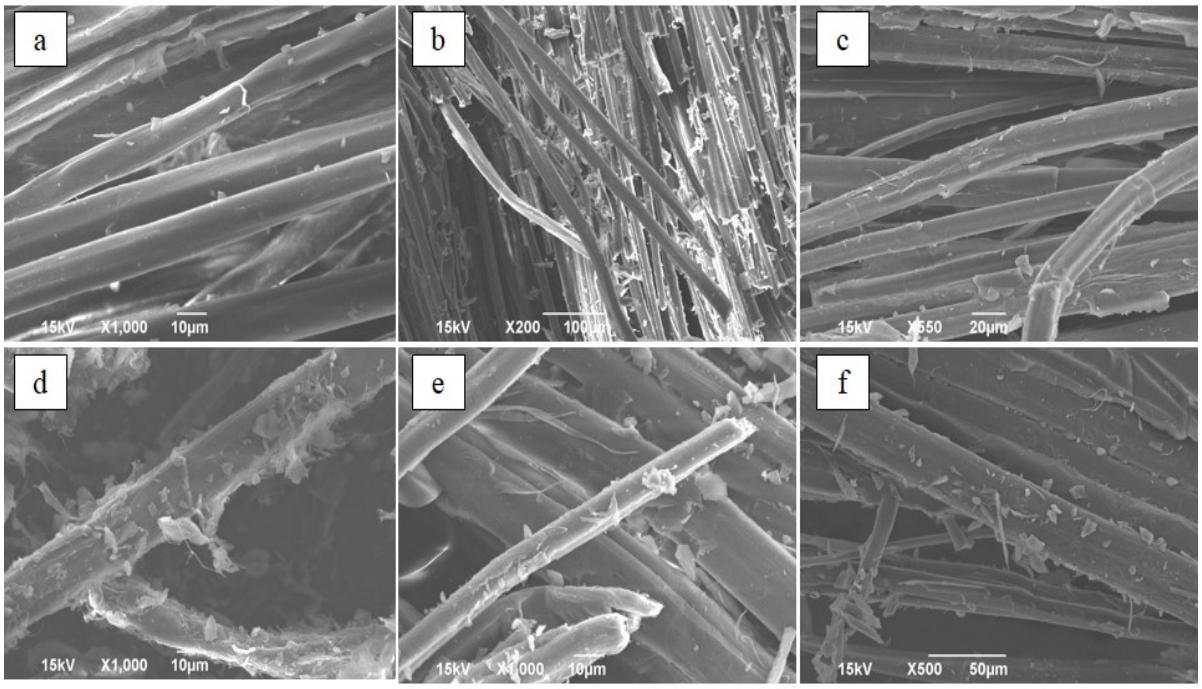

Figure 63. SEM images showing resin adhesion before and after alkaline treatment for a) UTUW-VE, b) UTUW-MESS, c) UTUW-DMESS, d) TUW-VE, d) TUW-MESS, f) TUW-DMESS

As shown in Figure 64c, the gap between the fiber and resin indicates poor bonding between the fiber and matrix. Unlike the untreated fibers, the treated fibers show a clean break at the matrix fiber plane. The minimal gap between the fiber and resin indicates a strong bond in the composite. In addition, Figure 64e, fiber breakage without fiber/matrix debonding. Also, the matrix cracks between fibers are indication of more efficient load sharing.

3.5.2. Mechanical Properties Before and After Weathering Exposure

Samples of the composites produced in this study were then subjected to accelerated weathering conditions. The designed cycles, the condensation and UV radiation cycles, emulate exposure to humidity & precipitation, and exposure to sunlight, respectively, as this is the usually the case for what composites in structural and aerospace applications would experience [222]. Figure 65 (a) presents the resulting losses in properties suffered by these samples. Properties across

all composite types show between 0.5% - 63% decrese after being exposed to accelarated weathering. The biggest loss in properties was observed in tensile strength of UTW-VE (untreated flax-VE) composites with 63% decrese while tensile strength of alkline treated flax using the same matrix decreased only 46%. Unexpectedly, tensile modulus of flax-VE and flexural modulus of treated flax-VE was increased after experincing weathering. This was also obsevred in the results presented in [212]. This could be attributed to loss of unreacted styrene monomer when exposed to higher temperature which will result in embroilment of the composite. Also, as stated by Taylor et. al. [212] this is likely result is a product of abnormally low un-weathered values.

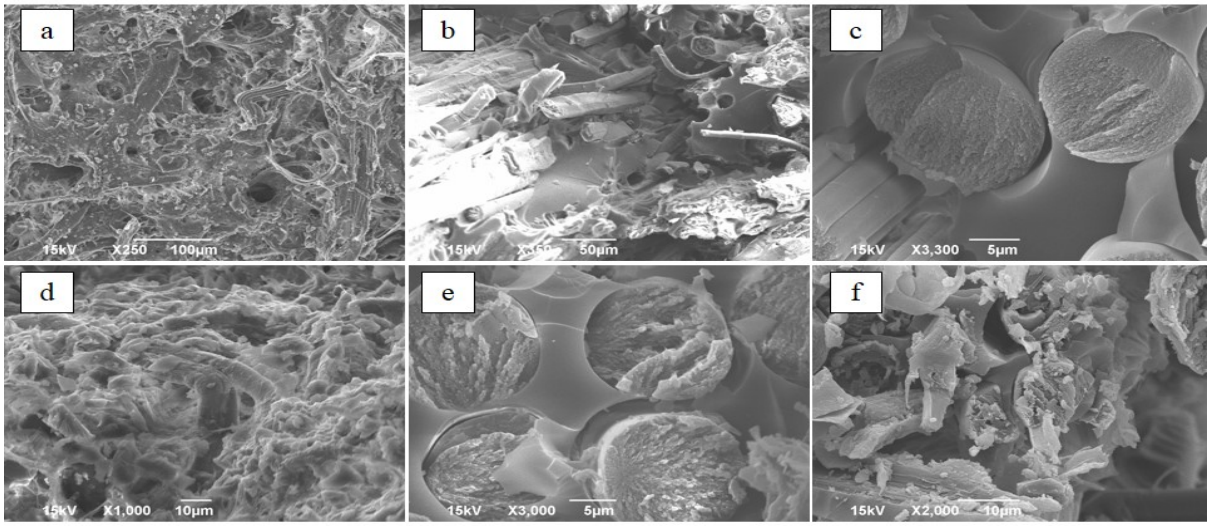

Figure 64. SEM images showing fiber pull-out before and after alkaline treatment for a) UTUW-VE, b) UTUW-MESS, c) UTUW-DMESS, d) TUW-VE, e) TUW-MESS, f) TUW-DMESS

In order to investigate the effect of fiber treatment on property decrease of manufactured composites, the average percentage of property decrease for composites using untreated vs treated fibers were plotted as presented in Figure 65 (b). As seen, except for the flexural strength, other properties fared better when incorporating alkaline treated flax fiber. Among all properties, ILSS had the least amount of decrease with 22% and 20% decrease for untreated and treated, respectively. Overall, tensile and flexural moduli of weathered composites using treated flax fiber,

are still within target range set for this study. For flexural strength and ILSS, this is true only for treated flax-VE composite sample.

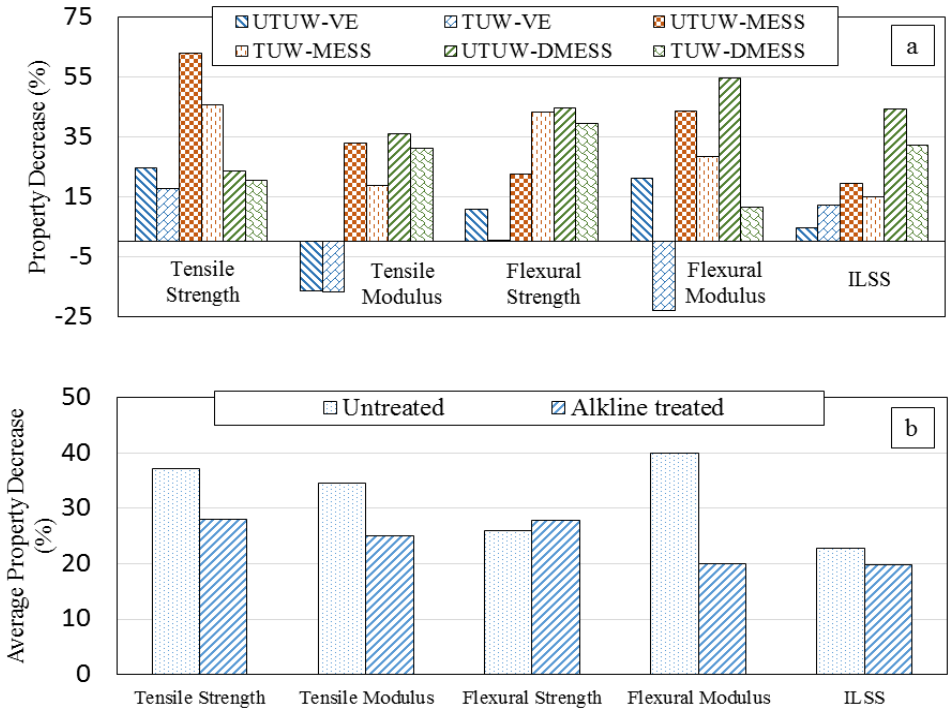

Figure 65. (a) Percent property decrease with weathering, and (b) average property decrease for untreated and alkaline treated flax fiber composites

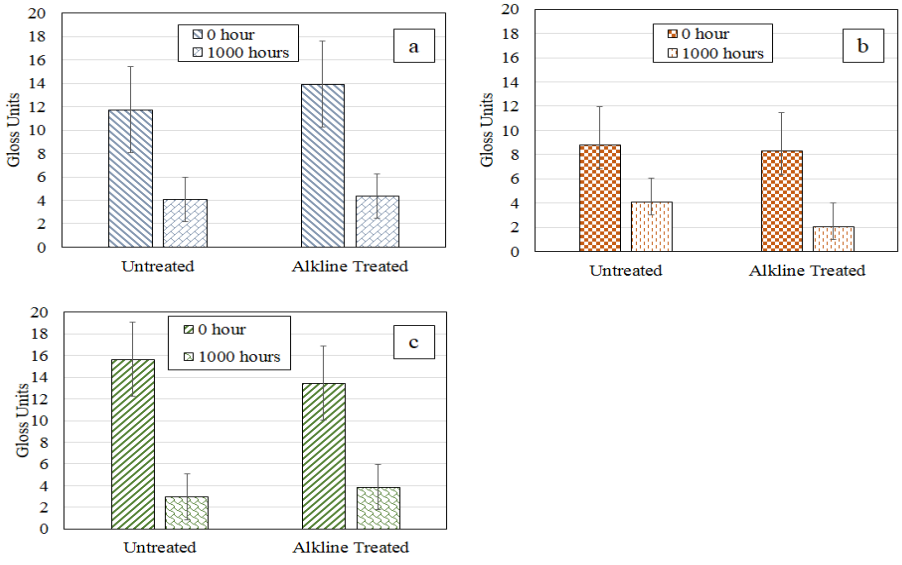

Figure 66. a) Flax-VE gloss at 85° before and after 1000h UV exposure, b) flax-MESS gloss at 85° before and after 1000h UV exposure, c) flax-DMESS gloss at 85° before and after 1000h UV exposure

3.5.3. Gloss and Color Change after Weathering Exposure

In general, manufactured composite panels exhibit minimal gloss before weathering; therefore, the gloss measurements at 85° reflectance are the most important. As shown in Figure 66, after 1000 hours of constant UV and moisture exposure, the UTW-VE and TW-VE showed a 65.1% and 68.5% gloss change, respectively. The UTW-MESS was 53.7% different, and TW-MESS was 75.4% changed. The DMESS weathered panels showed an 81% change in gloss for untreated fibers and 71.2% change for treated fibers. In general, the bio-resins MESS and DMESS showed greater propensity to lose gloss than petroleum based VE. UTW-MESS does not follow this trend which can be attributed to uneven weathering due to panel warpage during the process.

In addition to the gloss change, color change of the composites was observed. The measured value of ΔL denotes a bleaching of the composite and Δb is yellowing. As demonstrated by Figure 67, untreated resins showed less bleaching than treated fibers. Because the fiber treatment utilized sodium hydroxide which creates more hydroxide groups on the fiber surface [212], the increase in bleaching is expected in treated fibers. Also, VE yellowed significantly while the biobased resins did not. Due to the high aromatic content of vinyl ester resin, this result is expected.

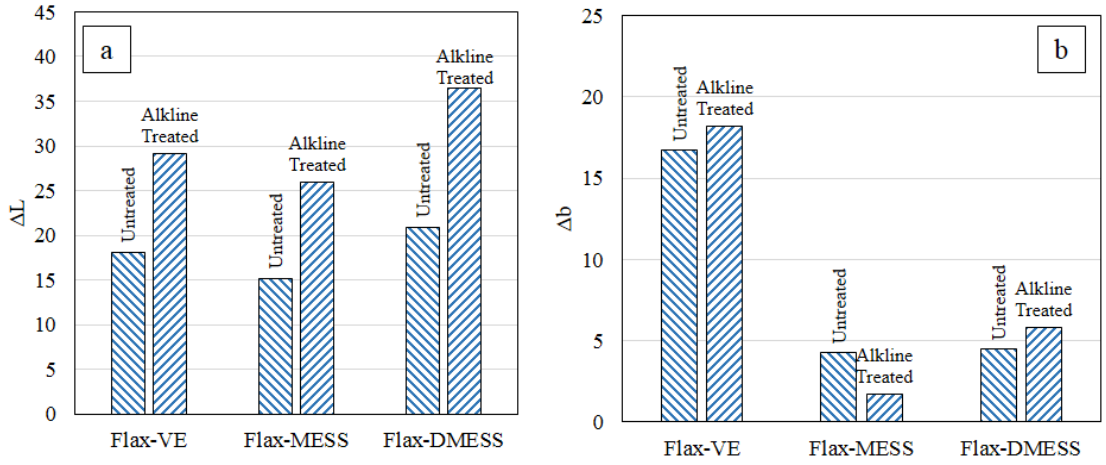

Figure 67. a) Lightness difference (ΔL*), b) yellow color difference (Δb*), after UV exposure

3.6. Characterization Methods Development

3.6.1. Void Fraction Calculation

3.6.1.1. Conventional Method

Results of fiber volume fraction and void fraction measurements using density measurements and Equations 16-19 are presented in Table 22.

Table 22. Results of fiber volume fraction and void fraction in manufactured composite samples

Composite description	Fiber volume fraction	Void fraction
Type 1 – VE	34.50%	9.14%
Type 2 – VE	39.13%	8.24%
Type 3 – VE	37.75%	8.29%
Type 4 – VE	36.60%	7.68%
Type 5 – VE	30.13%	6.88%
Type 1 – MESS	31.43%	13.46%
Type 2 – MESS	33.45%	13.54%
Type 3 – MESS	29.80%	13.43%
Type 4 – MESS	34.47%	11.58%
Type 5 – MESS	23.60%	7.23%

A typical 3D micro-CT image is shown in Figure 68. As observed, micro-CT can reveal any manufacturing flaws in the specimen, such as voids, delaminated plies and cracks.

In order to analyze the images and find the percentage of the void, after loading each image into the MATLAB® code, the opacity of the image is changes so as there is only black and white areas in the image. The white areas in the image are indication of fiber and matrix while black areas are either cracks or voids present in the material. In addition, the image is trimmed to remove the black background of the image. The original image and modified image is shown in Figure 69. After these corrections are made, percentage of black areas is calculated for one image, and the average over all images (300 images for a 3mm thick specimen) processed from one specimen is calculated.

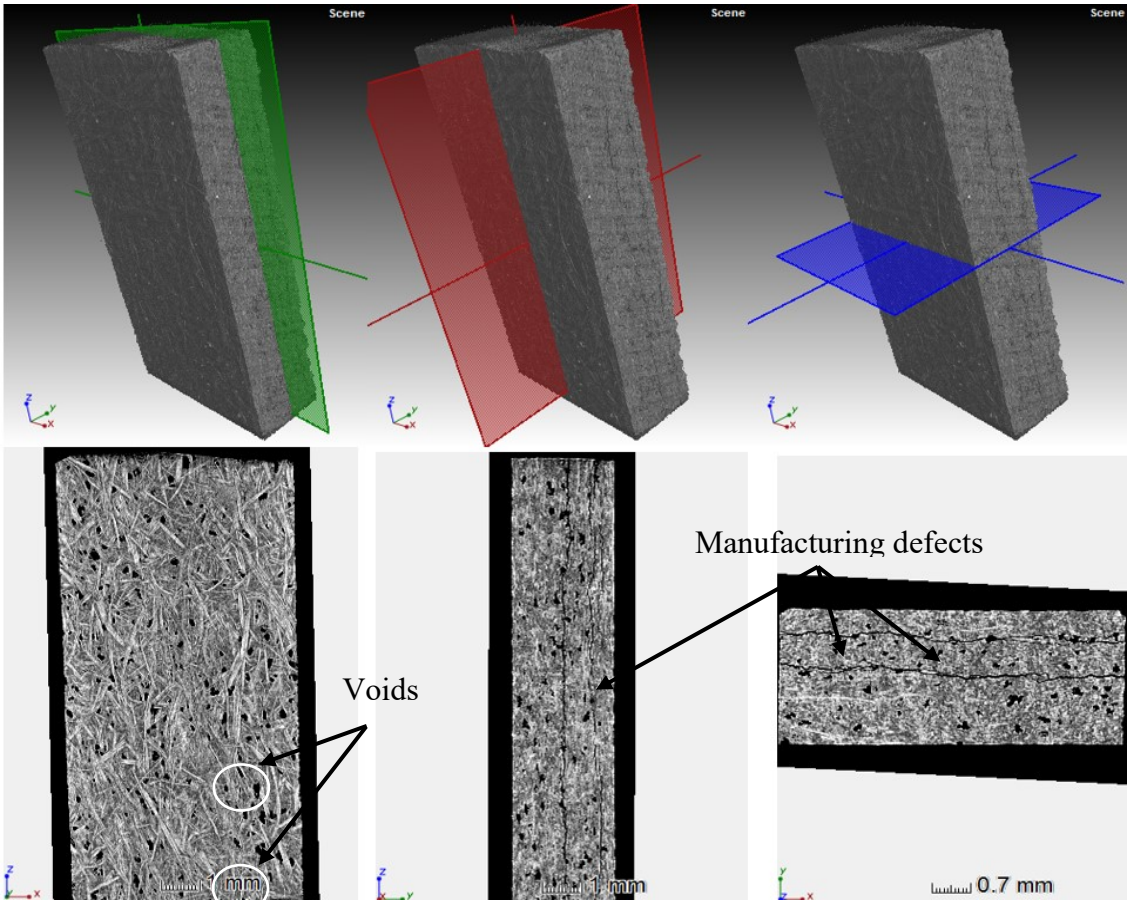

Figure 68. A typical micro-CT scan of a specimen from a composite panels

Table 23 compares the results of void fraction measurements by conventional method and use of image processing method. Also, the percentage differences in the results are presented.

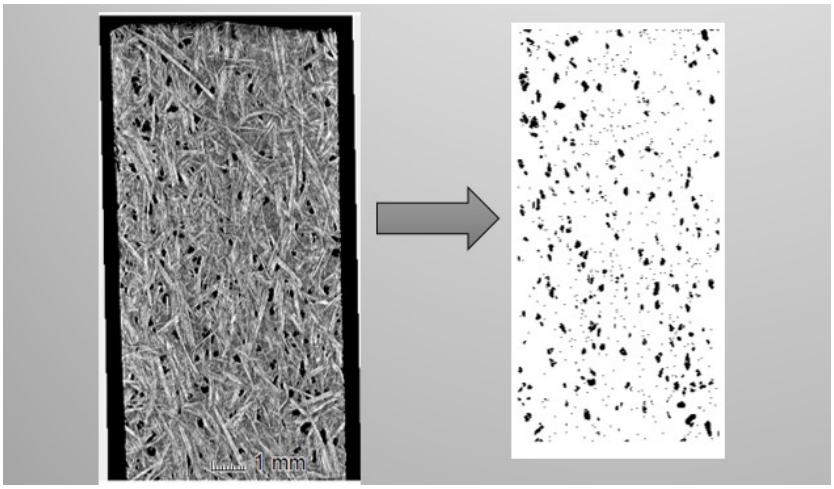

Figure 69. Correction on images done by the MATLAB® code (removal of black background)

As mentioned before, using submersion method to find the density of natural fibers and composites is always a challenging task which is never free of errors. The errors can be introduced in any stage of the measurements. One alternative is to find the density of natural fibers with more accurate methods such as gas pycnometry. One disadvantage of this method can be mentioned that it is not available in every lab setup. On the other hand, using micro-CT can be accurate and easier method to employ.

Table 23. Comparing results of void fraction measurements

Composite description	Void fraction		
	Conventional method	Micro-CT scans	Difference (%)
Type 1 – VE	9.14%	9.03%	1.2
Type 2 – VE	8.24%	7.98%	3.15
Type 3 – VE	8.29%	7.94%	4.22
Type 4 – VE	7.68%	7.21%	6.12
Type 5 – VE	6.88%	6.40%	6.97
Type 1 – MESS	13.46%	13.23%	1.71
Type 2 – MESS	13.54%	13.32%	1.62
Type 3 – MESS	13.43%	13.22%	1.56
Type 4 – MESS	11.58%	11.36%	1.89
Type 5 – MESS	7.23%	7.12%	1.52

3.6.2. Flax Fiber Density Development

3.6.2.1. First Set of Tests

Results of the initial stage of this study are presented in Table 24. For each test, minimum of three and maximum of seven specimens were tested. After a few samples were tested in distilled water with the mass of between 0.1 g to 0.2 g it was determined that minimum of 0.25 g specimens were needed so achieve better results. Therefore, all the results presented here are measurements based on 0.3 g of specimen size.

As observed, increased immersion time in distilled water from 1 min to 3 min has increased the value for density of the flax fiber. This is because of moisture absorption by the fiber due to hydrophilic property of flax. Because of this observation, distilled water was not considered to be used as an option for immersion fluid. Same trend is also observed when canola oil is used with different immersion times, however the difference in measured density is not significant for canola oil.

Table 24. Density measurements using Archimedes method using distilled water and canola oil

Immersion fluid	Density of fluid (g/cm^3)	Vacuum pressure (kPa)	Immersion time (min)	Density (g/cm^3)
Distilled Water	0.998	none	1	1.4227±0.1075
Distilled Water	0.998	none	3	1.4464±0.1487
Distilled Water	0.998	none	6	1.4779±0.1709
Canola Oil	0.9115	none	1	1.3641±0.0238
Canola Oil	0.9115	none	3	1.3665±0.0235
Canola Oil	0.9115	none	6	1.3698±0.0250
Canola Oil	0.9115	70	3-6	1.3691±0.0238
Canola Oil	0.9115	100	3-6	1.4698±0.0286

3.6.2.2. Ruggedness Test for Influential Factors

Ruggedness test were performed three times. The first test with lower pressure levels, pressure levels were increased for second ruggedness test and to confirm the results of second test, a third test was repeated with the same parameters as the second ruggedness test.

Density measurements were carried out based on buoyancy method as explained in the procedure section. All test were conducted at room temperature, 23 ºC. The design is replicated which means a second block of runs using the same factor settings as the original design is run. The density measurement results are presented in Table 25 in *Rep 1* and *Rep 2 Test Results* columns. Factors main effects were calculated using the average values (Rep Ave) of each design

point for the two replicates. For the current test results, S_d, S_{rep} and S_{effect} are also calculated and shown at the bottom of Table 25.

Statistical significance of the factor effects and half normal values for the half-normal plot are presented in Table 26. Student *t*-value was calculated by dividing each effect by S_{effect} with $(N-1)\times(rep-1)$ degrees of freedom, seven for the current design. The *p*-value is the two-sided tail probability of student's *t* with seven degrees of freedom.

The half-normal plot is shown in Figure 70 (a). Replicate error is shown with a line with slope of $1/S_{effect}$, plotted for the comparison. Estimated effects are plotted by black diamonds. The factors that fall the farthest from the replicate error line have the potential to be significant factors.

Table 25. Density measurements of flax fiber ruggedness test calculations for first test

PB order	Run#	A	B	C	E	Rep 1 Test Results	Rep 2 Test Results	Rep Ave	Rep Difference
1	2	+1	+1	+1	+1	1.270	1.359	1.314	0.089
2	4	-1	+1	+1	-1	1.501	1.430	1.465	-0.071
3	6	-1	-1	+1	+1	1.339	1.331	1.335	-0.008
4	8	+1	-1	-1	+1	1.341	1.324	1.332	-0.016
5	5	-1	+1	-1	+1	1.224	1.305	1.264	0.081
6	3	+1	-1	+1	-1	1.459	1.378	1.419	-0.081
7	1	+1	+1	-1	-1	1.375	1.413	1.394	0.037
8	7	-1	-1	-1	-1	1.367	1.442	1.405	0.075
Ave +		1.365	1.355	1.383	1.311			S_d	0.068
Ave -		1.367	1.373	1.349	1.421			S_{rep}	0.048
Main Effect		-0.002	-0.013	0.034	-0.109			S_{effect}	0.024

On the other hand, factor E, the immersion liquid used, is the farthest from the replicate error line and based on the p-value (p-value < 0.05), it is statistically significant. Based on results from the first test type of immersion liquid used can have the largest effect on the results of density

measurement for flax fiber and density measurement is rugged with regard to type of immersion liquid.

Table 26. Statistical significance of effects for density measurement of flax fiber (first test)

Effect Order	Effect	Estimated effect	Student's *t*	*p*-Value	Half-Normal Plotting Values
4	E	-0.109	-4.57	0.0026*	1.534
3	C	0.034	1.44	0.1922	0.887
2	B	-0.013	-0.56	0.5953	0.489
1	A	-0.002	-0.10	0.9197	0.157

* The marked value is statistically significant at 5% confidence level

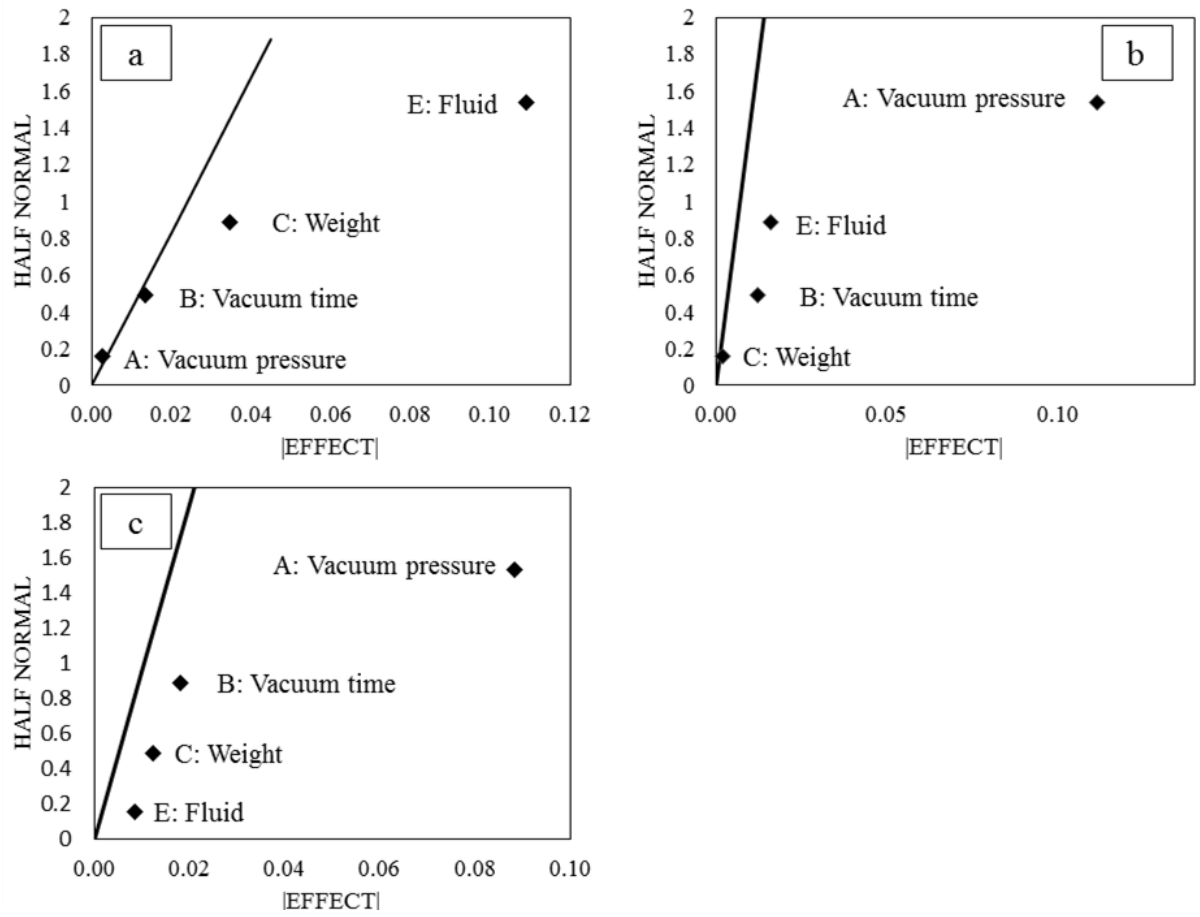

Figure 70. Half-normal plot for density measurements of flax fiber for ruggedness tests: a) first test, b) second test, c) third test

Results of the first test revealed that the type of liquid used for density measurements has the most significant effect of the results. However, during the tests, both at higher pressure and

lower pressure some amount of micro bubbles were visible attached to the specimens. Therefore, second ruggedness test was performed at higher pressures (both for Level – and Level +) and longer vacuum time. In this test, the upper levels and lower lever of pressure were 90 kPa and 50 kPa respectively. Same recommended design as Table 11 was used for this test and the results of measurements are presented in Table 27 and

To confirm this finding, a third ruggedness test was carried out with the same defined factors and levels as second test. Results are presented in Table 29, Table 30 and Figure 70 (c). As observed, again the only significant factor for this test is the vacuum pressure with the p-value < 0.001 and results of second ruggedness test was confirmed.

Table 28 and results of half-normal plot are presented in Figure 70 (b). As observed, the only significant factor for this test was the vacuum pressure with the *p*-value < 0.001.

Table 27. Density measurements of flax fiber ruggedness test calculations for second test

PB order	Run#	A	B	C	E	Rep 1 Test Results	Rep 2 Test Results	Rep Ave	Rep Difference
1	2	+1	+1	+1	+1	1.475	1.466	1.471	-0.008
2	4	-1	+1	+1	-1	1.364	1.347	1.355	-0.017
3	6	-1	-1	+1	+1	1.381	1.345	1.363	-0.036
4	8	+1	-1	-1	+1	1.494	1.492	1.493	-0.002
5	5	-1	+1	-1	+1	1.317	1.294	1.306	-0.022
6	3	+1	-1	+1	-1	1.428	1.402	1.415	-0.025
7	1	+1	+1	-1	-1	1.438	1.451	1.444	0.014
8	7	-1	-1	-1	-1	1.342	1.364	1.353	0.023
Ave +		1.456	1.394	1.401	1.408			S_d	0.020
Ave -		1.344	1.406	1.399	1.392			S_{rep}	0.014
Main Effect		0.112	-0.012	0.002	0.016			S_{effect}	0.007

To confirm this finding, a third ruggedness test was carried out with the same defined factors and levels as second test. Results are presented in Table 29, Table 30 and Figure 70 (c). As observed, again the only significant factor for this test is the vacuum pressure with the *p*-value < 0.001 and results of second ruggedness test was confirmed.

Table 28. Statistical significance of effects for density measurement of flax fiber ruggedness for the second test

Effect Order	Effect	Estimated effect	Student's *t*	*p*-Value	Half-Normal Plotting Values
4	A	0.112	15.78	0.0000*	1.534
3	E	0.016	2.27	0.0573	0.887
2	B	-0.012	-1.71	0.1316	0.489
1	C	0.002	0.28	0.7862	0.157

* The marked value is statistically significant at 5% confidence level.

Table 29. Density measurements of flax fiber ruggedness test calculations for third test

PB order	Run#	A	B	C	E	Rep 1 Test Results	Rep 2 Test Results	Rep Ave	Rep Difference
1	2	+1	+1	+1	+1	1.453	1.463	1.458	0.010
2	4	-1	+1	+1	-1	1.381	1.334	1.358	-0.047
3	6	-1	-1	+1	+1	1.367	1.371	1.369	0.022
4	8	+1	-1	-1	+1	1.457	1.441	1.449	-0.016
5	5	-1	+1	-1	+1	1.312	1.327	1.319	0.015
6	3	+1	-1	+1	-1	1.357	1.379	1.368	0.022
7	1	+1	+1	-1	-1	1.483	1.476	1.480	-0.007
8	7	-1	-1	-1	-1	1.386	1.325	1.356	-0.061
Ave +		1.439	1.404	1.388	1.399			S_d	0.030
Ave -		1.350	1.385	1.401	1.390			S_{rep}	0.021
Main Effect		0.089	0.018	-0.013	0.009			S_{effect}	0.011

Table 30. Statistical significance of effects for density measurement of flax fiber ruggedness for the third test

Order	Effect	Estimated effect	Student's *t*	*p*-Value	Half-Normal Plotting Values
4	A	0.089	7.92	0.0001*	1.534
3	B	0.018	1.65	0.1436	0.887
2	C	-0.013	-1.14	0.2912	0.489
1	E	0.009	0.75	0.4753	0.157

* The marked value is statistically significant at 5% confidence level

To confirm this finding, a third ruggedness test was carried out with the same defined factors and levels as second test. Results are presented in Table 29, Table 30 and Figure 70 (c). As observed, again the only significant factor for this test is the vacuum pressure with the *p*-value < 0.001 and results of second ruggedness test was confirmed. Based on the result of ruggedness tests, it can be concluded that factors A and B have no significant effect on the results. Based on half-normal plot, factor C has the potential to have an effect on the results of density measurement, however, by considering the p-value for this factor, indicates that the probability of a t-score as large as 1.44 is 0.1922. In other words, this factor effect is not statistically significant. Result of second and third ruggedness tests revealed that when the density measurements are taken at higher vacuum pressure, i.e. 50 & 90 kPa compared to 40 & 70 kPa, there is no significant effect from the type of fluid used to conduct the measurements. The effect order for B, C and E has changed, but according to

To confirm this finding, a third ruggedness test was carried out with the same defined factors and levels as second test. Results are presented in Table 29, Table 30 and Figure 70 (c). As observed, again the only significant factor for this test is the vacuum pressure with the *p-value* < 0.001 and results of second ruggedness test was confirmed.

Table 28 and Table 30, none has a significant effect on the results of density testing.

The average values of the measured densities for the factors that had significant effects are presented in Table 31. Each value is the average of eight measurements.

Table 31. Summary of ruggedness tests

	Significant Factor	Measured Density (g/m^3)	
		For Level (–) canola oil	For Level (+) mineral oil
Ruggedness Test 1	Fluid	1.420 ± 0.046	1.312 ± 0.044
		For Level (–) 50 kPa	For Level (+) 90 kPa
Ruggedness Test 2	Pressure	1.344 ± 0.028	1.456 ± 0.032
Ruggedness Test 3	Pressure	1.350 ± 0.029	1.439 ± 0.046

3.6.2.3. Density Testing with Different Immersion Fluids

Five different fluids were selected and minimum of 10 specimens were tested for each fluid type. The types of fluids used in this study are presented in materials and methods section and Table 32 summarized the fluid types and their measured densities. All densities were measured at 23 ± 0.2 ° C using Metler Toledo density measurement kit and a known standard density block.

Table 32. Properties of fluids used for density measurement of flax fiber

Type of fluid	Manufacturer	CAS Number	Density (g/cm^3)
Canola Oil - Grocery Store	Wesson	-	0.9058 ± 0.0163
Canola Oil – Certified	Sigma Aldrich	120962-03-0	0.9045 ± 0.0152
Soybean Oil- Grocery store	Crisco	-	0.9029 ± 0.0125
Soybean Oil - Certified	Sigma Aldrich	8001-22-7	0.9070 ± 0.0171
White Mineral Oil	W.S. Dodge Oil	8042-47-5	0.8448 ± 0.0147

Results of density measurements are presented in Table 33. Based on the results of ruggedness tests, 90 kPa vacuum pressure was applied and specimens were kept under the mentioned pressure for 10 minutes. It is worth mentioning result of density measurement for the same type of fiber with gas pycnometry was 1.49 ± 0.0022 g/cm^3.

Table 33. Results of density measurements of flax fiber (ten measurements)

Type of fluid Used	Density of Flax Fiber (g/cm^3)
Canola Oil - Grocery Store	1.4627 ± 0.0167
Canola Oil – Certified	1.4145 ± 0.0195
Soybean Oil- Grocery store	1.4663 ± 0.0083
Soybean Oil - Certified	1.4658 ± 0.0129
White Mineral Oil	1.4525 ± 0.0239
Pycnometry	1.4900 ± 0.0022

Based on the results presented in Table 33, certified lab grade soybean oil was selected and suggested to be used as submersion fluid for density measurements of flax fiber. The reason could be attributed to better affinity of soybean oil and flax fiber for one another from a chemical standpoint that leads to better wetting of the fiber and consequently a more accurate density values.

Five specimens were prepared for each flax fiber type and density test were performed using the parameters presented in Table 12. Results of measurements are presented in Table 34.

Table 34. Density of four types of flax fiber tested with Archimedes method and pycnometry

Fiber	Archimedes Density g/cm^3	Pycnometry Density g/cm^3
Flax Type 1	1.4894±0.0081	1.4900±0.0022
Flax Type 2	1.5065±0.0172	1.5241±0.0044
Flax Type 3	1.5005±0.0066	1.4945±0.0077
Flax Type 4	1.4869±0.0168	1.4927±0.0058

In general, Archimedes method would yield density values that are slightly lower compared to gas pycnometry method. This is due to entrapped air (microbubbles) on the surface of the fiber as well as the hollow center of the fiber. Although with the use of vacuum, some of these bubbles are extracted, entrapped air in the lumen will result in lower values of submerged weight o specimen and consequently lower value for density of fiber. Higher vacuum pressure of 90-100 kPa results in better removal of entrapped air and provides better density values. With utilization

of gas pycnometry, this problem is eliminated as the gas molecules (nitrogen or helium) can penetrate the hollow center of the fiber and yield accurate measures of volume of true the fiber and therefore accurate results of density of fiber.

4. CONCLUSIONS AND FUTURE WORK

4.1. Conclusions

4.1.1. Effect of Mechanical Processes

In this study, a novel highly-functional biobased resin from Methacrylated Epoxidized Sucrose Soyate (MESS) was used as the matrix. The mechanical properties of fibers with different mechanical treatments using novel MESS thermoset resin were compared with composites using Vinyl Ester (VE) as their thermoset resin. Three mechanical cleaning and processes were used to clean the fibers prior to use as reinforcement in the composites. Composite mechanical performance was characterized by performing tensile, flexure, and short beam shear tests. Untreated flax fibers, composites made from either MESS or VE resins exhibited improvements in tensile and flexural modulus when compared to composites made from mechanically treated flax fibers. Composites made from fibers treated with fluted rollers exhibited improved tensile, flexural, and inter-laminar shear strength when compared to untreated flax fiber composites and other mechanically treated fibers. However, composites made with MESS resin exhibited lower strengths compared to composites made with VE resin. This could be due to curing the resin at higher temperature which results in degradation of shive content of the fiber. Further study with different type of flax fiber with minimum to no shive content is required to confirm this conclusion.

4.1.2. Effect of Chemical Treatments

Lipase enzyme was used to clean flax fiber surface and mechanical properties of composites using untreated and treated flax fiber were evaluated. Lipase treatment has improved flexural strength of the fibers, however, this gain was not statistically significant. Also, it has minimal or no effect on flexural modulus and short beam strength. On the other hand, it has

decreased the tensile properties of the fiber significantly. Therefore, although this methods was helpful in cleaning up the surface of the fiber, it was decided not to pursue this method further.

Mechanical properties of untreated and alkaline treated linseed flax fiber (Type 1) with vinyl ester resin and vinyl ester containing 1% acrylic resin were investigated using static mechanical tests. Alkaline treatment was successful in increasing interlaminar shear strength and tensile strength of the composites. Although an increase in the flexural properties of the composite was observed after treatment, statistical analysis of results reveled that this gain was not significant. On the other hand, both tensile and flexural moduli of composites using alkaline treated flax fiber were decreased. Addition of 1% acrylic resin to the resin was effective in improving all mechanical properties except for flexural modulus where a decrease of 10% in modulus was observed. For all mechanical properties, the highest gain was observed where vinyl ester containing 1% acrylic resin was reinforced with alkaline treated flax fiber except for tensile modulus.

Vinyl ester resin was reinforced with flax fiber fabric (Type 6) to manufacture controlled composite. Alkaline treatment was employed to treat flax fiber fabric with the goal of increasing adhesion and mechanical interlocking of resin and matrix. Mechanical properties of manufactured composites using treated flax fiber were compared again those using untreated fiber. Overall, mechanical properties of manufactured composites showed improvement when using alkaline treated flax fiber as reinforcement. In addition, after exposing to accelerate weathering, mechanical properties of composites using treated flax fiber showed less reduction, except for flexural strength. In general, it is shown that biobased composites manufactured in this study, meet and most of the time exceed the target properties set based on commercially available pultruded fiberglass composites.

4.1.3. Long-Term Behavior - Creep

Creep tests with constant stress were carried out at different temperature intervals on flax/vinyl ester composite. A creep compliance master curve was generated by shifting creep compliance data along time scale in reference to the curve at 30 ºC. The horizontal shift factors were found to be governed by Arrhenius equation. The coefficients in Findley Power Law were computed and a strong agreement with 99.6% confidence level between experimental and simulated results was observed. Therefore, the resulting master curve and power law equation provides an accelerated creep characterization up to 1010 seconds for this composite. As a result, to predict creep behavior of a flax fiber/vinyl ester composite material in 20 years at 30 ºC, one can run creep tests at 100 ºC for 10 minutes and achieve fair accuracy.

Time temperature superposition (TTS) principle was applied to the results of creep compliance measurements at different temperatures to evaluate the effect of fiber and matrix treatment on long-term creep behavior. Results revealed that addition of acrylic resin to vinyl ester, slowed the process of creep in flax/vinyl ester composites in the steady state region. Moreover, combining alkaline treatment of flax fiber with manipulation of vinyl ester resin by addition of 1% acrylic resin delayed and extended creep response. In other words, by comparing creep compliance curves of untreated composites with composites using treatment of flax and vinyl ester, the former reached creep compliance of 350 1/MPa after 10^{10} seconds, where the latter reached the same value after 10^{12} seconds.

4.1.3.1. Summary of Frequency Sweep of Flax/VE

Frequency scans of flax/Vinyl ester composites were obtained at different temperatures and storage modulus, loss modulus and tan δ were recorded. The applications of horizontal and vertical shift factors to all three viscoelastic functions were studied. In addition, short-term strain

creep at different temperatures were measured and curves were shifted with solely horizontal, and with both horizontal and vertical shift factors. The resulting master curves were compared with a 24-hour creep test and two extrapolated creep models that were mentioned previously. It was shown that the use of solely horizontal shift factors are not adequate to achieve an acceptable and smooth creep master curve for all viscoelastic properties of these composites. In addition, the use of both horizontal and vertical shift factors will result in a broader range of time.

Comparing the Findley and Nutting models with the actual creep data for 24 hours, it was observed that the both underestimated the creep strain at longer times and deviated from the actual data. The deviation of Findley power law from experimental data could be a sign that the parameters in mentioned model are more dependent on temperature and therefore the effect of temperature is more pronounced compared to time. In addition, Nutting variables are temperature dependent, and the effect of temperature is more pronounced compared to time, this might be the reason foe deviation of experimental results from model at longer times [223].

In order to study the thermal and mechanical behavior of methacrylated epoxidized sucrose soyate (MESS) resin reinforced with flax fiber, frequency scans of flax/MESS composites were obtained at different temperatures and storage modulus, loss modulus (and tan δ as the ratio of these two functions) were recorded. The application of horizontal and vertical shift factors to loss modulus and storage modulus were studied. In addition, short-term strain creep at different temperatures were measured and curves were shifted with solely horizontal, and with both horizontal and vertical shift factors. The resulting master curves were compared with a 24-h creep test and two extrapolated creep models that were mentioned previously. It was shown that the use of solely horizontal shift factors is not adequate to achieve a satisfactory creep master curve for all

viscoelastic properties of these composites. In addition, the use of both horizontal and vertical shift factors will result in a broader range of time.

Comparing the Findley and Nutting models with the actual creep data for 24 h, it was observed that the former overestimated the creep strain at longer times and deviated from the actual data, while the latter showed good agreement with the experimental data. The deviation of Findley power law from experimental data could be a sign that the parameters in mentioned model are more dependent on temperature and therefore the effect of temperature is more pronounced compared to time.

Frequency scans of flax/Vinyl ester composites were obtained at different temperatures and storage modulus, loss modulus and tan δ were recorded. The applications of horizontal and vertical shift factors to all three viscoelastic functions were studied. In addition, short-term strain creep at different temperatures were measured and curves were shifted with solely horizontal, and with both horizontal and vertical shift factors. The resulting master curves were compared with a 24-hour creep test and two extrapolated creep models that were mentioned previously. It was shown that the use of solely horizontal shift factors are not adequate to achieve a satisfactory and smooth creep master curve for all viscoelastic properties of these composites. In addition, the use of both horizontal and vertical shift factors will result in a broader range of time.

Comparing the Findley and Nutting models with the actual creep data for 24 hours, it was observed that the both underestimated the creep strain at longer times and deviated from the actual data. The deviation of Findley power law from experimental data could be a sign that the parameters in mentioned model are more dependent on temperature and therefore the effect of temperature is more pronounced compared to time. In addition, Nutting variables are temperature

dependent, and the effect of temperature is more pronounced compared to time, this might be the reason for the deviation [223].

4.1.3.2. Long-Term Behavior – Accelerated Weathering

It is generally acknowledged that lab based accelerated weathering methods cannot be directly correlated to an equivalent degree of natural weathering using some sort of universal formula. This is a consequence of variations in the characteristics of each specific material. In addition, there is inherent variability in environmental conditions from season to season as well as between geographical regions. However, in an effort to provide some semblance of a benchmark by which the two methods can be correlated, a technical paper making this comparison was published by Q-Lab, the manufacturer of the chamber used in this study [29]. Assuming a linear correlation between irradiance and acceleration factor, accounting for the different irradiance levels employed during this study and that one (0.5 vs 0.85 W/m^2-nm) would suggest that the acceleration factor for this study's composites is 4.6. This would mean that they underwent the equivalent of 6.4 months of natural weathering.

Specimens were characterized after being exposed to accelerated weathering and percentage of degradation of mechanical properties as well as color gloss was calculated. The results of this study reveals that biobased composites using vinyl ester resin or 100% vegetable oil based resins have the potential of being used in structural applications such as aerospace applications.

4.1.4. Characterization of Flax Fiber and Flax Fiber Composites

4.1.4.1. Void Fraction Calculation

Void fractions of ten composite samples were calculated using two methods; density measurements and sets of equations, and using 3D scans of the composite samples and image

processing MATLAB® code. There were between 1.2% and 6.97% difference between the results from two methods. The focus of this study was to prove that using micro-CT scans is a feasible way of evaluating composites and with this novel method finding void fraction of manufactured composites is possible. Further investigation is required to confirm the accuracy of this method.

4.1.4.2. Density Measurement of Flax Fiber

In ordered to develop a standard test method for density measurement of flax fiber, this study was performed. The following could be summarized as results of this study:

Comparison of density tests using distilled water and canola oil with and without using a vacuum oven revealed that because of the hydrophilic nature of flax fiber, distilled water was not a suitable immersion fluid. In addition, use of vacuum oven improved the values of density of flax fiber by removing micro bubbles present in the oil and in the specimen.

Based on results of ruggedness tests, it was concluded that at lower vacuum pressure type of immersion fluid has a significant effect of values of density. However, at higher vacuum pressure, the effect of type of fluid used has no significant effect and instead the vacuum pressure plays an important role. Higher vacuum pressure results in removal of more entrapped air in the fiber and provide a more accurate value for density of fiber. Results suggested that vacuum pressure of 90-100 kPa and vacuum time of 10 minutes resulted in closer values to the actual values of density for flax fiber.

Based on the results from ruggedness test, higher vacuum pressure and longer vacuum time was considered and density of one type of flax was tested using immersion fluids and results were compared against values obtained from gas pycnometry. Results suggested that certified lab grade soybean oil is a suitable immersion fluid to be used in density measurement of flax fiber due to

better affinity of soybean oil and flax fiber for one another from a chemical standpoint that leads to better wetting of the fiber and consequently a more accurate density values.

Parameters mentioned in previous bullet points were used to measure density of four types of flax fiber and values were compared with density results from pycnometry method.

In conclusion, results of this study proves that use of Archimedes method with the mentioned parameters can yield acceptable results for density measurement of flax fiber in cases where gas pycnometry is not available and less accurate results of density are accepted.

4.2. Recommendations for Future Work

Based on results presented in this work, additional and future studies could be developed to further expand and extend the scope of current study:

- The chemical testaments of flax fiber and VE resins were proven to have a positive effect on enhancing performance of developed biobased composites. In the future studies effect of addition of AR to newly development resins (i.e. MESS and DMESS) could be investigated. In addition, effect of these treatments on other long-term behaviors such as fatigue life of biobased composites could be examined.
- Although in this study an existing empirical model was modified to predict long-term behavior of flax fiber reinforced biobased composites, applicability and development of other models to creep behavior of flax fiber/thermoset composites could be investigated in more depth. There has been a models being developed for predicting creep behavior of natural fibers and thermoplastic composites by Chandekar and Chaudhari [224]. Similar models could be developed to be used for flax fiber/thermoset resin composites.

- Weatherability of newly developed biocomposites were studies and mechanical performances before and after exposure to accelerated weather was examined. In the future studies, other weathering methods such as xenon arc testing, salt spray testing, or use of UV lights with different wavelength could be studied. In addition more characterization methods such as surface imaging (optical or SEM) and Attenuated Total Reflectance (ATR) should be employed to further explore the effect of weathering on these newly developed composites.
- In this study, the first steps were taken to develop advanced characterization methods for flax fiber and biocomposites. The first draft of an ASTM standard was prepared to be approve and published as standard test method for density measurement of flax fiber. This is the beginning of many more standard procedures and practices to be developed for natural fibers as well as natural fiber reinforced composites. As an example, as an expansion of the work presented in this study, a standard practice for drying and condition flax fiber prior to testing and characterization is to be developed.

REFERENCES

[1] P. A. Fowler, J. M. Hughes, and R. M. Elias, "Biocomposites: technology, environmental credentials and market forces," *Journal of the Science of Food and Agriculture,* vol. 86, no. 12, pp. 1781-1789, 2006.

[2] N. Chand, R. Tiwary, and P. Rohatgi, "Bibliography resource structure properties of natural cellulosic fibres—an annotated bibliography," *Journal of Materials Science,* vol. 23, no. 2, pp. 381-387, 1988.

[3] H. Lilholt and J. Lawther, "Natural organic fibers," *Comprehensive composite materials,* vol. 1, pp. 303-325, 2000.

[4] R. R. Franck, *Bast and other plant fibres*, Woodhead Publishing, Cambridge, England, 2005.

[5] A. Bolton, "Natural fibers for plastic reinforcement," *Materials Technology(USA),* vol. 9, no. 1, pp. 12-20, 1994.

[6] D. N. Saheb and J. Jog, "Natural fiber polymer composites: a review," *Advances in polymer technology,* vol. 18, no. 4, pp. 351-363, 1999.

[7] A. Mohanty and M. Misra, "Studies on jute composites—a literature review," *Polymer-Plastics Technology and Engineering,* vol. 34, no. 5, pp. 729-792, 1995.

[8] A. K. Bledzki, V. Sperber, and O. Faruk, *Natural and wood fibre reinforcement in polymers*, Rapra Publishing, Shropshire, UK, 2002.

[9] A. N. Netravali and S. Chabba, "Composites get greener," *Materials today,* vol. 6, no. 4, pp. 22-29, 2003.

[10] C. Baillie, *Green composites: polymer composites and the environment*, Crc Press, Cambridge, England, 2004.

[11] A. K. Mohanty, M. Misra, and L. T. Drzal, *Natural fibers, biopolymers, and biocomposites,* CRC Press, Boca Raton, FL, 2005.

[12] K. Pickering, *Properties and performance of natural-fibre composites*, Woodhead Publishing, Cambridge, England, 2008.

[13] J. Holbery and D. Houston, "Natural-fiber-reinforced polymer composites in automotive applications," *Jom,* vol. 58, no. 11, pp. 80-86, 2006.

[14] "Auto Body made of plastics resists denting under hard blows," *Popular Mechanics MagazinePopular Mechanics Magazine,* vol. 76, no. 6, p. 12, 1941.

[15] A. Amiri, "Experimental investigation of fatigue behavior of carbon fiber composites using fully-reversed four-point bending test,", master's thesis, University of NOrth Dakota, 2012.

[16] A. Amiri and M. N. Cavalli, *Experimental investigation of fatigue behavior of carbon fiber composites using fully reversed four point bending test. in: Composite matreials and joining technologies for composites*, vol. 7, Springer, East Lansing, MI, 2013.

[17] F. a. A. O. o. t. U. Nations. (2014). *Flax Production*. Available at: http://faostat3.fao.org/faostat-gateway/go/to/search/flax%20linseed/E

[18] D. F. Austin, "Plants for People," *Economic Botany,* vol. 57, no. 4, pp. 668-668, 2003.

[19] V. Salnikov, M. Ageeva, V. Yumashev, and V. Lozovaya, "Ultrastructural Analysis of Bast Fibers," *Russian Plant Physiology,* vol. 40, no. 3, pp. 416-421, 1993.

[20] G. Bogoeva-Gaceva *et al.*, "Natural fiber eco-composites," *Polymer Composites,* vol. 28, no. 1, pp. 98-107, 2007.

[21] A. Bledzki and J. Gassan, "Composites reinforced with cellulose based fibres," *Progress in polymer science,* vol. 24, no. 2, pp. 221-274, 1999.

[22] S. K. Batra, *Other long vegetable fibers: abaca, banana, sisal, henequen, flax, ramie, hemp, sunn, and coir,* Taylor and Francis Group, Boca Raton, 2007.

[23] H. Lilholt, H. Toftegaard, A. Thomsen, and A. Schmidt, "Natural composites based on cellulosic fibres and polypropylene matrix. Their processing and characterization," in *Proceedings of ICCM*, 1999, vol. 12, p. 9.

[24] M. Jawaid and H. Abdul Khalil, "Cellulosic/synthetic fibre reinforced polymer hybrid composites: A review," *Carbohydrate Polymers,* vol. 86, no. 1, pp. 1-18, 2011.

[25] A. Valadez-Gonzalez, J. Cervantes-Uc, R. Olayo, and P. Herrera-Franco, "Chemical modification of henequen fibers with an organosilane coupling agent," *Composites Part B: Engineering,* vol. 30, no. 3, pp. 321-331, 1999.

[26] D. Maldas, B. Kokta, and C. Daneault, "Influence of coupling agents and treatments on the mechanical properties of cellulose fiber–polystyrene composites," *Journal of Applied Polymer Science,* vol. 37, no. 3, pp. 751-775, 1989.

[27] H. A. Khalil, H. Ismail, H. Rozman, and M. Ahmad, "The effect of acetylation on interfacial shear strength between plant fibres and various matrices," *European Polymer Journal,* vol. 37, no. 5, pp. 1037-1045, 2001.

[28] B. E. Pallesen, "The quality of combine-harvested fibre flax for industrials purposes depends on the degree of retting," *Industrial crops and products,* vol. 5, no. 1, pp. 65-78, 1996.

[29] A. Bledzki, S. Reihmane, and J. Gassan, "Properties and modification methods for vegetable fibers for natural fiber composites," *Journal of Applied Polymer Science,* vol. 59, no. 8, pp. 1329-1336, 1996.

[30] C. Baley, "Analysis of the flax fibres tensile behaviour and analysis of the tensile stiffness increase," *Composites Part A: Applied Science and Manufacturing,* vol. 33, no. 7, pp. 939-948, 2002.

[31] H. L. Bos, *The potential of flax fibres as reinforcement for composite materials*. Technische Universiteit Eindhoven, 2004.

[32] G. C. Davies and D. M. Bruce, "Effect of environmental relative humidity and damage on the tensile properties of flax and nettle fibers," *Textile Research Journal,* vol. 68, no. 9, pp. 623-629, 1998.

[33] E. Pearce and M. Lewis, "Fiber Chemistry," in *Handbook of fibre science and technology*, vol. 4, Marcel Dekker Inc., New York, pp. 505-575, 1985.

[34] J. Brandrup, E. H. Immergut, E. A. Grulke, A. Abe, and D. R. Bloch, *Polymer handbook*. Wiley, New York, 1999.

[35] F. Tröger, G. Wegener, and C. Seemann, "Miscanthus and flax as raw material for reinforced particleboards," *Industrial Crops and Products,* vol. 8, no. 2, pp. 113-121, 1998.

[36] P. Hornsby, E. Hinrichsen, and K. Tarverdi, "Preparation and properties of polypropylene composites reinforced with wheat and flax straw fibres: part I fibre characterization," *Journal of Materials Science,* vol. 32, no. 2, pp. 443-449, 1997.

[37] C. Morvan, C. Andème-Onzighi, R. Girault, D. S. Himmelsbach, A. Driouich, and D. E. Akin, "Building flax fibres: more than one brick in the walls," *Plant Physiology and Biochemistry,* vol. 41, no. 11, pp. 935-944, 2003.

[38] A. Stamboulis, C. Baillie, and T. Peijs, "Effects of environmental conditions on mechanical and physical properties of flax fibers," *Composites Part A: Applied Science and Manufacturing,* vol. 32, no. 8, pp. 1105-1115, 2001.

[39] R. Rowell, "Natural fibres: types and properties," *Properties and performance of natural-fibre composites,* pp. 3-66, 2008.

[40] M. Z. Rong, M. Q. Zhang, Y. Liu, G. C. Yang, and H. M. Zeng, "The effect of fiber treatment on the mechanical properties of unidirectional sisal-reinforced epoxy composites," *Composites Science and Technology,* vol. 61, no. 10, pp. 1437-1447, 2001.

[41] J. Vallade, "Endosperme ou albumen? Petite histoire d'un choix terminologique relatif à l'organisation de l'ovule et de la graine chez les Phanérogames," *Acta botanica gallica,* vol. 151, no. 2, pp. 205-219, 2004.

[42] B. G. Bowes, *A colour atlas of plant structure*. Manson Publishing Ltd., London, UK, 1996.

[43] H. Bos and A. Donald, "In situ ESEM study of the deformation of elementary flax fibres," *Journal of materials science,* vol. 34, no. 13, pp. 3029-3034, 1999.

[44] F. Shafizadeh, T. Nevell, and S. Zeronian, "Cellulose Chemistry and Its Applications," Ellis Horwood Ltd., London, UK, 1985.

[45] A. Mustata, "Factors influencing fiber-fiber friction in the case of bleached flax," *Cellulose chemistry and technology,* vol. 31, no. 5-6, pp. 405-413, 1997.

[46] M. J. John and R. D. Anandjiwala, "Recent developments in chemical modification and characterization of natural fiber-reinforced composites," *Polymer composites,* vol. 29, no. 2, pp. 187-207, 2008.

[47] H. Yamamoto, F. Horii, and H. Odani, "Structural changes of native cellulose crystals induced by annealing in aqueous alkaline and acidic solutions at high temperatures," *Macromolecules,* vol. 22, no. 10, pp. 4130-4132, 1989.

[48] A. Bismarck, S. Mishra, and T. Lampke, "Plant fibers as reinforcement for green composites," *in Natural Fibers, Biopolymers and biocomposites*, CRC Press, Boca Raton, FL, 2005.

[49] M. Ehresmann, A. Amiri, and C. Ulven, "The effect of different variables on in-plane radial permeability of natural fiber mats," *Journal of Reinforced Plastics & Composites,* SAGE Publishing, UK, 2016.

[50] D. F. Caulfield, D. Feng, S. Prabawa, R. Young, and A. R. Sanadi, "Interphase effects on the mechanical and physical aspects of natural fiber composites," *Die Angewandte Makromolekulare Chemie,* vol. 272, no. 1, pp. 57-64, 1999.

[51] A. Amiri, C. A. Ulven, and S. Huo, "Effect of Chemical Treatment of Flax Fiber and Resin Manipulation on Service Life of Their Composites Using Time-Temperature Superposition," *Polymers,* vol. 7, no. 10, pp. 1965-1978, 2015.

[52] M. N. Belgacem and A. Gandini, "The surface modification of cellulose fibres for use as reinforcing elements in composite materials," *Composite Interfaces,* vol. 12, no. 1-2, pp. 41-75, 2005.

[53] M. A. Fuqua, S. Huo, and C. A. Ulven, "Natural fiber reinforced composites," *Polymer Reviews,* vol. 52, no. 3-4, pp. 259-320, 2012.

[54] D. Fengel and G. Wegener, *Wood: chemistry, ultrastructure, reactions*. Walter de Gruyter, New York, NY, 1983.

[55] S. a. Borysiak and J. Garbarczyk, "Applying the WAXS method to estimate the supermolecular structure of cellulose fibres after mercerisation," *Fibres and Textiles in Eastern Europe,* vol. 11, no. 5, pp. 104-106, 2003.

[56] X. Li, L. G. Tabil, and S. Panigrahi, "Chemical treatments of natural fiber for use in natural fiber-reinforced composites: a review," *Journal of Polymers and the Environment,* vol. 15, no. 1, pp. 25-33, 2007.

[57] A. Valadez-Gonzalez, J. Cervantes-Uc, R. Olayo, and P. Herrera-Franco, "Effect of fiber surface treatment on the fiber–matrix bond strength of natural fiber reinforced composites," *Composites Part B: Engineering,* vol. 30, no. 3, pp. 309-320, 1999.

[58] I. Van de Weyenberg, T. Chi Truong, B. Vangrimde, and I. Verpoest, "Improving the properties of UD flax fibre reinforced composites by applying an alkaline fibre treatment," *Composites Part A: Applied Science and Manufacturing,* vol. 37, no. 9, pp. 1368-1376, 2006.

[59] A. Jähn, M. Schröder, M. Füting, K. Schenzel, and W. Diepenbrock, "Characterization of alkali treated flax fibres by means of FT Raman spectroscopy and environmental scanning electron microscopy," *Spectrochimica Acta Part A: Molecular and Biomolecular Spectroscopy,* vol. 58, no. 10, pp. 2271-2279, 2002.

[60] S. Huo, A. Thapa, and C. Ulven, "Effect of surface treatments on interfacial properties of flax fiber-reinforced composites," *Advanced Composite Materials,* vol. 22, no. 2, pp. 109-121, 2013.

[61] R. Agrawal, N. Saxena, K. Sharma, S. Thomas, and M. Sreekala, "Activation energy and crystallization kinetics of untreated and treated oil palm fibre reinforced phenol formaldehyde composites," *Materials Science and Engineering: A,* vol. 277, no. 1, pp. 77-82, 2000.

[62] I. Van de Weyenberg, J. Ivens, A. De Coster, B. Kino, E. Baetens, and I. Verpoest, "Influence of processing and chemical treatment of flax fibres on their composites," *Composites Science and Technology,* vol. 63, no. 9, pp. 1241-1246, 2003.

[63] T. Yu, J. Ren, S. Li, H. Yuan, and Y. Li, "Effect of fiber surface-treatments on the properties of poly (lactic acid)/ramie composites," *Composites Part A: Applied Science and Manufacturing,* vol. 41, no. 4, pp. 499-505, 2010.

[64] C. Baley, F. Busnel, Y. Grohens, and O. Sire, "Influence of chemical treatments on surface properties and adhesion of flax fibre–polyester resin," *Composites Part A: Applied Science and Manufacturing,* vol. 37, no. 10, pp. 1626-1637, 2006.

[65] C. A. Hill, H. A. Khalil, and M. D. Hale, "A study of the potential of acetylation to improve the properties of plant fibres," *Industrial Crops and Products,* vol. 8, no. 1, pp. 53-63, 1998.

[66] A. Paul, K. Joseph, and S. Thomas, "Effect of surface treatments on the electrical properties of low-density polyethylene composites reinforced with short sisal fibers," *Composites Science and Technology,* vol. 57, no. 1, pp. 67-79, 1997.

[67] M. Sreekala and S. Thomas, "Effect of fibre surface modification on water-sorption characteristics of oil palm fibres," *Composites Science and Technology,* vol. 63, no. 6, pp. 861-869, 2003.

[68] A. Pietak, S. Korte, E. Tan, A. Downard, and M. P. Staiger, "Atomic force microscopy characterization of the surface wettability of natural fibres," *Applied Surface Science,* vol. 253, no. 7, pp. 3627-3635, 2007.

[69] C. Hill and H. Abdul Khalil, "Effect of fiber treatments on mechanical properties of coir or oil palm fiber reinforced polyester composites," *Journal of Applied Polymer Science,* vol. 78, no. 9, pp. 1685-1697, 2000.

[70] L. A. Pothan and S. Thomas, "Effect of hybridization and chemical modification on the water-absorption behavior of banana fiber–reinforced polyester composites," *Journal of applied polymer science,* vol. 91, no. 6, pp. 3856-3865, 2004.

[71] V. A. Alvarez and A. Vazquez, "Influence of fiber chemical modification procedure on the mechanical properties and water absorption of MaterBi-Y/sisal fiber composites," *Composites Part A: Applied Science and Manufacturing,* vol. 37, no. 10, pp. 1672-1680, 2006.

[72] N. Zafeiropoulos, C. Baillie, and J. Hodgkinson, "Engineering and characterisation of the interface in flax fibre/polypropylene composite materials. Part II. The effect of surface treatments on the interface," *Composites Part A: Applied Science and Manufacturing,* vol. 33, no. 9, pp. 1185-1190, 2002.

[73] H. Sharma and C. Van Sumere, "Enzyme treatment of flax," *Genetic Engineer and Biotechnologist,* Vol. March/April, pp. 19-23, 1992.

[74] A. E. Brown, "Epicoccum nigrum, a primary saprophyte involved in the retting of flax," *Transactions of the British Mycological Society,* vol. 83, no. 1, pp. 29-35, 1984.

[75] H. Schunke, C. Sanio, H. Pape, U. Schunke, and C. Matz, "Reduction of time required for dew retting of flax: Influence of agricultural, mechanical and microbiological techniques on fibre processing," *Melliand,* vol. 76, pp. E101-E104, 1995.

[76] D. E. Akin, J. A. Foulk, R. B. Dodd, and D. D. McAlister, "Enzyme-retting of flax and characterization of processed fibers," *Journal of Biotechnology,* vol. 89, no. 2, pp. 193-203, 2001.

[77] J. Rout, S. Tripathy, M. Misra, A. Mohanty, and S. Nayak, "The influence of fiber surface modification on the mechanical properties of coir-polyester composites," *Polymer Composites,* vol. 22, no. 4, pp. 468-476, 2001.

[78] A. Mohanty, L. Drzal, and M. Misra, "Engineered natural fiber reinforced polypropylene composites: influence of surface modifications and novel powder impregnation processing," *Journal of adhesion science and technology,* vol. 16, no. 8, pp. 999-1015, 2002.

[79] W. Thielemans and R. P. Wool, "Butyrated kraft lignin as compatibilizing agent for natural fiber reinforced thermoset composites," *COMPOSITES part A: applied science and manufacturing,* vol. 35, no. 3, pp. 327-338, 2004.

[80] S. A. Paul, A. Boudenne, L. Ibos, Y. Candau, K. Joseph, and S. Thomas, "Effect of fiber loading and chemical treatments on thermophysical properties of banana fiber/polypropylene commingled composite materials," *Composites Part A: Applied Science and Manufacturing,* vol. 39, no. 9, pp. 1582-1588, 2008.

[81] M. Sreekala, M. Kumaran, and S. Thomas, "Water sorption in oil palm fiber reinforced phenol formaldehyde composites," *Composites Part A: Applied science and manufacturing,* vol. 33, no. 6, pp. 763-777, 2002.

[82] K. Joseph, S. Thomas, and C. Pavithran, "Effect of chemical treatment on the tensile properties of short sisal fibre-reinforced polyethylene composites," *Polymer,* vol. 37, no. 23, pp. 5139-5149, 1996.

[83] J. George, R. Janardhan, J. Anand, S. Bhagawan, and S. Thomas, "Melt rheological behaviour of short pineapple fibre reinforced low density polyethylene composites," *Polymer,* vol. 37, no. 24, pp. 5421-5431, 1996.

[84] J. Gassan, V. S. Gutowski, and A. K. Bledzki, "About the surface characteristics of natural fibres," *Macromolecular materials and engineering,* vol. 283, no. 1, pp. 132-139, 2000.

[85] P. Bataille, M. Dufourd, and S. Sapieha, "Copolymerization of styrene on to cellulose activated by corona," *Polymer international,* vol. 34, no. 4, pp. 387-391, 1994.

[86] S. Nowak, H. P. Haerri, L. Schlapbach, and J. Vogt, "Surface analysis and adhesion of polypropylene after low-pressure plasma treatment," *Surface and interface Analysis,* vol. 16, no. 1-12, pp. 418-423, 1990.

[87] J. Jeong *et al.*, "Etching materials with an atmospheric-pressure plasma jet," *Plasma Sources Science and Technology,* vol. 7, no. 3, p. 282, 1998.

[88] B. Miller, L. S. Penn, and S. Hedvat, "Wetting force measurements on single fibers," *Colloids and Surfaces,* vol. 6, no. 1, pp. 49-61, 1983.

[89] J. Laine and D. Goring, "Influence of ultrasonic irradiation on the properties of cellulosic fibres," *Cellul Chem Technol,* Vol. 11, pp. 561-567, 1977.

[90] J. Gassan and V. S. Gutowski, "Effects of corona discharge and UV treatment on the properties of jute-fibre epoxy composites," *Composites Science and Technology,* vol. 60, no. 15, pp. 2857-2863, 2000.

[91] O. H. TP, "Vinyl esters in engineered materials handbook," *Engineering plastics.,* vol. 2, pp. 272-275, 1988.

[92] T. F. Scott, W. D. Cook, and J. S. Forsythe, "Kinetics and network structure of thermally cured vinyl ester resins," *European polymer journal,* vol. 38, no. 4, pp. 705-716, 2002.

[93] B. T. Åström, *Manufacturing of polymer composites*. CRC Press, Boca Raton, FL, 1997.

[94] M. M. Denn, "Encyclopedia of polymer science and engineering." Vols. 1–10: *A-pentadiene polymers* by H. F. Mark, N. M. Bikales, C. G. Overberger, and G. Menges, eds., Wiley-Interscience, New York, 1987.

[95] G. Marsh, "Vinyl ester–the midway boat building resin," *Reinforced Plastics,* vol. 51, no. 8, pp. 20-23, 2007.

[96] S. Taillemite and R. Pauer, "Bright future for vinyl ester resins in corrosion applications," *Reinforced Plastics,* vol. 53, no. 4, pp. 34-37, 2009.

[97] A. B. Strong and B. Strong, "Plastics: materials and processing," Pearson, Upper Saddle River, NJ, 2000.

[98] A. M. Atta, A. M. Elsaeed, R. K. Farag, and S. M. El-Saeed, "Synthesis of unsaturated polyester resins based on rosin acrylic acid adduct for coating applications," *Reactive and Functional Polymers,* vol. 67, no. 6, pp. 549-563, 2007.

[99] B. A. Milleville and W. Bladergroen, "New organic peroxide catalyst for curing vinyl ester resins," in *45th Annual Conference, Composites Institute, Society of the Plastic Industry*, pp. 12-15, 1990

[100] C. D. Han and K. W. Lem, "Chemorheology of thermosetting resins. IV. The chemorheology and curing kinetics of vinyl ester resin," *Journal of applied polymer science,* vol. 29, no. 5, pp. 1879-1902, 1984.

[101] T. Grentzer, D. Rust, S. Lo, C. Spencer, and G. HACKWAORTH, "Influence of catalyst and reaction exotherm on the cure of unsaturated polyester and vinyl ester laminates," *Composite polymers,* vol. 5, no. 6, pp. 459-481, 1992.

[102] C. D. Han and K. W. Lem, "Rheology of unsaturated polyester resins. I. Effects of filler and low-profile additive on the rheological behavior of unsaturated polyester resin," *Journal of Applied Polymer Science,* vol. 28, no. 2, pp. 743-762, 1983.

[103] C. D. Han and K. W. Lem, "Rheology of unsaturated polyester resins. II. Thickening behavior of unsaturated polyester and vinyl ester resins," *Journal of Applied Polymer Science,* vol. 28, no. 2, pp. 763-778, 1983.

[104] G. Palmese, O. Andersen, and V. Karbhari, "Effect of glass fiber sizing on the cure kinetics of vinyl–ester resins," *Composites Part A: Applied Science and Manufacturing,* vol. 30, no. 1, pp. 11-18, 1999.

[105] H. J. Kim and D. W. Seo, "Effect of water absorption fatigue on mechanical properties of sisal textile-reinforced composites," *International Journal of Fatigue,* vol. 28, no. 10, pp. 1307-1314, 2006.

[106] S. Huo, V. S. Chevali, and C. A. Ulven, "Study on interfacial properties of unidirectional flax/vinyl ester composites: resin manipulation on vinyl ester system," *Journal of Applied Polymer Science,* vol. 128, no. 5, pp. 3490-3500, 2013.

[107] S. Huo, "The physico-chemical investigation of interfacial properties in natural fiber/vinyl ester biocomposites," Dissertation, North Dakota State University, 2012.

[108] S. Huo, M. Fuqua, V. S. Chevali, and C. A. Ulven, "Effects of Natural Fiber Surface Treatments and Matrix Modification on Mechanical Properties of Their Composites," SAE Technical Paper0148-7191, 2010.

[109] V. Antonucci, A. Cusano, M. Giordano, J. Nasser, and L. Nicolais, "Cure-induced residual strain build-up in a thermoset resin," *Composites Part A: Applied Science and Manufacturing,* vol. 37, no. 4, pp. 592-601, 2006.

[110] FLSmidth Co., "Rotary kilns for cement plants," FLSmidth Publications, Copenhagen, Denmark, 2011.

[111] Z. W. Wicks Jr, F. N. Jones, S. P. Pappas, and D. A. Wicks, *Organic coatings: science and technology*. John Wiley & Sons, Hoboken, NJ, 2007.

[112] P. Tran, D. Graiver, and R. Narayan, "Biocomposites synthesized from chemically modified soy oil and biofibers," *Journal of applied polymer science,* vol. 102, no. 1, pp. 69-75, 2006.

[113] K. Carlson and S. Chang, "Chemical epoxidation of a natural unsaturated epoxy seed oil fromVernonia galamensis and a look at epoxy oil markets," *Journal of the American Oil Chemists' Society,* vol. 62, no. 5, pp. 934-939, 1985.

[114] S. Warwel, "Complete and partial epoxidation of plant oils by lipase-catalyzed perhydrolysis," *Industrial Crops and Products,* vol. 9, no. 2, pp. 125-132, 1999.

[115] M. Zhan and R. P. Wool, "Biobased composite resins design for electronic materials," *Journal of applied polymer science,* vol. 118, no. 6, pp. 3274-3283, 2010.

[116] J. Lu, S. Khot, and R. P. Wool, "New sheet molding compound resins from soybean oil. I. Synthesis and characterization," *Polymer,* vol. 46, no. 1, pp. 71-80, 2005.

[117] E. Can, S. Küsefoğlu, and R. Wool, "Rigid, thermosetting liquid molding resins from renewable resources. I. Synthesis and polymerization of soy oil monoglyceride maleates," *Journal of applied polymer science,* vol. 81, no. 1, pp. 69-77, 2001.

[118] G. I. Williams and R. P. Wool, "Composites from natural fibers and soy oil resins," *Applied Composite Materials,* vol. 7, no. 5-6, pp. 421-432, 2000.

[119] K. Adekunle, D. Åkesson, and M. Skrifvars, "Biobased composites prepared by compression molding with a novel thermoset resin from soybean oil and a natural-fiber reinforcement," *Journal of applied polymer science,* vol. 116, no. 3, pp. 1759-1765, 2010.

[120] M. A. Sithique, S. Nagendiran, and M. Alagar, "Synthesis and Characterization of Bismaleimide-modified, Soy-based Epoxy Matrices for Flame-retardant Applications," *High Performance Polymers,* vol. 22, no. 3, pp. 328-344, 2010.

[121] V. Thulasiraman, S. Rakesh, and M. Sarojadevi, "Synthesis and characterization of chlorinated soy oil based epoxy resin/glass fiber composites," *Polymer Composites,* vol. 30, no. 1, pp. 49-58, 2009.

[122] S. N. Khot *et al.*, "Development and application of triglyceride-based polymers and composites," *Journal of Applied Polymer Science,* vol. 82, no. 3, pp. 703-723, 2001.

[123] X. Pan, P. Sengupta, and D. C. Webster, "Novel biobased epoxy compounds: epoxidized sucrose esters of fatty acids," *Green Chemistry,* vol. 13, no. 4, pp. 965-975, 2011.

[124] X. Pan, P. Sengupta, and D. C. Webster, "High biobased content epoxy–anhydride thermosets from epoxidized sucrose esters of fatty acids," *Biomacromolecules,* vol. 12, no. 6, pp. 2416-2428, 2011.

[125] E. Kontou, G. Spathis, and P. Georgiopoulos, "Modeling of nonlinear viscoelasticity-viscoplasticity of bio-based polymer composites," *Polymer Degradation and Stability,* vol. 110, pp. 203-207, 2014.

[126] E. M. Monono, D. C. Webster, and D. P. Wiesenborn, "Pilot scale (10kg) production and characterization of epoxidized sucrose soyate," *Industrial Crops and Products,* vol. 74, pp. 987-997, 2015.

[127] E. Bodros, I. Pillin, N. Montrelay, and C. Baley, "Could biopolymers reinforced by randomly scattered flax fibre be used in structural applications?," *Composites Science and Technology,* vol. 67, no. 3, pp. 462-470, 2007.

[128] M. Assarar, D. Scida, A. El Mahi, C. Poilâne, and R. Ayad, "Influence of water ageing on mechanical properties and damage events of two reinforced composite materials: Flax–fibres and glass–fibres," *Materials & Design,* vol. 32, no. 2, pp. 788-795, 2011.

[129] L. Yan, N. Chouw, and X. Yuan, "Improving the mechanical properties of natural fibre fabric reinforced epoxy composites by alkali treatment," *Journal of Reinforced Plastics and Composites,* Vol. 31*,* pp. 425-437, 2012.

[130] A. Amiri and C. Ulven, "Surface Treatment of Flax Fiber," in *65th Flax Institute of the United States*, Fargo, ND, pp. 117-125, 2014.

[131] J. L. Vold, C. A. Ulven, and B. J. Chisholm, "Torrefied biomass filled polyamide biocomposites: mechanical and physical property analysis," *Journal of Materials Science,* vol. 50, no. 2, pp. 725-732, 2015.

[132] P. Herrera-Franco and A. Valadez-Gonzalez, "A study of the mechanical properties of short natural-fiber reinforced composites," *Composites Part B: Engineering,* vol. 36, no. 8, pp. 597-608, 2005.

[133] J. Hearle, "The fine structure of fibers and crystalline polymers. III. Interpretation of the mechanical properties of fibers," *Journal of Applied Polymer Science,* vol. 7, no. 4, pp. 1207-1223, 1963.

[134] V. Keryvin, M. Lan, A. Bourmaud, T. Parenteau, L. Charleux, and C. Baley, "Analysis of flax fibres viscoelastic behaviour at micro and nano scales," *Composites Part A: Applied Science and Manufacturing,* Vol. 68, pp. 219-225, 2014.

[135] R. Joffe, L. Rozite, and A. Pupurs, "Nonlinear Behavior of Natural Fiber/Bio-Based Matrix Composites," in *Challenges in Mechanics of Time-Dependent Materials and Processes in Conventional and Multifunctional Materials,* vol. 2, Springer, East Lansing, MI, pp. 131-137, 2013.

[136] L. Pupure, R. Joffe, J. Varna, and B. Nyström, "Development of constitutive model for composites exhibiting time dependent properties," in *IOP Conference Series: Materials Science and Engineering*, vol. 48, IOP Publishing, Bristol, UK, 2013.

[137] Y. S. Song, J. T. Lee, D. S. Ji, M. W. Kim, S. H. Lee, and J. R. Youn, "Viscoelastic and thermal behavior of woven hemp fiber reinforced poly (lactic acid) composites," *Composites Part B: Engineering,* vol. 43, no. 3, pp. 856-860, 2012.

[138] H.-S. Yang, D. J. Gardner, and H.-J. Kim, "Viscoelastic and thermal analysis of lignocellulosic material filled polypropylene bio-composites," *Journal of thermal analysis and calorimetry,* vol. 98, no. 2, pp. 553-558, 2009.

[139] L. Yan, N. Chouw, and K. Jayaraman, "Flax fibre and its composites–A review," *Composites Part B: Engineering,* vol. 56, pp. 296-317, 2014.

[140] F. Achereiner, K. Engelsing, M. Bastian, and P. Heidemeyer, "Accelerated creep testing of polymers using the stepped isothermal method," *Polymer Testing,* vol. 32, no. 3, pp. 447-454, 2013.

[141] M. L. Williams, R. F. Landel, and J. D. Ferry, "The temperature dependence of relaxation mechanisms in amorphous polymers and other glass-forming liquids," *Journal of the American Chemical Society,* vol. 77, no. 14, pp. 3701-3707, 1955.

[142] J. D. Ferry, *Viscoelastic properties of polymers*. John Wiley & Sons, Hoboken, NJ, 1980.

[143] R. A. Schapery, "On the characterization of nonlinear viscoelastic materials," *Polymer Engineering & Science,* vol. 9, no. 4, pp. 295-310, 1969.

[144] R. Gupta, B. Baldewa, and Y. M. Joshi, "Time temperature superposition in soft glassy materials," *Soft Matter,* vol. 8, no. 15, pp. 4171-4176, 2012.

[145] D. Pedrazzoli and A. Pegoretti, "Long-term creep behavior of polypropylene/fumed silica nanocomposites estimated by time–temperature and time–strain superposition approaches," *Polymer Bulletin,* vol. 71, no. 9, pp. 2247-2268, 2014.

[146] A. Dorigato, A. Pegoretti, and J. Kolařík, "Nonlinear tensile creep of linear low density polyethylene/fumed silica nanocomposites: Time-strain superposition and creep prediction," *Polymer Composites,* vol. 31, no. 11, pp. 1947-1955, 2010.

[147] J. Kolařík and A. Pegoretti, "Non-linear tensile creep of polypropylene: Time-strain superposition and creep prediction," *Polymer,* vol. 47, no. 1, pp. 346-356, 2006.

[148] J. Kolařík and A. Pegoretti, "Proposal of the Boltzmann-like superposition principle for nonlinear tensile creep of thermoplastics," *Polymer Testing,* vol. 27, no. 5, pp. 596-606, 2008.

[149] R. F. Landel and L. E. Nielsen, *Mechanical properties of polymers and composites*. CRC Press, Boca Ranton, FL, 1993.

[150] M. A. Meyers and K. K. Chawla, *Mechanical behavior of materials*. Cambridge University Press, Cambridge, England, 2009.

[151] *ASTM D2990-09 Standard Test Methods for Tensile, Compressive, and Flexural Creep and Creep-Rupture of Plastics*, ASTM International, West Conshocken, PA, 2009.

[152] W. N. Findley, J. S. Lai, and K. Onaran, "Creep and relaxation of nonlinear viscoelastic materials," North-Holland Publishing, Amsterdam, Netherlands, 1976.

[153] V. S. Chevali, D. R. Dean, and G. M. Janowski, "Flexural creep behavior of discontinuous thermoplastic composites: Non-linear viscoelastic modeling and time–temperature–stress superposition," *Composites Part A: Applied Science and Manufacturing,* vol. 40, no. 6, pp. 870-877, 2009.

[154] H. Leaderman, "Elastic and creep properties of filamentous materials and other high polymers," *J. of Phys. Chem.*, vol. 53, no. 3, pp. 886-886, 1947.

[155] L. Boltzmann, "On the theory of the elastic aftereffect," *J. of Phys. Chem,* vol. 7, pp. 624-645, 1876.

[156] J. G. Zornberg, B. R. Byler, and J. W. Knudsen, "Creep of geotextiles using time-temperature superposition methods," *Journal of geotechnical and geoenvironmental engineering,* vol. 130, no. 11, pp. 1158-1168, 2004.

[157] M. T. Shaw and W. J. MacKnight, *Introduction to polymer viscoelasticity*. John Wiley & Sons, Hoboken, NJ, 2005.

[158] L. W. Ting and Q. An Qunli, "Time-temperature-stress equivalence and its application to nonlinear viscoelastic materials," *Acta Mechanica Solida Sinica,* vol. 14, no. 3, pp. 195-199. 2001.

[159] R. M. Koerner, A. E. Lord, and Y. H. Hsuan, "Arrhenius modeling to predict geosynthetic degradation," *Geotextiles and Geomembranes,* vol. 11, no. 2, pp. 151-183, 1992.

[160] K. Alwis and C. Burgoyne, "Time-temperature superposition to determine the stress-rupture of aramid fibres," *Applied Composite Materials,* vol. 13, no. 4, pp. 249-264, 2006.

[161] P. A. O'Connell and G. B. McKenna, "Arrhenius-type temperature dependence of the segmental relaxation below Tg," *The Journal of chemical physics,* vol. 110, no. 22, pp. 11054-11060, 1999.

[162] S. Siengchin, T. Pohl, L. Medina, and P. Mitschang, "Structure and properties of flax/polylactide/alumina nanocomposites," *Journal of Reinforced Plastics and Composites,* vol. 32, no. 1, pp. 23-33, 2012.

[163] P. Mannberg, B. Nyström, and R. Joffe, "Service life assessment and moisture influence on bio-based thermosetting resins," *Journal of Materials Science,* vol. 49, no. 10, pp. 3687-3693, 2014.

[164] B. Wielage, T. Lampke, H. Utschick, and F. Soergel, "Processing of natural-fibre reinforced polymers and the resulting dynamic–mechanical properties," *Journal of materials processing technology,* vol. 139, no. 1, pp. 140-146, 2003.

[165] A. Vazquez, V. Dominguez, and J. Kenny, "Bagasse fiber-polypropylene based composites," *Journal of Thermoplastic Composite Materials,* vol. 12, no. 6, pp. 477-497, 1999.

[166] V. S. Chevali, D. R. Dean, and G. M. Janowski, "Effect of environmental weathering on flexural creep behavior of long fiber-reinforced thermoplastic composites," *Polymer Degradation and Stability,* vol. 95, no. 12, pp. 2628-2640, 2010.

[167] M. Tajvidi, R. H. Falk, and J. C. Hermanson, "Time–temperature superposition principle applied to a kenaf-fiber/high-density polyethylene composite," *Journal of applied polymer science,* vol. 97, no. 5, pp. 1995-2004, 2005.

[168] W. Luo, C. Wang, X. Hu, and T. Yang, "Long-term creep assessment of viscoelastic polymer by time-temperature-stress superposition," *Acta Mechanica Solida Sinica,* vol. 25, no. 6, pp. 571-578, 2012.

[169] S. A. Miller, W. V. Srubar, S. L. Billington, and M. D. Lepech, "Integrating durability-based service-life predictions with environmental impact assessments of natural fiber–reinforced composite materials," *Resources, Conservation and Recycling,* vol. 99, pp. 72-83, 2015.

[170] R. M. Guedes, *Creep and fatigue in polymer matrix composites*. Elsevier, Amsterdam, Netherlands, 2010.

[171] R. H. Newman, M. A. Battley, J. E. Carpenter, and M. J. Le Guen, "Energy loss in a unidirectional flax-polyester composite subjected to multiple tensile load–unload cycles," *Journal of Materials Science,* vol. 47, no. 3, pp. 1164-1170, 2012.

[172] M. Hughes, J. Carpenter, and C. Hill, "Deformation and fracture behaviour of flax fibre reinforced thermosetting polymer matrix composites," *Journal of Materials Science,* vol. 42, no. 7, pp. 2499-2511, 2007.

[173] A. Amiri, N. Hosseini, C. Ulven, and D. Webster, "Advanced Bio-composites Made from Methacrylated Epoxidized Sucrose Soyate Resin Reinforced with Flax Fibers," proceedings of *20th International Conference on Composite Materials*, Copenhagen, Denmark, vol. 20, p. 3503, 2015.

[174] A. Michel and S. Billington, "Nonlinear Constitutive Model for Anisotropic Biobased Composite Materials," *Journal of Engineering Mechanics,* vol. 140, no. 11, p. 04014083, 2014.

[175] P. Nutting, "A study of elastic viscous deformation," *Proc. ASTM,* vol. 21, pp. 1162-1171, 1921.

[176] G. S. Blair and J. Caffyn, "An application of the theory of quasi-properties to the treatment of anomalous strain-stress relations," *Philosophical Magazine,* vol. 40, no. 300, pp. 80-94, 1949.

[177] G. S. Blair and B. Veinoglou, "A study of the firmness of soft materials based on Nutting's equation," *Journal of Scientific Instruments,* vol. 21, no. 9, p. 149, 1944.

[178] J. Betten, *Creep mechanics*. Springer, East Lansing, MI, 2008.

[179] H. Schürmann, *Konstruieren mit Faser-Kunststoff-Verbunden*. Springer, East Lansing, MI, 2005.

[180] P. Morgan, *Carbon fibers and their composites*. CRC press, Boca Ranton, FL, 2005.

[181] R. Whitacre, A. Amiri, and C. Ulven, "The effects of corn zein protein coupling agent on mechanical properties of flax fiber reinforced composites," *Industrial Crops and Products,* vol. 77, pp. 232-238, 2015.

[182] M. Truong, W. Zhong, S. Boyko, and M. Alcock, "A comparative study on natural fibre density measurement," *The Journal of The Textile Institute,* vol. 100, no. 6, pp. 525-529, 2009.

[183] P. G. Tortora and B. J. Collier, *Understanding textiles*. Prentice-Hall, Englewood Cliffs, New Jersey, United States, 1997.

[184] A. Arbelaiz, B. Fernandez, G. Cantero, R. Llano-Ponte, A. Valea, and I. Mondragon, "Mechanical properties of flax fibre/polypropylene composites. Influence of fibre/matrix modification and glass fibre hybridization," *Composites Part A: Applied Science and Manufacturing,* vol. 36, no. 12, pp. 1637-1644, 2005.

[185] J. Flynn, A. Amiri, and C. Ulven, "Hybridized carbon and flax fiber composites for tailored performance," *Materials & Design,* vol. 102, pp. 21-29, 2016.

[186] N. Soykeabkaew, P. Supaphol, and R. Rujiravanit, "Preparation and characterization of jute-and flax-reinforced starch-based composite foams," *Carbohydrate Polymers,* vol. 58, no. 1, pp. 53-63, 2004.

[187] T. Rude, L. Strait, and L. Ruhala, "Measurement of fiber density by helium pycnometry," *Journal of composite materials,* vol. 34, no. 22, pp. 1948-1958, 2000.

[188] W. Steinmann and A.-K. Saelhoff, "Essential Properties of Fibres for Composite Applications," in *Fibrous and Textile Materials for Composite Applications*: Springer, East Lansing, MI, pp. 39-73, 2016.

[189] R. Joffe, J. Andersons, and L. Wallström, "Strength and adhesion characteristics of elementary flax fibres with different surface treatments," *Composites Part A: Applied Science and Manufacturing,* vol. 34, no. 7, pp. 603-612, 2003.

[190] T. Stuart, Q. Liu, M. Hughes, R. McCall, H. Sharma, and A. Norton, "Structural biocomposites from flax—Part I: Effect of bio-technical fibre modification on composite properties," *Composites Part A: Applied Science and Manufacturing,* vol. 37, no. 3, pp. 393-404, 2006.

[191] B. Wang, S. Panigrahi, L. Tabil, W. Crerar, S. Sokansanj, and L. Braun, "Modification of flax fibers by chemical treatment," in *Proceeding CSAE/SCGR Meeting,* pp. 6-9, 2003.

[192] B. Wang, S. Panigrahi, L. Tabil, and W. Crerar, "'Effects of Chemical Treatments on Mechanical and Physical Properties of Flax Fiber-reinforced Rotationally Molded Composites," in *ASAE Annual Meeting,* Paper no. 046083, 2004.

[193] B. Wang, L. Tabil, and S. Panigrahi, "Effects of chemical treatments on mechanical and physical properties of flax fiber-reinforced composites," *Science and Engineering of Composite Materials,* vol. 15, no. 1, pp. 43-58, 2008.

[194] A. Amiri and C. Ulven, "Durabiliy of flax fiber biocomposites" in *In 66th Flax Institute of the United States*, Fargo, ND, vol. 66, pp. 39-47, 2016.

[195] "Araldite ® LY 8601 / Aradur ® 8602 System.," Huntsman Corporation, The Woodlands, TX, pp. 4-7. 2010.

[196] "Epoxy Systems Specifications.," Huntsman Corporation, The Woodlands, TX , p.4065, 2001.

[197] N. Correia, F. Robitaille, A. Long, C. Rudd, P. Simacek, and S. G. Advani, "Use of resin transfer molding simulation to predict flow, saturation, and compaction in the VARTM process," *Journal of fluids engineering,* vol. 126, no. 2, pp. 210-215, 2004.

[198] M. Kang, W. Lee, and H. Hahn, "Analysis of vacuum bag resin transfer molding process," *Composites Part A: Applied Science and Manufacturing,* vol. 32, no. 11, pp. 1553-1560, 2001.

[199] T. S. Lundström and B. R. Gebart, "Influence from process parameters on void formation in resin transfer molding," *Polymer Composites,* vol. 15, no. 1, pp. 25-33, 1994.

[200] J. Yan and D. C. Webster, "Thermosets from highly functional methacrylated epoxidized sucrose soyate," *Green Materials,* vol. 2, no. 3, pp. 132-143, 2014.

[201] I. M. Daniel, O. Ishai, I. M. Daniel, and I. Daniel, *Engineering mechanics of composite materials*. Oxford university press New York, 1994.

[202] J. Lawson and J. Erjavec, *Modern statistics for engineering and quality improvement*. Duxbury Press, Pacific Grove, CA, 2000.

[203] ASTM E1169-14: Standard Practice for Conducting Ruggedness Tests, ASTM International, West Conshocken, PA, 2014.

[204] W. Hu, M. Zhang, M.-T. Ton-That, and T.-d. Ngo, "A comparison of flax shive and extracted flax shive reinforced PP composites," *Fibers and Polymers,* vol. 15, no. 8, pp. 1722-1728, 2014.

[205] J. L. Vold, C. A. Ulven, and B. J. Chisholm, "Torrefied biomass filled polyamide biocomposites: mechanical and physical property analysis," *Journal of Materials Science,* vol. 50, no. 2, pp. 725-732, 2015.

[206] P. K. Kushwaha and R. Kumar, "Influence of chemical treatments on the mechanical and water absorption properties of bamboo fiber composites," *Journal of Reinforced Plastics and Composites,* vol. 30, no. 1, pp. 73-85, 2010.

[207] T. F. Scott, W. D. Cook, and J. S. Forsythe, "Photo-DSC cure kinetics of vinyl ester resins II: influence of diluent concentration," *Polymer,* vol. 44, no. 3, pp. 671-680, 2003.

[208] J. Zhu, A. Imam, R. Crane, K. Lozano, V. N. Khabashesku, and E. V. Barrera, "Processing a glass fiber reinforced vinyl ester composite with nanotube enhancement of interlaminar shear strength," *Composites Science and Technology,* vol. 67, no. 7, pp. 1509-1517, 2007.

[209] A. J. Michell, "Second derivative Ft-ir spectra of celluloses I and II and related mono-and oligo-saccharides," *Carbohydrate research,* vol. 173, no. 2, pp. 185-195, 1988.

[210] N. Nosbi, H. M. Akil, Z. M. Ishak, and A. A. Bakar, "Degradation of compressive properties of pultruded kenaf fiber reinforced composites after immersion in various solutions," *Materials & Design,* vol. 31, no. 10, pp. 4960-4964, 2010.

[211] B. Barkakaty, "Some structural aspects of sisal fibers," *Journal of Applied Polymer Science,* vol. 20, no. 11, pp. 2921-2940, 1976.

[212] C. Taylor, A. Amiri, A. Paramarta, C. Ulven, and D. Webster, "Development and weatherability of bio-based composites of structural quality using flax fiber and epoxidized sucrose soyate," *Materials & Design,* vol. 113, pp. 17-26, 2017.

[213] B. Herzog, D. J. Gardner, R. Lopez-Anido, and B. Goodell, "Glass-transition temperature based on dynamic mechanical thermal analysis techniques as an indicator of the adhesive performance of vinyl ester resin," *Journal of applied polymer science,* vol. 97, no. 6, pp. 2221-2229, 2005.

[214] A. Amiri, N. Hosseini, and C. A. Ulven, "Long-Term Creep Behavior of Flax/Vinyl Ester Composites Using Time-Temperature Superposition Principle," *Journal of Renewable Materials,* vol. 3, no. 3, pp. 224-233, 2015.

[215] ASTM D790-03: Standard Test Methods for Flexural Properties of Unreinforced and Reinforced Plastic and Electrical Insulating Materials, ASTM International, West Conshohocken, PA, 2003.

[216] H. H. Horowitz and G. Metzger, "A New Analysis of Thermogravimetric Traces," *Analytical Chemistry,* vol. 35, no. 10, pp. 1464-1468, 1963.

[217] K. Van De Velde and P. Kiekens, "Thermal degradation of flax: The determination of kinetic parameters with thermogravimetric analysis," *Journal of Applied Polymer Science,* vol. 83, no. 12, pp. 2634-2643, 2002.

[218] S. Huo and C. A. Ulven, "Study on Residual Stresses in Unidirectional Flax Fiber/Vinyl Ester Composites by XRD Technique," *Journal of Renewable Materials,* 2017.

[219] I. M. Ward and J. Sweeney, *Mechanical properties of solid polymers*. John Wiley & Sons, Hoboken, NJ, 2012.

[220] B. Harper and Y. Weitsman, "Characterization method for a class of thermorheologically complex materials," *Journal of Rheology,* vol. 29, no. 1, pp. 49-66, 1985.

[221] D. Feng, D. Caulfield, and A. Sanadi, "Effect of compatibilizer on the structure-property relationships of kenaf-fiber/polypropylene composites," *Polymer composites,* vol. 22, no. 4, pp. 506-517, 2001.

[222] C. A. Taylor, A. Amiri, D. C. Webster, and C. A. Ulven, "long-term behavior of bio-composites for structural applications," in proceedings of *CAMX The Composites and Advanced Materials Conference*, Anaheim, California, 2016.

[223] C. Marais and G. Villoutreix, "Analysis and modeling of the creep behavior of the thermostable PMR-15 polyimide," *Journal of applied polymer science,* vol. 69, no. 10, pp. 1983-1991, 1998.

[224] H. Chandekar and V. Chaudhari, "Flexural creep behaviour of jute polypropylene composites," *Materials Science and Engineering*, vol. 149, no. 1, p. 012107, 2016

APPENDIX A. PROPERTIES OF MATERIALS

Table A1. Constituent of the enzyme used for the treatment of the flax fiber

Ingredients	% (w/w)
Water, CAS no. 7732-18-5	64.8
Propylen glycol, CAS no. 57-55-6	30
Lipase, CAS no. 9001-62-1	5
Proxel, CAS no. 2634-33-5	0.20

Table A2. Literature values for epoxy 8601/Aradur

Density	Tensile Modulus	Tensile Strength	Max Elongation	Transverse Modulus	Shear Modulus,G_{12}	Poisson's Ratio, υ_{12}
kg/m^3	GPa	MPa	%	GPa	MPa	GPa
1120	2.22	54.3	6	2.22	822	0.35

APPENDIX B. PROPERTIES OF MESS RESIN

Table B1. Properties of MESS

	Acid Number	% Solid	Viscosity (Pa•s)[a]	M_n (kg/mol)[b]	Đ[c]
MESS	19	98.51	438.73	3610	1.009

[a]Measured by rheometry at 25°C, taken at a frequency of 10 MHz.
[b]Measured by GPC.
[c]Polydispersity index

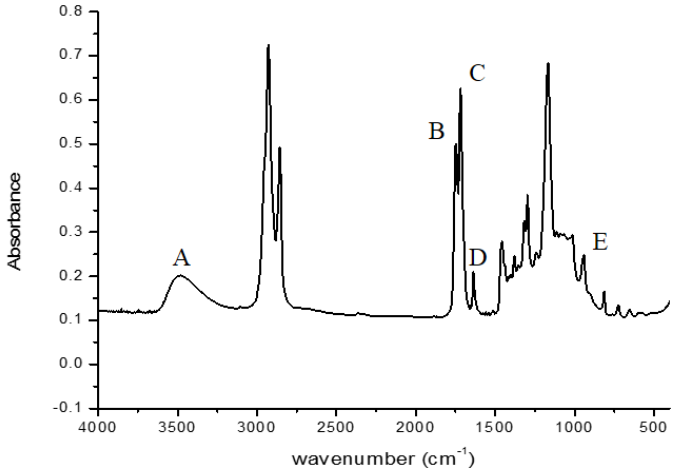

Figure B1. Fourier transform infrared spectrum of MESS

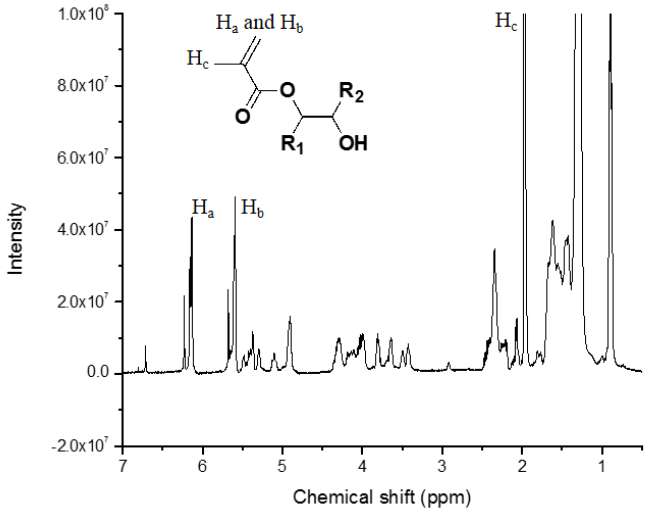

Figure B2. Proton nuclear magnetic resonance spectrum of the methacrylated epoxidized sucrose soyate (MESS) in $CDCl_3$

APPENDIX C. PROPERTIES OF DMESS RESIN

Table C1. Properties of DMESS

	Acid Number	% Solid	Viscosity (Pa•s)[a]	M_n (g/mol)[b]	Đ[c]
DMESS	24	99.24	21.08	3630	1.013

[a]Measured by rheometry at 25°C, taken at a frequency of 10 MHz
[b]Measured by GPC
[c]Polydispersity index

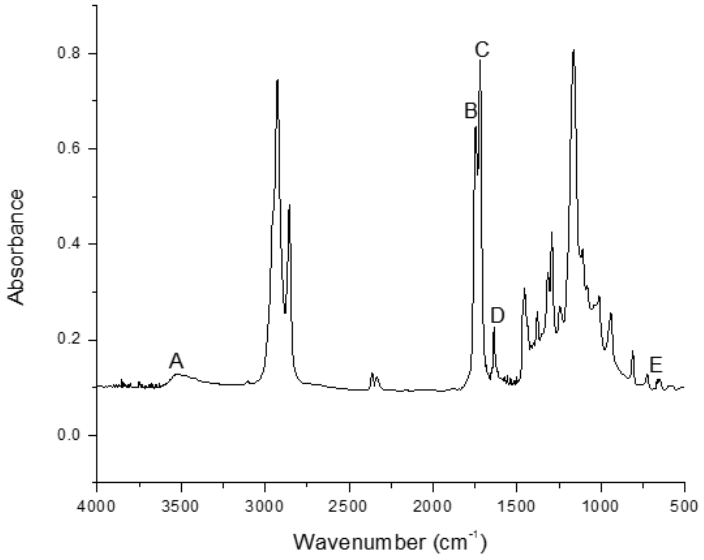

Figure C1. Fourier transform infrared spectrum of DMESS

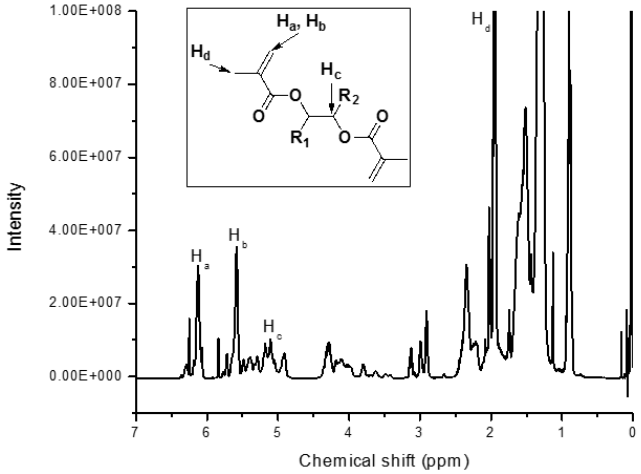

Figure C2. Proton nuclear magnetic resonance spectrum of the double methacrylated epoxidized sucrose soyate (DMESS) in $CDCl_3$

APPENDIX D. MATLAB CODE FOR IMAGE PROCESSING

```
clear all
close all
clc
Avg=0;

% Reading the sliced images
srcFiles = dir('Z:\Ali Amiri\images\*.tif');
for i = 1 : length(srcFiles)
    filename = strcat('Z:\Ali Amiri\Void Fraction
papers\Sampe\images\',srcFiles(i).name);
    I = imread(filename);
    I2 = imcrop(I,[65.5 15.51 191.98 392.98]);
    BW = im2bw(I2,0.275);
    percentageBlack=(1-nnz(BW)/numel(BW))*100;
    Avg=percentageBlack+Avg;
end
Avg=Avg/i
```

APPENDIX E. SUGGESTED TEST METHOD FOR DENSITY MEASUREMENT OF FLAX FIBER USING BUOYANCY METHOD

1 Apparatus

1.1 Buoyancy method kits can be commercially purchased for some balances. The kits or custom laboratory set ups should include the comparable or better of the following.

1.2 Thermometer, capable of reading the test temperature during the test to 0.1ºC.

1.3 Balance, analytical, capable of weighting to 0.0001 g (or 0.005 mg from D1577).

1.4 Balance Stand, depending on the type of balance used; two recommended stands are shown in Figs. 1 and 2.

1.5 Suspension Wire, nickel or stainless steel, approximately 0.4 mm in diameter, cut and shaped to match the system used.

1.6 Density Standard, A solid piece of borosilicate glass (approximate density 2.2 g/mL) of known density to four significant figures as determined by water immersion[1]. A NIST standard of this type (SRM 1825) is recommended.

1.7 Vacuum Desiccator (with Pump), an airtight container in which a low vacuum (less than 75 kPa [560 Torr]) can be maintained.

1.8 Container, glass or other transparent container resistant to a liquid medium is recommended.

1.9 Immersion Liquid, the liquid used shall not dissolve or otherwise affect the specimen, but should wet it and have a specific gravity less than that of the specimen. The specific gravity of the immersion liquid shall be determined shortly before and after each use.

1.10 Gloves, clean, non-linting (or lint free) gloves for use when handling fibers.

---

[1] A No. 19 “Pyrex” glass stopper with a 3.175-mm diameter hole bored through the top for suspension purposes has proved satisfactory

1.11 Laboratory Jack, heavy-duty precision.

1.12 Hydrometer, capable of reading liquid density.

2 Reagents and Materials

2.1 Canola oil with the average density of 0.92 g/ml ± 0.05 g/ml

3 Hazards

3.1 This test method should be used only by laboratory workers with general training in the safe handling of chemicals. A source of useful information is Prudent Practices in the Laboratory: Handling and Disposal of Chemicals, National Academy Press, 1995, 448 pp., ISBN 0-309-05229-7. (Warning—In addition to other warnings, consult the appropriate material safety data sheet for each material used, including reagent materials and test specimen materials, for specific recommendations on safety and handling.)

4 Sampling, Test Specimens, and Test Units

4.1 A minimum of five test specimens shall be tested for each sample.

4.2 The test specimen weight shall be a minimum of 0.5 g.

5 Preparation of Apparatus

5.1 The assembly of the apparatus is shown in Fig. 1 or Fig. 2. The balance stand must be firmly secured to a stable surface with the balance resting on the stand directly over the hole provided for the suspension system. Place the immersion fluid container on the laboratory jack directly under the suspension hook.

5.2 To prevent stray air currents between the bottom of the balance and the top of the stand, it is advisable to shield this area. If excessive vibration is observed while weighing, vibration damping pads must be used.

6 Calibration and Standardization

6.1 All measuring equipment shall have certified calibrations that are current at the time of use of the equipment. The calibration documentation shall be available for inspection.

6.2 The following steps should be undertaken at least once prior to a series of tests and again if the test environment changed temperature by greater than ±1ºC or a new batch of immersion fluid is required.

6.2.1 *Density Standard Calibration*—Fill the immersion fluid container 3/4 to 7/8 full with distilled water. Place the container on a collapsed laboratory jack and zero the balance. Attach the suspension wire and weigh. Record as M1, g. Raise the laboratory jack to the immersion point of the suspension wire and record the weight as M2, g. Rinse the wire with acetone and let air dry. Attach the wire plus glass standard and weigh. Record asM3, g. Again raise the jack to the immersion point and weigh. Record as M4, g. Lower the jack, remove the standard plus wire, and rinse them with acetone to dry. Measure the temperature of the water to 0.1°C and record the water density at that temperature.

6.3 *Immersion Fluid Standardization* — This step should be done at the beginning of each series of density determinations with a new batch of specimen, when a new batch of immersion fluid is to be used or there is temperature change greater than ±1ºC. Fill the clean and dry fluid container 3/4 to 7/8 full with liquid (canola oil for example) and allow to come to temperature equilibrium. Proceed by weighing the suspension wire. Record as M1, g. Raise the laboratory jack to the immersion point of the suspension wire and record the weight as M2, g. Rinse the wire with acetone and let air dry. Attach the wire plus glass standard and weigh. Record as M3, g. Again raise the jack to the immersion point and weigh. Record as M4, g. Remove wire and standard and rinse with acetone.

7 Conditioning

7.1 All fibers need to be placed in the oven at 80ºC for at least 4 hours prior to testing.

7.2 Specimen temperature at time of testing should be within ± 1 ºC of the test temperature.

7.3 Condition the liquid to a test temperature, typically 23°C.

8 Procedure

8.1 Select a specimen. Wrap the specimen (the end of a small winding cone is suitable) and intertwine the ends of the fiber tow to prevent unraveling. Proceed by weighing the suspension wire. Record as M1, g. Raise the laboratory jack to the immersion point of the suspension wire and record the weight as M2, g. Rinse the wire with acetone and let air dry. Attach the specimen to the wire and weigh. Record as M3, g.

8.2 Raise the laboratory jack to the immersion point of the suspension wire. Remove the wire and soak in the liquid. Put the container with the specimen and liquid into a vacuum desiccator and pull vacuum to approximately 10-mm Hg or until boiling of the solution begins. Hold vacuum for a minimum of 3 min or until all trapped air on the fiber surface is removed.

8.3 Reattach the specimen and wire to the balance. Again raise the jack to the immersion point and weigh. Record as M4, g. Remove wire and standard and rinse with acetone.

8.4 Repeat for each specimen

9 Calculation or Interpretation of Results

9.1 Density of Glass Standard, g/mL:

$$\rho s = \frac{(M3 - M1)\rho w}{((M3 - M1) - (M4 - M2))}$$

where: the liquid is water and the sample is the glass standard.

The density of the standard should remain consistent to ± 0.0001 g/mL

9.2 Density of Immersion Liquid, g/ml

$$\rho l = \rho s \frac{(M3 - M1)\rho l}{((M3 - M1) - (M4 - M2))}$$

where: the liquid is the test liquid and the sample is the glass standard.

9.3 Density of fiber specimen, g/ml

$$\rho f = \frac{(M3 - M1)\rho l}{((M3 - M1) - (M4 - M2))}$$

where : the liquid is the canola oil and the specimen is the fiber.

10 Report

10.1 Report the following information:

10.1.1 Reporting of items that are beyond the control of a given test laboratory, such as material details shall be the responsibility of the requestor.

10.1.2 Complete identification of the material in accordance with Guide E1309, including fiber type, surface treatment, and fiber manufacturer.

10.1.3 This standard and the test method used

10.1.4 Complete test parameters including test temperature in degrees Celsius

10.1.5 The specimen conditioning performed prior to testing

10.1.6 The immersion liquid(s) used and their temperature.

10.1.7 Each measured density and average, g/mL. A measure of the degree of variation in the density such as standard deviation.

11 Precision and Bias

11.1 The data required for the development of a precision and bias statement is not available for this test method. Committee D13 is currently planning a round-robin test for this test method to determine precision

APPENDIX F. ADDITIONAL DENSITY MEASUREMENT DATA

Table F1. Distilled water, liquid density = .998 g/cc

	Initial		3 Minutes		6 Minutes	
Dry Mass (g)	Immersed (g)	Calc Dens (g/cc)	Immersed (g)	Calc Dens (g/cc)	Immersed (g)	Calc Dens (g/cc)
0.1237	0.0789	2.7556	0.0857	3.2488	0.0877	3.4292
0.1360	0.0750	2.2250	0.0851	2.6666	0.0910	3.0162
0.1322	0.0706	2.1418	0.0822	2.6387	0.0868	2.9061
0.1112	0.0400	1.5587	0.0458	1.6969	0.0479	1.7532
0.1404	0.0440	1.4535	0.0418	1.4211	0.0418	1.4211
0.1907	0.0435	1.2929	0.0440	1.2973	0.0448	1.3044
0.1243	0.0377	1.4325	0.0378	1.4341	0.0443	1.5506
0.1858	0.0430	1.2985	0.0440	1.3077	0.0440	1.3077
0.1523	0.0510	1.5004	0.0524	1.5215	0.0530	1.5307

Table F2. Canola oil, no vacuum, liquid density =0 .9155 g/cc

	Initial		3 Minutes		6 Minutes	
Dry Mass (g)	Immersed (g)	Calc Dens (g/cc)	Immersed (g)	Calc Dens (g/cc)	Immersed (g)	Calc Dens (g/cc)
0.4185	0.1395	1.3733	0.1402	1.3767	0.1426	1.3887
0.4275	0.1481	1.4008	0.1485	1.4028	0.1487	1.4038
0.3511	0.1112	1.3399	0.1120	1.3443	0.1124	1.3466
0.3856	0.1242	1.3505	0.1244	1.3515	0.1244	1.3515
0.4014	0.1304	1.3560	0.1307	1.3575	0.1309	1.3585

Table F3. Canola oil, vacuum low, liquid density = .9155 g/cc

Dry Mass (g)	Immersed (g)	Calc Dens (g/cc)
0.3535	0.1124	1.3423
0.4400	0.1498	1.3881
0.3264	0.1094	1.3770

Table F4. Canola oil, vacuum high, liquid density = .9155 g/cc

	Before Vac		After Vac	
Dry Mass (g)	Immersed (g)	Calc Dens (g/cc)	Immersed (g)	Calc Dens (g/cc)
0.3074	0.1100	1.4257	0.1205	1.5058
0.3847	0.1300	1.3828	0.1445	1.4662
0.3572	0.1263	1.4163	0.1286	1.4305
0.3495	0.1230	1.4127	0.1344	1.4875
0.4438	0.1552	1.4078	0.1654	1.4594

APPENDIX G. STATISTICAL ANALYSIS OF DATA

Table G1. Statistical analysis, interlaminar shear stress for treated and untreated flax fiber Type 1 presented in Table 14

SUMMARY					
Groups	*Count*	*Sum*	*Mean*	*St. Deviation*	
Unt./8601	5	81.6	16.32	0.80	
treated/8601	5	80	16	0.50	
Anova: Single Factor					
Source of Variation	*SS*	*df*	*MS*	*F*	*P-value*
Between Groups	0.4919	1	0.4919	0.7838	0.3781
Within Groups	78.5808	8	0.6275		
Total	79.0727	9			

Table G2. Statistical analysis, tensile strength for treated and untreated flax fiber Type 1 presented in Table 14

SUMMARY					
Groups	*Count*	*Sum*	*Mean*	*St. Deviation*	
Unt./8601	5	81.6	140.52	15.98	
treated/8601	5	80	96.26	12.43	
Anova: Single Factor					
Source of Variation	*SS*	*df*	*MS*	*F*	*P-value*
Between Groups	9409.78	1	9409.7852	37.3199	0.0000
Within Groups	31572.8073	8	252.1387		
Total	40982.5873	9			

Table G3. Statistical analysis, tensile modulus for treated and untreated flax fiber Type 1 presented in Table 14

SUMMARY				
Groups	*Count*	*Sum*	*Mean*	*St. Deviation*
Unt./8601	5	63.35	12.67	1.54
treated/8601	5	57.35	11.47	0.41

Anova: Single Factor					
Source of Variation	*SS*	*df*	*MS*	*F*	*P-value*
Between Groups	6.917	1	6.9170	3.0058	0.0857
Within Groups	288.1578	8	2.3012		
Total	295.0748	9			

Table G4. Statistical analysis, flexural strength for treated and untreated flax fiber Type 1 presented in Table 14

SUMMARY				
Groups	*Count*	*Sum*	*Mean*	*St. Deviation*
Unt./8601	5	615	123	8.90
treated/8601	5	650	130	7.90

Anova: Single Factor					
Source of Variation	*SS*	*df*	*MS*	*F*	*P-value*
Between Groups	235.371	1	235.3710	2.9918	0.0864
Within Groups	9851.4762	8	78.6733		
Total	10086.8472	9			

Table G5. Statistical analysis, flexural modulus of treated and untreated flax fiber Type 1 presented in Table 14

SUMMARY

Groups	*Count*	*Sum*	*Mean*	*St. Deviation*
Unt./8601	5	41	8.2	0.71
treated/8601	5	39	7.8	0.28

Anova: Single Factor

Source of Variation	*SS*	*df*	*MS*	*F*	*P-value*
Between Groups	0.7686	1	0.7686	1.5669	0.2134
Within Groups	61.4206	8	0.4905		
Total	62.1892	9			

Table G6. Statistical analysis, tensile strength of flax/VE and flax/MESS composites presented in Table 16

SUMMARY

Groups	*Count*	*Sum*	*Mean*	*St. Dev.*
Type 1- VE	5	540.4	108.08	2.27
Type 1- MESS	5	139.1	27.82	1.61
Type 2- VE	5	469.6	93.92	3.26
Type 2- MESS	5	210.0	42.01	4.69
Type 3- VE	5	407	81.4	2.67
Type 3- MESS	5	131.5	26.3	5.61
Type 4- VE	5	524.75	104.95	3.85
Type 4- MESS	5	247.85	49.57	5.78

Anova: Single Factor

Source of Variation	*SS*	*df*	*MS*	*F*	*P-value*
Between Groups	91823.6554	7	131117.6651	1758.9624	0.0000
Within Groups	1112.8253	192	7.4576		
Total	92936.4807	199			

Tukey-HSD Post-hoc Test

Groups	*p-value*	*Groups*	*p-value*
T1- VE vs T1 - MESS	0.0000	T2 - VE vs T3 - VE	0.0000
T1 - VE vs T2 - VE	0.0000	T2 - VE vs T3 - MESS	0.0000
T1 - VE vs T2 - MESS	0.0000	T2 - VE vs T4 - VE	0.0000
T1 - VE vs T3 - VE	0.0000	T2 - VE vs T4 - MESS	0.0000
T1 - VE vs T3 - MESS	0.0000	T2 - MESS vs T3 - VE	0.0000
T1 - VE vs T4 - VE	0.0000	T2 - MESS vs T3 - MESS	0.0000
T1 - VE vs T4 - MESS	0.0000	T2 - MESS vs T4 - VE	0.0000
T1 - MESS vs T2 - VE	0.0000	T2 - MESS vs T4 - MESS	0.0006
T1 - MESS vs T2 - MESS	0.0000	T3 - VE vs T3 - MESS	0.0000
T1 - MESS vs T3 - VE	0.0000	T3 - VE vs T4 - VE	0.0000
T1 - MESS vs T3 - MESS	0.0000	T3 - VE vs T4 - MESS	0.0000
T1 - MESS vs T4 - VE	0.0000	T3 - MESS vs T4 - VE	0.0000
T1 - MESS vs T4 - MESS	0.0000	T3 - MESS vs T4 - MESS	0.0000
T2 - VE vs T2 - MESS	0.0000	T4 - VE vs T4 - MESS	0.0000

Table G7. Statistical analysis, tensile modulus of flax/VE and flax/MESS composites presented in Table 16

SUMMARY

Groups	*Count*	*Sum*	*Mean*	*St. Dev.*
Type 1- VE	5	77.15	15.43	0.45
Type 1- MESS	5	85.3	17.06	1.67
Type 2- VE	5	64.35	12.87	0.45
Type 2- MESS	5	71.5	14.3	0.41
Type 3- VE	5	62.95	12.59	0.87
Type 3- MESS	5	64.35	12.87	1.26
Type 4- VE	5	70.15	14.03	1
Type 4- MESS	5	82.05	16.41	2.55

Anova: Single Factor

Source of Variation	*SS*	*df*	*MS*	*F*	*P-value*
Between Groups	130.2612	7	18.6087	36.2634	0.0000
Within Groups	76.573	192	0.5132		
Total	206.8342	199			

Tukey-HSD Post-hoc Test

Groups	*p-value*	*Groups*	*p-value*
T1- VE vs T1 - MESS	0.0001	T2 - VE vs T3 - VE	0.9986
T1 - VE vs T2 - VE	0.0000	T2 - VE vs T3 - MESS	1.0000
T1 - VE vs T2 - MESS	0.0159	T2 - VE vs T4 - VE	0.1791
T1 - VE vs T3 - VE	0.0000	T2 - VE vs T4 - MESS	0.0000
T1 - VE vs T3 - MESS	0.0000	T2 - MESS vs T3 - VE	0.0055
T1 - VE vs T4 - VE	0.0008	T2 - MESS vs T3 - MESS	0.0396
T1 - VE vs T4 - MESS	0.0616	T2 - MESS vs T4 - VE	0.9989
T1 - MESS vs T2 - VE	0.0000	T2 - MESS vs T4 - MESS	0.0002
T1 - MESS vs T2 - MESS	0.0000	T3 - VE vs T3 - MESS	0.9986
T1 - MESS vs T3 - VE	0.0000	T3 - VE vs T4 - VE	0.0372
T1 - MESS vs T3 - MESS	0.0000	T3 - VE vs T4 - MESS	0.0000
T1 - MESS vs T4 - VE	0.0000	T3 - MESS vs T4 - VE	0.1791
T1 - MESS vs T4 - MESS	0.8397	T3 - MESS vs T4 - MESS	0.0000
T2 - VE vs T2 - MESS	0.0396	T4 - VE vs T4 - MESS	0.0000

Table G8. Statistical analysis, tensile modulus of flax/VE and flax/MESS composites presented in Table 16

SUMMARY

Groups	*Count*	*Sum*	*Mean*	*St. Dev.*
Type 1- VE	5	77.15	15.43	0.45
Type 1- MESS	5	85.3	17.06	1.67
Type 2- VE	5	64.35	12.87	0.45
Type 2- MESS	5	71.5	14.3	0.41
Type 3- VE	5	62.95	12.59	0.87
Type 3- MESS	5	64.35	12.87	1.26
Type 4- VE	5	70.15	14.03	1
Type 4- MESS	5	82.05	16.41	2.55

Anova: Single Factor

Source of Variation	*SS*	*df*	*MS*	*F*	*P-value*
Between Groups	130.2612	7	18.6087	36.2634	0.0000
Within Groups	76.573	192	0.5132		
Total	206.8342	199			

Tukey-HSD Post-hoc Test

Groups	*p-value*	*Groups*	*p-value*
T1- VE vs T1 - MESS	0.0001	T2 - VE vs T3 - VE	0.9986
T1 - VE vs T2 - VE	0.0000	T2 - VE vs T3 - MESS	1.0000
T1 - VE vs T2 - MESS	0.0159	T2 - VE vs T4 - VE	0.1791
T1 - VE vs T3 - VE	0.0000	T2 - VE vs T4 - MESS	0.0000
T1 - VE vs T3 - MESS	0.0000	T2 - MESS vs T3 - VE	0.0055
T1 - VE vs T4 - VE	0.0008	T2 - MESS vs T3 - MESS	0.0396
T1 - VE vs T4 - MESS	0.0616	T2 - MESS vs T4 - VE	0.9989
T1 - MESS vs T2 - VE	0.0000	T2 - MESS vs T4 - MESS	0.0002
T1 - MESS vs T2 - MESS	0.0000	T3 - VE vs T3 - MESS	0.9986
T1 - MESS vs T3 - VE	0.0000	T3 - VE vs T4 - VE	0.0372
T1 - MESS vs T3 - MESS	0.0000	T3 - VE vs T4 - MESS	0.0000
T1 - MESS vs T4 - VE	0.0000	T3 - MESS vs T4 - VE	0.1791
T1 - MESS vs T4 - MESS	0.8397	T3 - MESS vs T4 - MESS	0.0000
T2 - VE vs T2 - MESS	0.0396	T4 - VE vs T4 - MESS	0.0000

Table G9. Statistical analysis, flexural strength of flax/VE and flax/MESS composites presented in Table 16

SUMMARY

Groups	*Count*	*Sum*	*Mean*	*St. Dev.*
Type 1- VE	5	623.85	124.77	3.15
Type 1- MESS	5	209.15	41.83	1.46
Type 2- VE	5	574.65	114.93	5.54
Type 2- MESS	5	309.6	61.92	6.83
Type 3- VE	5	518.05	103.61	2.44
Type 3- MESS	5	177.15	35.43	5.97
Type 4- VE	5	659.8	131.96	3.37
Type 4- MESS	5	324.85	64.97	2.63

Anova: Single Factor

Source of Variation	*SS*	*df*	*MS*	*F*	*P-value*
Between Groups	98760.6049	7	14108.6578	1196.0762	0.0000
Within Groups	17600.1671	192	11.7958		
Total	116360.772	199			

Tukey-HSD Post-hoc Test

Groups	*p-value*	*Groups*	*p-value*
T1- VE vs T1 - MESS	0.0000	T2 - VE vs T3 - VE	0.0000
T1 - VE vs T2 - VE	0.0000	T2 - VE vs T3 - MESS	0.0000
T1 - VE vs T2 - MESS	0.0000	T2 - VE vs T4 - VE	0.0000
T1 - VE vs T3 - VE	0.0000	T2 - VE vs T4 - MESS	0.0000
T1 - VE vs T3 - MESS	0.0000	T2 - MESS vs T3 - VE	0.0000
T1 - VE vs T4 - VE	0.0003	T2 - MESS vs T3 - MESS	0.0000
T1 - VE vs T4 - MESS	0.0000	T2 - MESS vs T4 - VE	0.0000
T1 - MESS vs T2 - VE	0.0000	T2 - MESS vs T4 - MESS	0.8542
T1 - MESS vs T2 - MESS	0.0000	T3 - VE vs T3 - MESS	0.0000
T1 - MESS vs T3 - VE	0.0000	T3 - VE vs T4 - VE	0.0000
T1 - MESS vs T3 - MESS	0.0707	T3 - VE vs T4 - MESS	0.0000
T1 - MESS vs T4 - VE	0.0000	T3 - MESS vs T4 - VE	0.0000
T1 - MESS vs T4 - MESS	0.0000	T3 - MESS vs T4 - MESS	0.0000
T2 - VE vs T2 - MESS	0.0000	T4 - VE vs T4 - MESS	0.0000

Table G10. Statistical analysis, flexural modulus of flax/VE and flax/MESS composites presented in Table 16

SUMMARY				
Groups	*Count*	*Sum*	*Mean*	*St. Dev.*
Type 1- VE	5	46.5	9.3	0.08
Type 1- MESS	5	75.2	15.04	0.44
Type 2- VE	5	44.25	8.85	0.71
Type 2- MESS	5	73.55	14.71	1.7
Type 3- VE	5	30.05	6.01	0.34
Type 3- MESS	5	47.95	9.59	0.55
Type 4- VE	5	42.55	8.51	1.13
Type 4- MESS	5	64.25	12.85	1.6

Anova: Single Factor					
Source of Variation	*SS*	*df*	*MS*	*F*	*P-value*
Between Groups	415.3671	7	59.3382	275.4394	0.0000
Within Groups	32.1466	192	0.2154		
Total	447.5137	199			

Tukey-HSD Post-hoc Test			
Groups	*p-value*	*Groups*	*p-value*
T1- VE vs T1 - MESS	0.0000	T2 - VE vs T3 - VE	0.0000
T1 - VE vs T2 - VE	0.4040	T2 - VE vs T3 - MESS	0.1949
T1 - VE vs T2 - MESS	0.0000	T2 - VE vs T4 - VE	0.9423
T1 - VE vs T3 - VE	0.0000	T2 - VE vs T4 - MESS	0.0000
T1 - VE vs T3 - MESS	0.8697	T2 - MESS vs T3 - VE	0.0000
T1 - VE vs T4 - VE	0.0064	T2 - MESS vs T3 - MESS	0.0000
T1 - VE vs T4 - MESS	0.0000	T2 - MESS vs T4 - VE	0.0000
T1 - MESS vs T2 - VE	0.0000	T2 - MESS vs T4 - MESS	0.0000
T1 - MESS vs T2 - MESS	0.9506	T3 - VE vs T3 - MESS	0.0000
T1 - MESS vs T3 - VE	0.0000	T3 - VE vs T4 - VE	0.0000
T1 - MESS vs T3 - MESS	0.0000	T3 - VE vs T4 - MESS	0.0000
T1 - MESS vs T4 - VE	0.0000	T3 - MESS vs T4 - VE	0.0077
T1 - MESS vs T4 - MESS	0.0000	T3 - MESS vs T4 - MESS	0.0000
T2 - VE vs T2 - MESS	0.0000	T4 - VE vs T4 - MESS	0.0000

Table G11. Statistical analysis, interlaminar shear strength of flax/VE and flax/MESS composites presented in Table 16

SUMMARY				
Groups	*Count*	*Sum*	*Mean*	*St. Dev.*
Type 1- VE	5	61.95	12.39	0.7
Type 1- MESS	5	39.85	7.97	2.66
Type 2- VE	5	65.3	13.06	0.74
Type 2- MESS	5	45.8	9.16	1.34
Type 3- VE	5	50.3	10.06	0.46
Type 3- MESS	5	21.4	4.28	0.67
Type 4- VE	5	54.1	10.82	0.69
Type 4- MESS	5	35.15	7.03	0.68

Anova: Single Factor					
Source of Variation	*SS*	*df*	*MS*	*F*	*P-value*
Between Groups	569.7862	7	81.3980	117.3899	0.0000
Within Groups	103.469	192	0.6934		
Total	673.2552	199			

Tukey-HSD Post-hoc Test			
Groups	*p-value*	*Groups*	*p-value*
T1- VE vs T1 - MESS	0.0000	T2 - VE vs T3 - VE	0.0000
T1 - VE vs T2 - VE	0.6456	T2 - VE vs T3 - MESS	0.0000
T1 - VE vs T2 - MESS	0.0000	T2 - VE vs T4 - VE	0.0010
T1 - VE vs T3 - VE	0.0000	T2 - VE vs T4 - MESS	0.0000
T1 - VE vs T3 - MESS	0.0000	T2 - MESS vs T3 - VE	0.6815
T1 - VE vs T4 - VE	0.0015	T2 - MESS vs T3 - MESS	0.0000
T1 - VE vs T4 - MESS	0.0000	T2 - MESS vs T4 - VE	0.0401
T1 - MESS vs T2 - VE	0.0000	T2 - MESS vs T4 - MESS	0.0021
T1 - MESS vs T2 - MESS	0.3231	T3 - VE vs T3 - MESS	0.0000
T1 - MESS vs T3 - VE	0.0028	T3 - VE vs T4 - VE	0.8356
T1 - MESS vs T3 - MESS	0.0000	T3 - VE vs T4 - MESS	0.0000
T1 - MESS vs T4 - VE	0.0000	T3 - MESS vs T4 - VE	0.0000
T1 - MESS vs T4 - MESS	0.6313	T3 - MESS vs T4 - MESS	0.0000
T2 - VE vs T2 - MESS	0.0000	T4 - VE vs T4 - MESS	0.0000

Table G12. Statistical analysis, interlaminar shear stress for treated and untreated flax fiber Type 1 presented in Table 19

SUMMARY

Groups	*Count*	*Sum*	*Mean*	*St. Deviation*
Unt./VE	5	61.1	12.22	0.92
Unt./VE+AR	5	79.7	15.94	1.01
Alkaline/VE	5	104.4	20.88	0.93
Alkaline/VE+AR	5	110.2	22.04	2.32

Anova: Single Factor

Source of Variation	*SS*	*df*	*MS*	*F*	*P-value*
Between Groups	39580.282	3	13193.4273	6504.1915	0.0000
Within Groups	32.4552	16	2.0284		
Total	39612.7372	19			

Tukey-HSD Post-hoc Test

Groups	*Diff*	*p-value*
Unt./VE vs Unt.VE+AR	-106.2800	0.9344
Unt./VE vs Alkaline/VE	-101.3400	0.9345
Unt./VE vs Alkaline/VE+AR	-100.1800	0.9345
Unt.VE+AR vs Alkaline/VE	4.9400	0.0003
Unt.VE+AR vs Alkaline/VE+AR	6.1000	0.0000
Alkaline/VE vs Alkaline/VE+AR	1.1600	0.5833

Table G13. Statistical analysis, tensile strength for treated and untreated flax fiber Type 1 presented in Table 19

SUMMARY

Groups	*Count*	*Sum*	*Mean*	*St. Deviation*
Unt./VE	5	502.45	100.49	11.02
Unt./VE+AR	5	539.35	107.87	3.40
Alkaline/VE	5	526.6	105.32	2.82
Alkaline/VE+AR	5	584.5	116.9	0.12

Anova: Single Factor

Source of Variation	*SS*	*df*	*MS*	*F*	*P-value*
Between Groups	1586.175	3	528.7250	4.7595	0.0035
Within Groups	14799.1125	16	111.0878		
Total	16385.2875	19			

Tukey-HSD Post-hoc Test

Groups	*Diff*	*p-value*
Unt./VE vs Unt.VE+AR	7.38	0.4198
Unt./VE vs Alkaline/VE	4.83	0.7471
Unt./VE vs Alkaline/VE+AR	16.41	0.0047
Unt.VE+AR vs Alkaline/VE	2.55	0.9809
Unt.VE+AR vs Alkaline/VE+AR	9.03	0.5300
Alkaline/VE vs Alkaline/VE+AR	11.58	0.3087

Table G14. Statistical analysis, tensile modulus for treated and untreated flax fiber Type 1 presented in Table 19

SUMMARY

Groups	*Count*	*Sum*	*Mean*	*St. Deviation*
Unt./VE	5	68.55	13.71	2.10
Unt./VE+AR	5	79.7	15.94	2.25
Alkaline/VE	5	60.2	12.04	1.67
Alkaline/VE+AR	5	69.95	13.99	0.17

Anova: Single Factor

Source of Variation	*SS*	*df*	*MS*	*F*	*P-value*
Between Groups	39.0724	3	13.0241	3.0650	0.0303
Within Groups	566.1014	16	4.2494		
Total	605.1738	19			

Tukey-HSD Post-hoc Test

Groups	*Diff*	*p-value*
Unt./VE vs Unt.VE+AR	2.23	0.0877
Unt./VE vs Alkaline/VE	1.67	0.2897
Unt./VE vs Alkaline/VE+AR	0.28	0.9908
Unt.VE+AR vs Alkaline/VE	3.90	0.0172
Unt.VE+AR vs Alkaline/VE+AR	1.95	0.4430
Alkaline/VE vs Alkaline/VE+AR	1.95	0.4430

Table G15. Statistical analysis, flexural strength for treated and untreated flax fiber Type 1 presented in Table 19

SUMMARY

Groups	*Count*	*Sum*	*Mean*	*St. Deviation*
Unt./VE	5	766.25	153.25	29.90
Unt./VE+AR	5	771.45	154.29	7.20
Alkaline/VE	5	815.15	163.03	10.27
Alkaline/VE+AR	5	790.2	158.04	20.10

Anova: Single Factor

Source of Variation	*SS*	*df*	*MS*	*F*	*P-value*
Between Groups	553.9761	3	184.6587	0.2224	0.8807
Within Groups	110617.184	16	830.3347		
Total	111171.16	19			

Table G16. Statistical analysis, flexural modulus for treated and untreated flax fiber Type 1 presented in Table 19

SUMMARY

Groups	*Count*	*Sum*	*Mean*	*St. Deviation*
Unt./VE	5	62.5	12.5	2.90
Unt./VE+AR	5	59.2	11.84	0.75
Alkaline/VE	5	54.1	10.82	1.16
Alkaline/VE+AR	5	68.1	13.62	1.10

Anova: Single Factor

Source of Variation	*SS*	*df*	*MS*	*F*	*P-value*
Between Groups	22.2908	3	7.4303	0.9592	0.4141
Within Groups	1031.9326	16	7.7461		
Total	1054.2234	19			

Table G17. Statistical analysis, tensile strength for unweathered treated and untreated flax fiber Type 7 presented in Table 20

SUMMARY

Groups	*Count*	*Sum*	*Mean*	*St. Dev.*
UTUW-VE	5	913.95	182.79	15.00
TUW-VE	5	1048.65	209.73	27.46
UTUW-MESS	5	614.85	122.97	2.56
TUW-MESS	5	1039.60	207.92	18.13
UTUW-DMESS	5	652.95	130.59	11.57
TUW-DMESS	5	751.95	150.39	2.20

Anova: Single Factor

Source of Variation	*SS*	*df*	*MS*	*F*	*P-value*
Between Groups	40652.968	5	8130.5936	35.6734	0.0000
Within Groups	32186.528	24	227.9176		
Total	72839.496	29			

Tukey-HSD Post-hoc Test

Groups	*p-value*	*Groups*	*p-value*
UTUW-VE vs TUW-VE	0.0007	TUW-VE vs TUW-DMESS	0.0000
UTUW-VE vs UTUW-MESS	0.0000	UTUW-MESS vs TUW-MESS	0.0000
UTUW-VE vs TUW-MESS	0.0018	UTUW-MESS vs UTUW-DMESS	0.9674
UTUW-VE vs UTUW-DMESS	0.0000	UTUW-MESS vs TUW-DMESS	0.0524
UTUW-VE vs TUW-DMESS	0.0003	TUW-MESS vs UTUW-DMESS	0.0000
TUW-VE vs UTUW-MESS	0.0000	TUW-MESS vs TUW-DMESS	0.0000
TUW-VE vs TUW-MESS	0.9999	UTUW-DMESS vs TUW-DMESS	0.3071
TUW-VE vs UTUW-DMESS	0.0000		

Table G18. Statistical analysis, tensile modulus for unweathered treated and untreated flax fiber Type 7 presented in Table 20

SUMMARY

Groups	*Count*	*Sum*	*Mean*	*St. Dev.*
UTUW-VE	5	113.80	22.76	1.08
TUW-VE	5	134.80	26.96	3.88
UTUW-MESS	5	96.15	19.23	1.72
TUW-MESS	5	146.40	29.28	13.63
UTUW-DMESS	5	101.40	20.28	15.36
TUW-DMESS	5	124.50	24.90	2.14

Anova: Single Factor

Source of Variation	*SS*	*df*	*MS*	*F*	*P-value*
Between Groups	408.7384	5	81.7477	6.0171	0.0000
Within Groups	1918.5866	24	13.5858		
Total	2327.325	29			

Tukey-HSD Post-hoc Test

Groups	*p-value*	*Groups*	*p-value*
UTUW-VE vs TUW-VE	0.1319	TUW-VE vs TUW-DMESS	0.9499
UTUW-VE vs UTUW-MESS	0.2938	UTUW-MESS vs TUW-MESS	0.0004
UTUW-VE vs TUW-MESS	0.0022	UTUW-MESS vs UTUW-DMESS	0.9976
UTUW-VE vs UTUW-DMESS	0.6809	UTUW-MESS vs TUW-DMESS	0.1523
UTUW-VE vs TUW-DMESS	0.7995	TUW-MESS vs UTUW-DMESS	0.0023
TUW-VE vs UTUW-MESS	0.0145	TUW-MESS vs TUW-DMESS	0.4194
TUW-VE vs TUW-MESS	0.9188	UTUW-DMESS vs TUW-DMESS	0.3579
TUW-VE vs UTUW-DMESS	0.0532		

Table G19. Statistical analysis, flexural strength for unweathered treated and untreated flax fiber Type 7 presented in Table 20

SUMMARY

Groups	*Count*	*Sum*	*Mean*	*St. Dev.*
UTUW-VE	5	907.65	181.53	26.28
TUW-VE	5	1395.15	279.03	27.38
UTUW-MESS	5	681.25	136.25	7.09
TUW-MESS	5	1145.35	229.07	19.00
UTUW-DMESS	5	667.05	133.41	12.02
TUW-DMESS	5	1000.25	200.05	40.95

Anova: Single Factor

Source of Variation	*SS*	*df*	*MS*	*F*	*P-value*
Between Groups	81539.628	5	16307.9256	24.0778	0.0000
Within Groups	95648.448	24	677.3010		
Total	177188.08	29			

Tukey-HSD Post-hoc Test

Groups	*p-value*	*Groups*	*p-value*
UTUW-VE vs TUW-VE	0.0000	TUW-VE vs TUW-DMESS	0.0001
UTUW-VE vs UTUW-MESS	0.0027	UTUW-MESS vs TUW-MESS	0.0000
UTUW-VE vs TUW-MESS	0.0014	UTUW-MESS vs UTUW-DMESS	0.9999
UTUW-VE vs UTUW-DMESS	0.0012	UTUW-MESS vs TUW-DMESS	0.0022
UTUW-VE vs TUW-DMESS	0.6263	TUW-MESS vs UTUW-DMESS	0.0000
TUW-VE vs UTUW-MESS	0.0000	TUW-MESS vs TUW-DMESS	0.4929
TUW-VE vs TUW-MESS	0.0334	UTUW-DMESS vs TUW-DMESS	0.0012
TUW-VE vs UTUW-DMESS	0.0000		

Table G20. Statistical analysis, flexural modulus for unweathered treated and untreated flax fiber Type 7 presented in Table 20

SUMMARY

Groups	*Count*	*Sum*	*Mean*	*St. Dev.*
UTUW-VE	5	94.75	18.95	3.72
TUW-VE	5	126.75	25.35	3.24
UTUW-MESS	5	89.30	17.86	4.99
TUW-MESS	5	132.15	26.43	2.73
UTUW-DMESS	5	84.20	16.84	1.99
TUW-DMESS	5	101.75	20.35	5.25

Anova: Single Factor

Source of Variation	*SS*	*df*	*MS*	*F*	*P-value*
Between Groups	497.7727	5	99.5545	7.1186	0.0000
Within Groups	1974.9836	24	13.9852		
Total	2472.7563	29			

Tukey-HSD Post-hoc Test

Groups	*p-value*	*Groups*	*p-value*
UTUW-VE vs TUW-VE	0.0034	TUW-VE vs TUW-DMESS	0.2861
UTUW-VE vs UTUW-MESS	0.9879	UTUW-MESS vs TUW-MESS	0.0053
UTUW-VE vs TUW-MESS	0.0003	UTUW-MESS vs UTUW-DMESS	0.9981
UTUW-VE vs UTUW-DMESS	0.8181	UTUW-MESS vs TUW-DMESS	0.8989
UTUW-VE vs TUW-DMESS	0.9633	TUW-MESS vs UTUW-DMESS	0.0011
TUW-VE vs UTUW-MESS	0.0228	TUW-MESS vs TUW-DMESS	0.1114
TUW-VE vs TUW-MESS	0.9975	UTUW-DMESS vs TUW-DMESS	0.6750
TUW-VE vs UTUW-DMESS	0.0058		

Table G21. Statistical analysis, interlaminar shear strength for unweathered treated and untreated flax fiber Type 7 presented in Table 20

SUMMARY

Groups	*Count*	*Sum*	*Mean*	*St. Dev.*
UTUW-VE	5	93.95	18.79	1.81
TUW-VE	5	156.35	31.27	1.03
UTUW-MESS	5	58.40	11.68	1.07
TUW-MESS	5	68.40	13.68	0.51
UTUW-DMESS	5	63.60	12.72	0.66
TUW-DMESS	5	94.00	18.80	3.73

Anova: Single Factor

Source of Variation	*SS*	*df*	*MS*	*F*	*P-value*
Between Groups	1340.5855	5	268.1171	81.53.45	0.0000
Within Groups	464.3864	24	3.2884		
Total	1804.9719	29			

Tukey-HSD Post-hoc Test

Groups	*p-value*	*Groups*	*p-value*
UTUW-VE vs TUW-VE	0.0000	TUW-VE vs TUW-DMESS	0.0000
UTUW-VE vs UTUW-MESS	0.0000	UTUW-MESS vs TUW-MESS	0.5054
UTUW-VE vs TUW-MESS	0.0000	UTUW-MESS vs UTUW-DMESS	0.9442
UTUW-VE vs UTUW-DMESS	0.0000	UTUW-MESS vs TUW-DMESS	0.0000
UTUW-VE vs TUW-DMESS	0.0000	TUW-MESS vs UTUW-DMESS	0.9601
TUW-VE vs UTUW-MESS	0.0000	TUW-MESS vs TUW-DMESS	0.0002
TUW-VE vs TUW-MESS	0.0000	UTUW-DMESS vs TUW-DMESS	0.0000
TUW-VE vs UTUW-DMESS	0.0000		